(12) INTERNATIONAL APPLICATION PUBLISHED UNDER THE PATENT COOPERATION TREATY (PCT)

(19) World Intellectual Property Organization
International Bureau

(43) International Publication Date
18 April 2019 (18.04.2019)

WIPO | PCT

(10) International Publication Number
WO 2019/072885 A1

(51) International Patent Classification:
A61K 31/704 (2006.01) *A61K 47/69* (2017.01)
A61K 45/06 (2006.01) *A61P 35/00* (2006.01)

(21) International Application Number:
PCT/EP2018/077547

(22) International Filing Date:
10 October 2018 (10.10.2018)

(25) Filing Language: English

(26) Publication Language: English

(30) Priority Data:
17306375.1 11 October 2017 (11.10.2017) EP

(71) Applicants: **INSERM (INSTITUT NATIONAL DE LA SANTÉ ET DE LA RECHERCHE MÉDICALE)** [FR/FR]; 101, rue de Tolbiac, 75013 Paris (FR). **INSTITUT NATIONAL DES SCIENCES APPLIQUÉES** [FR/FR]; 135 Avenue de Rangueil, 31400 Toulouse (FR). **CENTRE NATIONAL DE LA RECHERCHE SCIENTIFIQUE (CNRS)** [FR/FR]; 3, Rue Michel Ange, 75016 Paris (FR). **UNIVERSITÉ PAUL SABATIER TOULOUSE III** [FR/FR]; 118 route de Narbonne, 31400 Toulouse (FR).

(72) Inventors: **GIGOUX, Véronique**; INSERM ERL1226, Réceptologie et ciblage thérapeutique en cancérologie (RCTC), 1 avenue Jean Poulhès, 31432 Toulouse cedex 4 (FR). **CLERC, Pascal**; INSERM ERL1226, Réceptologie et ciblage thérapeutique en cancérologie (RCTC), 1 avenue Jean Poulhès, 31432 Toulouse cedex 4 (FR). **FOURMY, Daniel**; INSERM ERL1226, Réceptologie et ciblage thérapeutique en cancérologie (RCTC), 1 avenue Jean Poulhès, 31432 Toulouse cedex 4 (FR). **CARREY, Julian**; LPCNO, 135 Avenue de Rangueil, 31077 Toulouse (FR).

(74) Agent: **INSERM TRANSFERT**; 7 rue Watt, 75013 Paris (FR).

(81) Designated States *(unless otherwise indicated, for every kind of national protection available)*: AE, AG, AL, AM, AO, AT, AU, AZ, BA, BB, BG, BH, BN, BR, BW, BY, BZ, CA, CH, CL, CN, CO, CR, CU, CZ, DE, DJ, DK, DM, DO, DZ, EC, EE, EG, ES, FI, GB, GD, GE, GH, GM, GT, HN, HR, HU, ID, IL, IN, IR, IS, JO, JP, KE, KG, KH, KN, KP, KR, KW, KZ, LA, LC, LK, LR, LS, LU, LY, MA, MD, ME, MG, MK, MN, MW, MX, MY, MZ, NA, NG, NI, NO, NZ, OM, PA, PE, PG, PH, PL, PT, QA, RO, RS, RU, RW, SA, SC, SD, SE, SG, SK, SL, SM, ST, SV, SY, TH, TJ, TM, TN, TR, TT, TZ, UA, UG, US, UZ, VC, VN, ZA, ZM, ZW.

(84) Designated States *(unless otherwise indicated, for every kind of regional protection available)*: ARIPO (BW, GH, GM, KE, LR, LS, MW, MZ, NA, RW, SD, SL, ST, SZ, TZ, UG, ZM, ZW), Eurasian (AM, AZ, BY, KG, KZ, RU, TJ, TM), European (AL, AT, BE, BG, CH, CY, CZ, DE, DK, EE, ES, FI, FR, GB, GR, HR, HU, IE, IS, IT, LT, LU, LV, MC, MK, MT, NL, NO, PL, PT, RO, RS, SE, SI, SK, SM, TR), OAPI (BF, BJ, CF, CG, CI, CM, GA, GN, GQ, GW, KM, ML, MR, NE, SN, TD, TG).

Published:
— *with international search report (Art. 21(3))*

(54) Title: MAGNETIC NANOPARTICLES FOR THE TREATMENT OF CANCER

(57) Abstract: The present invention relates to methods and pharmaceutical compositions for the treatment of cancer in a subject in need thereof. Therapeutic strategies using drugs which cause Lysosomal Cell Death have been proposed for eradication of resistant cancer cells. Nanotherapy based on Magnetic Intra-Lysosomal Hyperthermia (MILH) generated by magnetic nanoparticles (MNPs) that are grafted with ligands of receptors overexpressed in tumors appears to be a very promising therapeutic option. The inventors investigated the mechanisms whereby MILH induces cell death using Gastrin-grafted MNPs specifically delivered to lysosomes of tumor cells from different cancers. The inventors provide evidences that MILH causes cell death through a non-apoptotic signaling pathway. The mechanism of cell death involves temperature elevation at the nanoparticle periphery which enhances the production of reactive oxygen species through the lysosomal Fenton reaction. Subsequently, MILH induces lipid peroxidation, lysosomal membrane permeabilization and leakage of lysosomal enzymes into the cytosol, including Cathepsin-B which activates Caspase-1 but not apoptotic Caspase-3. Thus, the invention relates to a magnetic nanoparticle grafted with a tumor targeting agent for use in a method for inducing non-apoptotic signaling of cancer cell in a subject afflicted with cancer in need thereof.

WO 2019/072885 A1

MAGNETIC NANOPARTICLES FOR THE TREATMENT OF CANCER

FIELD OF THE INVENTION:

The present invention relates to methods and pharmaceutical compositions for the treatment of cancer in a subject in need thereof.

BACKGROUND OF THE INVENTION:

Cancer is a leading cause of death with millions of new people diagnosed with cancer every year. One major reason that limits outcome and drug response of anti-cancer therapies is multidrug resistance (1). However, recent studies have shown that cancer cells resistant to traditional therapies can be sensitive to agents which induce lysosomal cell death through lysosome membrane permeabilization (LMP) (2). In fact, LMP can be triggered by a wide variety of stimuli including death ligands, oxidative stress and treatment by lysosomotropic agents (3). In some circumstances (i.e. treatment by lysosomotropic agents), LMP appears to be an early event triggering apoptosis whereas in others (i.e. treatment by death ligands), LMP results from the activation of apoptosis signaling pathways and contributes to the amplification of death signals.

Alternatively to these above agents, we (4) and others (5,6) have recently proposed that magnetic intra-lysosomal hyperthermia (termed MILH), induced by application of a high frequency alternating magnetic field (AMF) to cells containing magnetic nanoparticles (MNPs) in their lysosomes, is an effective way to specifically trigger lysosomal cell death in cancer cells (7). This is the result of the heat released by MNPs when exposed to AMF. Moreover, MNPs offer the potential to be driven into lysosomes of tumor cells by grafting them with ligands or antibodies that recognize receptors overexpressed in tumors. Subsequently to their activation, receptors are internalized together with ligand-grafted MNPs and traffic to lysosomes (4,5). Using this strategy, we showed that minute amounts of iron oxide MNPs targeting gastrin receptors (CCK2R), overexpressed in most endocrine tumors, caused the death of cancer cells upon AMF exposure, making this approach an attractive therapeutic option (4,8). Strikingly, in this study, as in others, no perceptible temperature rise in the cell medium occurred during AMF exposure (4-6). Thus, MILH differs from standard magnetic hyperthermia whereby tumor eradication is achieved with large doses of MNPs which cause a temperature elevation of the whole tumor (9). In MILH, it is expected that MNPs, even of low heating power (Specific Absorption Rate), generate a local temperature rise causing LMP (4-6,10). In spite of this recent

proof-of-concept, the precise mechanisms leading to cell death by MILH remains largely unknown. Insight into these mechanisms is essential to optimize this approach in a therapeutic perspective.

To date, molecular mechanisms of lysosomal cell death of epithelial cells were mainly elucidated using lysosomotropic agents or death ligands which do not exclusively target lysosomes of cancer cells (11-13). Lysosomal cell death through apoptosis was demonstrated to involve the release of lysosomal hydrolases into the cytosol, especially Cathepsin-D and Cathepsin-B (CathB) which digest apoptosis-regulated proteins, leading to mitochondrial outer membrane permeabilization (MOMP) and apoptotic caspases activation (3,14).

The inventors investigated the cellular and molecular mechanisms involved in cancer cell death induced by MILH. Here, the inventors report that, under an AMF, lysosome-accumulated MNPs enhanced reactive oxygen species (ROS) production through the Fenton reaction within lysosomes causing lipid peroxidation of lysosome membrane, LMP and subsequent cell death by a non-conventional mechanism which is dependent of Caspase-1 and CathB but independent of apoptotic Caspase-3. These major advances in the understanding of the cell death mechanism occurring during MILH will facilitate optimization of the strategy in a therapeutic perspective.

SUMMARY OF THE INVENTION:

The present invention relates to methods and pharmaceutical compositions for the treatment of cancer in a subject in need thereof.

DETAILED DESCRIPTION OF THE INVENTION:

Therapeutic strategies using drugs which cause Lysosomal Cell Death have been proposed for eradication of resistant cancer cells. In this context, nanotherapy based on Magnetic Intra-Lysosomal Hyperthermia (MILH) generated by magnetic nanoparticles (MNPs) that are grafted with ligands of receptors overexpressed in tumors appears to be a very promising therapeutic option. However, mechanisms whereby MILH induces cell death are still elusive. Herein, using Gastrin-grafted MNPs specifically delivered to lysosomes of tumor cells from different cancers, the inventors provide evidences that MILH causes cell death through a non-apoptotic signaling pathway. The mechanism of cell death involves temperature elevation at the nanoparticle periphery which enhances the production of reactive oxygen species through the lysosomal Fenton reaction. Subsequently, MILH induces lipid peroxidation, lysosomal membrane permeabilization and leakage of lysosomal enzymes into the cytosol, including Cathepsin-B which activates Caspase-1 but not apoptotic Caspase-3. These data highlight the clear potential of MILH for the eradication of tumors overexpressing receptors.

Accordingly, the present invention relates to a magnetic nanoparticle grafted with a tumor targeting agent for use in a method for inducing non-apoptotic signaling of cancer cell in a subject afflicted with cancer in need thereof.

In a particular embodiment, the invention relates to a magnetic nanoparticle grafted with a tumor targeting agent and application of a high frequency alternating magnetic field (AMF) for use in a method for inducing non-apoptotic signaling of cancer cell in a subject afflicted with cancer in need thereof.

In some embodiments, the present invention relates to the magnetic nanoparticle grafted with a tumor targeting agent for use in a method for inducing non-apoptotic signaling of resistant cancer cell in a subject afflicted with cancer in need thereof.

In some embodiments, the present invention relates to the magnetic nanoparticle grafted with a tumor targeting agent for use in the treatment of cancer by inducing non-apoptotic signaling of cancer cell in a subject in need thereof.

As used herein, the term “subject” denotes a mammal. Typically, a subject according to the invention refers to any subject (preferably human) afflicted with or susceptible to be afflicted with a cancer. Typically, a subject according to the invention refers to any subject (preferably human) afflicted with or susceptible to be afflicted with a pancreatic endocrine cancer, pancreatic exocrine cancer or gastric cancer.

As used herein, the term "cancer" has its general meaning in the art and includes, but is not limited to, solid tumors and blood borne tumors. The term cancer includes diseases of the skin, tissues, organs, bone, cartilage, blood and vessels. The term "cancer" further encompasses both primary and metastatic cancers. Examples of cancers that may be treated by methods and compositions of the present invention include, but are not limited to, cancer cells from the bladder, blood, bone, bone marrow, brain, breast, colon, esophagus, gastrointestine, gum, head, kidney, liver, lung, nasopharynx, neck, ovary, prostate, skin, stomach, testis, tongue, or uterus. In addition, the cancer may specifically be of the following histological type, though it is not limited to these: neoplasm, malignant; carcinoma; carcinoma, undifferentiated; giant and spindle cell carcinoma; small cell carcinoma; papillary carcinoma; squamous cell carcinoma; lymphoepithelial carcinoma; basal cell carcinoma; pilomatrix carcinoma; transitional cell carcinoma; papillary transitional cell carcinoma; adenocarcinoma; gastrinoma, malignant; cholangiocarcinoma; hepatocellular carcinoma; combined hepatocellular carcinoma and cholangiocarcinoma; trabecular adenocarcinoma; adenoid cystic carcinoma; adenocarcinoma in adenomatous polyp; adenocarcinoma, familial polyposis coli; solid carcinoma; carcinoid tumor, malignant; branchiolo-alveolar adenocarcinoma; papillary adenocarcinoma;

chromophobe carcinoma; acidophil carcinoma; oxyphilic adenocarcinoma; basophil carcinoma; clear cell adenocarcinoma; granular cell carcinoma; follicular adenocarcinoma; papillary and follicular adenocarcinoma; nonencapsulating sclerosing carcinoma; adrenal cortical carcinoma; endometroid carcinoma; skin appendage carcinoma; apocrine adenocarcinoma; sebaceous adenocarcinoma; ceruminous; adenocarcinoma; mucoepidermoid carcinoma; cystadenocarcinoma; papillary cystadenocarcinoma; papillary serous cystadenocarcinoma; mucinous cystadenocarcinoma; mucinous adenocarcinoma; signet ring cell carcinoma; infiltrating duct carcinoma; medullary carcinoma; lobular carcinoma; inflammatory carcinoma; paget's disease, mammary; acinar cell carcinoma; adenosquamous carcinoma; adenocarcinoma w/squamous metaplasia; thymoma, malignant; ovarian stromal tumor, malignant; thecoma, malignant; granulosa cell tumor, malignant; and roblastoma, malignant; Sertoli cell carcinoma; leydig cell tumor, malignant; lipid cell tumor, malignant; paraganglioma, malignant; extra-mammary paraganglioma, malignant; pheochromocytoma; glomangiosarcoma; malignant melanoma; amelanotic melanoma; superficial spreading melanoma; malig melanoma in giant pigmented nevus; epithelioid cell melanoma; blue nevus, malignant; sarcoma; fibrosarcoma; fibrous histiocytoma, malignant; myxosarcoma; liposarcoma; leiomyosarcoma; rhabdomyosarcoma; embryonal rhabdomyosarcoma; alveolar rhabdomyosarcoma; stromal sarcoma; mixed tumor, malignant; mullerian mixed tumor; nephroblastoma; hepatoblastoma; carcinosarcoma; mesenchymoma, malignant; brenner tumor, malignant; phyllodes tumor, malignant; synovial sarcoma; mesothelioma, malignant; dysgerminoma; embryonal carcinoma; teratoma, malignant; struma ovarii, malignant; choriocarcinoma; mesonephroma, malignant; hemangiosarcoma; hemangioendothelioma, malignant; kaposi's sarcoma; hemangiopericytoma, malignant; lymphangiosarcoma; osteosarcoma; juxtacortical osteosarcoma; chondrosarcoma; chondroblastoma, malignant; mesenchymal chondrosarcoma; giant cell tumor of bone; ewing's sarcoma; odontogenic tumor, malignant; ameloblastic odontosarcoma; ameloblastoma, malignant; ameloblastic fibrosarcoma; pinealoma, malignant; chordoma; glioma, malignant; ependymoma; astrocytoma; protoplasmic astrocytoma; fibrillary astrocytoma; astroblastoma; glioblastoma; oligodendroglioma; oligodendroblastoma; primitive neuroectodermal; cerebellar sarcoma; ganglioneuroblastoma; neuroblastoma; retinoblastoma; olfactory neurogenic tumor; meningioma, malignant; neurofibrosarcoma; neurilemmoma, malignant; granular cell tumor, malignant; malignant lymphoma; Hodgkin's disease; Hodgkin's lymphoma; paragranuloma; malignant lymphoma, small lymphocytic; malignant lymphoma, large cell, diffuse; malignant lymphoma, follicular; mycosis fungoides; other specified non-Hodgkin's lymphomas;

malignant histiocytosis; multiple myeloma; mast cell sarcoma; immunoproliferative small intestinal disease; leukemia; lymphoid leukemia; plasma cell leukemia; erythroleukemia; lymphosarcoma cell leukemia; myeloid leukemia; basophilic leukemia; eosinophilic leukemia; monocytic leukemia; mast cell leukemia; megakaryoblastic leukemia; myeloid sarcoma; and hairy cell leukemia.

In some embodiments, the subject suffers from a cancer selected from the group consisting of pancreatic cancer, breast cancer, colon cancer, lung cancer, prostate cancer, testicular cancer, brain cancer, skin cancer, rectal cancer, gastric cancer, esophageal cancer, sarcomas, tracheal cancer, head and neck cancer, liver cancer, ovarian cancer, lymphoid cancer, cervical cancer, vulvar cancer, melanoma, mesothelioma, renal cancer, bladder cancer, thyroid cancer, bone cancers, carcinomas, sarcomas, and soft tissue cancers.

In some embodiments, the subject suffers from cancer resistant to anti-cancer treatment.

As used herein, the term “cancer resistant to anti-cancer treatment” denotes cancer resistant to conventional treatments like chemotherapy and/or immunotherapy.

As used herein, the term "treatment" or "treat" refer to both prophylactic or preventive treatment as well as curative or disease modifying treatment, including treatment of subjects at risk of contracting the disease or suspected to have contracted the disease as well as subjects who are ill or have been diagnosed as suffering from a disease or medical condition, and includes suppression of clinical relapse. The treatment may be administered to a subject having a medical disorder or who ultimately may acquire the disorder, in order to prevent, cure, delay the onset of, reduce the severity of, or ameliorate one or more symptoms of a disorder or recurring disorder, or in order to prolong the survival of a subject beyond that expected in the absence of such treatment. By "therapeutic regimen" is meant the pattern of treatment of an illness, e.g., the pattern of dosing used during therapy. A therapeutic regimen may include an induction regimen and a maintenance regimen. The phrase "induction regimen" or "induction period" refers to a therapeutic regimen (or the portion of a therapeutic regimen) that is used for the initial treatment of a disease. The general goal of an induction regimen is to provide a high level of drug to a subject during the initial period of a treatment regimen. An induction regimen may employ (in part or in whole) a "loading regimen", which may include administering a greater dose of the drug than a physician would employ during a maintenance regimen, administering a drug more frequently than a physician would administer the drug during a maintenance regimen, or both. The phrase "maintenance regimen" or "maintenance period" refers to a therapeutic regimen (or the portion of a therapeutic regimen) that is used for the maintenance of a subject during treatment of an illness, e.g., to keep the subject in remission

for long periods of time (months or years). A maintenance regimen may employ continuous therapy (e.g., administering a drug at a regular intervals, e.g., weekly, monthly, yearly, etc.) or intermittent therapy (e.g., interrupted treatment, intermittent treatment, treatment at relapse, or treatment upon achievement of a particular predetermined criteria [e.g., disease manifestation, etc.]).

The term "magnetic nanoparticle" or "MNP" has its general meaning in the art and refers to magnetic nanoparticle used in nanotherapy by inducing Magnetic Intra-Lysosomal Hyperthermia (MILH). The term "magnetic nanoparticle" also refers to magnetic nanoparticle inducing Lysosomal Cell Death. The term "magnetic nanoparticle" also refers to iron oxide magnetic nanoparticles (MNPs) but not limited to iron oxide magnetic nanoparticles (MNPs) coated with PEG-COOH and iron oxide magnetic nanoparticles (MNPs) coated with PEG-amine. The term "magnetic nanoparticle" also refers to iron oxide magnetic nanoparticles (MNPs) coated with PEG-Amine such as described in the example. The term "magnetic nanoparticle" also refers to magnetic nanoparticle comprised an iron-oxide core such as magnetite-Fe_3O_4 or maghemite-γ-Fe_2O_3 and magnetic nanoparticle such as described in WO2012078745; Sanchez *et al.*, 2014; Domenech *et al.*, 2013; Creixell *et al.*, 2011; Fourmy *et al.*, 2015; Silva *et al.*, 2011; Cole *et al.*, 2011; Kim *et al.,* 2012; Yang *et al.,* 2012.

The term "tumor targeting agent" has its general meaning in the art and refers to ligand of receptor overexpressed or specifically expressed in cancer cell. The term "tumor targeting agent" also refers to ligands, agents or antibodies interacting with tumor membrane-bound and intracellular targets overexpressed or specifically expressed in cancer cell. Tumor targeting agent include but are not limited to gastrin, the ligand of gastrin receptors (CCK2R), antibodies directed against the EDB domain of fibronectin, antibodies or agents binding Vascular endothelial growth factor receptor 2, antibodies or molecules binding fibroblast growth factor receptor-1, antibodies or agents that interact with CD31, antibodies or agents interacting with tumor lymphatic endothelium (Podoplanin, Lyve-1), or antibodies or agents binding to $\alpha V\beta 3$ integrin such as RGD peptides.

In some embodiments, the "tumor tageting agent" is gastrin, the ligand of gastrin receptors (CCK2R) overexpressed in pancreatic endocrine cancer cells.

The term "non-apoptotic signaling" has its general meaning in the art and refers to non-apoptotic cell death. The term "non-apoptotic signaling" also refers to cell death by the non-conventional mechanism which is dependent of Caspase-1 and Cathepsin B but independent of apoptotic Caspase-3.

In a further aspect, the present invention relates to the magnetic nanoparticle grafted with a tumor targeting agent according to the invention in combination with one or more compound selected from the group consisting of:

Compound inducing iron excess or iron enrichment (such as FeCl3, transferrin),

Compound increasing the acidification of the lysosomal pH (such as Artesunate, activator of ATPase proton pump),

HSP70 inhibitor,

Cathepsin-B activator, and

Caspase-1 activator,

for use in the treatment of cancer in a subject in need thereof.

In a further aspect, the present invention relates to the magnetic nanoparticle grafted with a tumor targeting agent according to the invention in combination with one or more compound selected from the group consisting of:

Compound inducing iron excess or iron enrichment (such as transferrin),

Compound increasing the acidification of the lysosomal pH (such as Artesunate, activator of ATPase proton pump),

HSP70 inhibitor,

Cathepsin-B activator, and

Caspase-1 activator,

for use in a method for inducing non-apoptotic signaling and/or inducing a signaling death pathway of cancer cell in a subject afflicted with cancer in need thereof.

The term "Compound inducing iron excess or iron enrichment" has its general meaning in the art and refers to compound inducing iron overload such as transferrin, ferrous sulphate such as Ferrosanol®, FeCl3, and iron composition for iron-enriched diet.

The term "Compound increasing the acidification of the lysosomal pH" has its general meaning in the art and refers to compounds reducing lysosomal pH such as Artesunate, activator of ATPase proton pump, epinephrine, norepinephrine, cAMP (Cyclic adenosine monophosphate), β-adrenergic receptor agonist such as isoproterenol, adenosine receptor agonist 5'-(N-ethylcarboxamido)-adenosine (NECA), A2A adenosine receptors agonist such as CGS21680, cell-permeable analogues chlorophenylthio-cAMP (cpt-cAMP) and 8-bromo-cAMP, 3-isobutyl-1-methylxanthine (IBMX) and forskolin such as described in Liu *et al.,* 2008 and WO2012149285.

The term "HSP70" has its general meaning in the art and refers to the heat shock protein 70 involved in assisting protein folding, preventing protein aggregation and transporting

proteins across membranes (Li *et al.,* 2016; Assimon *et al.,* 2013; Reikvam *et al.,* 2014; Patury *et al.,* 2009).

The term "HSP70 inhibitor" has its general meaning in the art and refers to a compound that selectively blocks or inactivates the HSP70. The term "HSP70 inhibitor" also refers to a compound that selectively blocks the binding of HSP70 to its molecular chaperones (such as HSP40 (DNAJ) (Heat shock protein 40); Auxilin (DNAJ6); HSP110 (HSPH) Heat shock protein 110; BAG (Bcl-2-associated athanogene); GrpE; Bap; HIP HSP70-interacting protein; CHIP (Carboxyl terminus of HSP70-interacting protein); HOP (HSP70/HSP90-organizing protein); and Tom70 (Translocases of outer membrane 70). The term "HSP70 inhibitor" also refers to a compound able to prevent the action of HSP70 for example by inhibiting the activity of HSP70 or the HSP70 chaperone pathway. As used herein, the term "selectively blocks or inactivates" refers to a compound that preferentially binds to and blocks or inactivates HSP70 with a greater affinity and potency, respectively, than its interaction with the other sub-types of the HSP family. Compounds that block or inactivate HSP70, but that may also block or inactivate other HSP sub-types, as partial or full inhibitors, are contemplated. The term "HSP70 inhibitor" also refers to a compound that inhibits HSP70 expression. Typically, a HSP70 inhibitor is a small organic molecule, a polypeptide, an aptamer, an antibody, intra-antibody, an oligonucleotide, a ribozyme or a CRISPR.

The HSP70 inhibitors are well-known in the art as illustrated by Li *et al.,* 2016; Assimon *et al.,* 2013; Reikvam *et al.,* 2014; Patury *et al.,* 2009; WO2015130922; and US20150025052.

In one embodiment of the invention, the HSP70 inhibitor is selected from the group consisting of inhibitors of the N-terminal ATP-binding domain such as MKT-077, YM-1, VER-155008, NSC 630668, MAL3-101, MAL2-11B, Apoptozole, Myricetin; inhibitors of the C-terminal peptide-binding domain such as 2-phenylethynesulfonamide/Pifithrin-μ (PES), ADD70; Inhibitory blocking antibodies such as cmHSP70.1 mAb; Inhibitors of HSF-1 such as Quercetin, KNK437, Triptolide, KRIBB11; inhibitors of the HSP40 co-chaperone such as Phenoxy-N-arylacetamides (Reikvam et al., 2014; Li et al., 2016; Patury et al., 2009); YK5 (Li et al., 2016); epigallocatechin gallate (EGCG); Sulfoglycolipids; Dihydropyrimidines; Geranylgeranyl acetone (GGA); Acyl benzamides; Spergualin Derivatives (Patury et al., 2009); 2-Phenylethynesulfonamide (PES), biotinylated PES analog (B-PES), chlorinated derivative, 2-(3-chlorophenyl) ethynesulfonamide (PES-Cl) (WO2010/033771; US2011/0189125); capsaicin and capsaicinoids (US20150025052); and compounds such as described in Li *et al.,* 2016; Assimon *et al.,* 2013; Reikvam *et al.,* 2014; Patury *et al.,* 2009; WO2015130922; US20150025052).

In one embodiment, the HSP70 inhibitor of the invention is a HSP70 expression inhibitor.

The term "expression" when used in the context of expression of a gene or nucleic acid refers to the conversion of the information, contained in a gene, into a gene product. A gene product can be the direct transcriptional product of a gene (e.g., mRNA, tRNA, rRNA, antisense RNA, ribozyme, structural RNA or any other type of RNA) or a protein produced by translation of a mRNA. Gene products also include messenger RNAs, which are modified, by processes such as capping, polyadenylation, methylation, and editing, and proteins (e.g., HSP70) modified by, for example, methylation, acetylation, phosphorylation, ubiquitination, SUMOylation, ADP-ribosylation, myristilation, and glycosylation.

An "inhibitor of expression" refers to a natural or synthetic compound that has a biological effect to inhibit the expression of a gene.

HSP70 expression inhibitors for use in the present invention may be based on antisense oligonucleotide constructs. Anti-sense oligonucleotides, including anti-sense RNA molecules and anti-sense DNA molecules, would act to directly block the translation of HSP70 mRNA by binding thereto and thus preventing protein translation or increasing mRNA degradation, thus decreasing the level of HSP70 proteins, and thus activity, in a cell. For example, antisense oligonucleotides of at least about 15 bases and complementary to unique regions of the mRNA transcript sequence encoding HSP70 can be synthesized, e.g., by conventional phosphodiester techniques and administered by e.g., intravenous injection or infusion. Methods for using antisense techniques for specifically alleviating gene expression of genes whose sequence is known are well known in the art (e.g. see U.S. Pat. Nos. 6,566,135; 6,566,131; 6,365,354; 6,410,323; 6,107,091; 6,046,321; and 5,981,732).

Small inhibitory RNAs (siRNAs) can also function as expression inhibitors for use in the present invention. Gene expression can be reduced by contacting the subject or cell with a small double stranded RNA (dsRNA), or a vector or construct causing the production of a small double stranded RNA, such that HSP70 expression is specifically inhibited (i.e. RNA interference or RNAi). Methods for selecting an appropriate dsRNA or dsRNA-encoding vector are well known in the art for genes whose sequence is known (e.g. see Tuschl, T. et al. (1999); Elbashir, S. M. et al. (2001); Hannon, GJ. (2002); McManus, MT. et al. (2002); Brummelkamp, TR. et al. (2002); U.S. Pat. Nos. 6,573,099 and 6,506,559; and International Patent Publication Nos. WO 01/36646, WO 99/32619, and WO 01/68836).

Ribozymes can also function as expression inhibitors for use in the present invention. Ribozymes are enzymatic RNA molecules capable of catalyzing the specific cleavage of RNA.

The mechanism of ribozyme action involves sequence specific hybridization of the ribozyme molecule to complementary target RNA, followed by endonucleolytic cleavage. Engineered hairpin or hammerhead motif ribozyme molecules that specifically and efficiently catalyze endonucleolytic cleavage of mRNA sequences are thereby useful within the scope of the present invention. Specific ribozyme cleavage sites within any potential RNA target are initially identified by scanning the target molecule for ribozyme cleavage sites, which typically include the following sequences, GUA, GUU, and GUC. Once identified, short RNA sequences of between about 15 and 20 ribonucleotides corresponding to the region of the target gene containing the cleavage site can be evaluated for predicted structural features, such as secondary structure, that can render the oligonucleotide sequence unsuitable. The suitability of candidate targets can also be evaluated by testing their accessibility to hybridization with complementary oligonucleotides, using, e.g., ribonuclease protection assays.

Both antisense oligonucleotides and ribozymes useful as HSP70 inhibitors can be prepared by known methods. These include techniques for chemical synthesis such as, e.g., by solid phase phosphoramadite chemical synthesis. Alternatively, anti-sense RNA molecules can be generated by in vitro or in vivo transcription of DNA sequences encoding the RNA molecule. Such DNA sequences can be incorporated into a wide variety of vectors that incorporate suitable RNA polymerase promoters such as the T7 or SP6 polymerase promoters. Various modifications to the oligonucleotides of the invention can be introduced as a means of increasing intracellular stability and half-life. Possible modifications include but are not limited to the addition of flanking sequences of ribonucleotides or deoxyribonucleotides to the 5' and/or 3' ends of the molecule, or the use of phosphorothioate or 2'-O-methyl rather than phosphodiesterase linkages within the oligonucleotide backbone.

Antisense oligonucleotides siRNAs and ribozymes of the invention may be delivered in vivo alone or in association with a vector. In its broadest sense, a "vector" is any vehicle capable of facilitating the transfer of the antisense oligonucleotide siRNA or ribozyme nucleic acid to the cells and preferably cells expressing HSP70. Preferably, the vector transports the nucleic acid to cells with reduced degradation relative to the extent of degradation that would result in the absence of the vector. In general, the vectors useful in the invention include, but are not limited to, plasmids, phagemids, viruses, other vehicles derived from viral or bacterial sources that have been manipulated by the insertion or incorporation of the antisense oligonucleotide siRNA or ribozyme nucleic acid sequences. Viral vectors are a preferred type of vector and include, but are not limited to nucleic acid sequences from the following viruses: retrovirus, such as moloney murine leukemia virus, harvey murine sarcoma virus, murine mammary tumor

virus, and rouse sarcoma virus; adenovirus, adeno-associated virus; SV40-type viruses; polyoma viruses; Epstein-Barr viruses; papilloma viruses; herpes virus; vaccinia virus; polio virus; and RNA virus such as a retrovirus. One can readily employ other vectors not named but known to the art.

Preferred viral vectors are based on non-cytopathic eukaryotic viruses in which non-essential genes have been replaced with the gene of interest. Non-cytopathic viruses include retroviruses (e.g., lentivirus), the life cycle of which involves reverse transcription of genomic viral RNA into DNA with subsequent proviral integration into host cellular DNA. Retroviruses have been approved for human gene therapy trials. Most useful are those retroviruses that are replication-deficient (i.e., capable of directing synthesis of the desired proteins, but incapable of manufacturing an infectious particle). Such genetically altered retroviral expression vectors have general utility for the high-efficiency transduction of genes in vivo. Standard protocols for producing replication-deficient retroviruses (including the steps of incorporation of exogenous genetic material into a plasmid, transfection of a packaging cell lined with plasmid, production of recombinant retroviruses by the packaging cell line, collection of viral particles from tissue culture media, and infection of the target cells with viral particles) are provided in KRIEGLER (A Laboratory Manual," W.H. Freeman C.O., New York, 1990) and in MURRY ("Methods in Molecular Biology," vol.7, Humana Press, Inc., Cliffton, N.J., 1991).

Preferred viruses for certain applications are the adeno-viruses and adeno-associated viruses, which are double-stranded DNA viruses that have already been approved for human use in gene therapy. The adeno-associated virus can be engineered to be replication deficient and is capable of infecting a wide range of cell types and species. It further has advantages such as, heat and lipid solvent stability; high transduction frequencies in cells of diverse lineages, including hemopoietic cells; and lack of superinfection inhibition thus allowing multiple series of transductions. Reportedly, the adeno-associated virus can integrate into human cellular DNA in a site-specific manner, thereby minimizing the possibility of insertional mutagenesis and variability of inserted gene expression characteristic of retroviral infection. In addition, wild-type adeno-associated virus infections have been followed in tissue culture for greater than 100 passages in the absence of selective pressure, implying that the adeno-associated virus genomic integration is a relatively stable event. The adeno-associated virus can also function in an extrachromosomal fashion.

Other vectors include plasmid vectors. Plasmid vectors have been extensively described in the art and are well known to those of skill in the art. See e.g., SANBROOK et al., "Molecular Cloning: A Laboratory Manual," Second Edition, Cold Spring Harbor Laboratory Press, 1989.

In the last few years, plasmid vectors have been used as DNA vaccines for delivering antigen-encoding genes to cells in vivo. They are particularly advantageous for this because they do not have the same safety concerns as with many of the viral vectors. These plasmids, however, having a promoter compatible with the host cell, can express a peptide from a gene operatively encoded within the plasmid. Some commonly used plasmids include pBR322, pUC18, pUCl9, pRC/CMV, SV40, and pBlueScript. Other plasmids are well known to those of ordinary skill in the art. Additionally, plasmids may be custom designed using restriction enzymes and ligation reactions to remove and add specific fragments of DNA. Plasmids may be delivered by a variety of parenteral, mucosal and topical routes. For example, the DNA plasmid can be injected by intramuscular, intradermal, subcutaneous, or other routes. It may also be administered by intranasal sprays or drops, rectal suppository and orally. It may also be administered into the epidermis or a mucosal surface using a gene-gun. The plasmids may be given in an aqueous solution, dried onto gold particles or in association with another DNA delivery system including but not limited to liposomes, dendrimers, cochleate and microencapsulation.

In one embodiment of the invention, HSP70 expression inhibitors include but are not limited to siRNAs and compounds such as described in Patury et al., 2009; Reikvam et al., 2014; Guo et al., 2005.

The term "Cathepsin-B" has its general meaning in the art and refers to a lysosomal cysteine protease linked to general protein turnover in lysosomes (Aggarwal and Sloane, 2014).

The term "Cathepsin-B activator" refers to any compound that can directly or indirectly stimulate the signal transduction cascade related to the Cathepsin-B. The term "Cathepsin-B activator" also refers to a compound that selectively activates the Cathepsin-B. As used herein, the term "selectively activates" refers to a compound that preferentially binds to and activates Cathepsin-B with a greater affinity and potency, respectively, than its interaction with the other sub-types or isoforms of the Cathepsin family. Compounds that prefer Cathepsin-B, but that may also activate other Cathepsin sub-types, as partial or full activators, and thus that may have multiple Cathepsin activities, are contemplated. Typically, a Cathepsin-B activator is a small organic molecule or a peptide. Typically, a Cathepsin-B activator is a small organic molecule, a peptide, a modified Cathepsin-B or an activator of Cathepsin-B expression.

In one embodiment of the invention, the Cathepsin-B activator is selected from the group consisting of Compounds described in CN106220735; WO2005060663.

The term "Caspase-1" has its general meaning in the art and refers to a cysteine protease implicated in cell death by pyroptosis, known to occur in cells of the immune system during

inflammatory processes. The term "Caspase-1" also refers to caspase implicated in apoptosis and non-apoptotic cell death pathway (32; 44-49).

The term "Caspase-1 activator" refers to any compound that can directly or indirectly stimulate the signal transduction cascade related to the Caspase-1. The term "Caspase-1 activator" also refers to a compound that selectively activates the Caspase-1. As used herein, the term "selectively activates" refers to a compound that preferentially binds to and activates Caspase-1 with a greater affinity and potency, respectively, than its interaction with the other sub-types or isoforms of the Caspase family. Compounds that prefer Caspase-1, but that may also activate other Cathepsin sub-types, as partial or full activators, and thus that may have multiple Caspase activities, are contemplated. Typically, a Caspase-1 activator is a small organic molecule or a peptide. Typically, a Caspase-1 activator is a small organic molecule, a peptide, a modified Caspase-1 or an activator of Caspase-1 expression.

An "activator of expression" refers to a natural or synthetic compound that has a biological effect to activate the expression of a gene.

In a further aspect, the present invention relates to the magnetic nanoparticle grafted with a tumor targeting agent according to the invention in combination with one or more anti-cancer compound for use in a method for inducing non-apoptotic signaling of cancer cell in a subject afflicted with cancer in need thereof.

In a further aspect, the present invention relates to the magnetic nanoparticle grafted with a tumor targeting agent according to the invention which sensitizes cancer cells to anti-cancer compound.

Accordingly, the present invention relates to the magnetic nanoparticle grafted with a tumor targeting agent according to the invention for use in a method for enhancing therapeutic efficacy of anti-cancer compound such as doxorubicin in a subject in need thereof.

In some embodiment, the present invention relates to the magnetic nanoparticle grafted with a tumor targeting agent according to the invention in combination with doxorubicin for use in a method for inducing non-apoptotic signaling of cancer cell in a subject afflicted with cancer in need thereof.

The term "anti-cancer compound" has its general meaning in the art and refers to compounds used in anti-cancer therapy such as anti-angiogenic compound, tyrosine kinase inhibitors, tyrosine kinase receptor (TKR) inhibitors, Vascular Endothelial Growth Factor Receptors (VEGFRs) pathway inhibitors, interferon therapy, anti-HER2 compounds, anti-EGFR compounds, alkylating agents, anti-metabolites, immunotherapeutic agents, Interferons (IFNs), Interleukins, and chemotherapeutic agents such as described below.

The term "anti-angiogenic compound" has its general meaning in the art and refers to compounds used in anti-angiogenic therapy such as tyrosine kinase inhibitors, anti-angiogenic tyrosine kinase receptor (TKR) inhibitors, anti-angiogenics targeting the Vascular Endothelial Growth Factor Receptors (VEGFRs) pathway such anti-VEGF antibody bevacizumab (Avastin) and VEGF receptor tyrosine kinase inhibitor (TKI) compounds such as sunitinib (Sutent), vandetanib (Zactima), pazopanib (Votrient), sorafenib (Nexavar) and cediranib, interferon therapy and anti-HER2 compounds such as Trastuzumab (herceptin) and pertuzumab. In one embodiment, the term "anti-angiogenic compound" refers to Sunitinib (Sutent), an anti-angiogenic TKR inhibitor of VEGFRs, platelet-derived growth factor receptors (PDGF-Rs), and c-kit.

The term "tyrosine kinase inhibitor" or "TKI" has its general meaning in the art and refers to any of a variety of therapeutic agents or drugs such as compounds inhibiting tyrosine kinase, tyrosine kinase receptor inhibitors (TKRI), EGFR tyrosine kinase inhibitors, EGFR antagonists. The term "tyrosine kinase inhibitor" or "TKI" has its general meaning in the art and refers to any of a variety of therapeutic agents or drugs that act as selective or non-selective inhibitors of receptor and/or non-receptor tyrosine kinases. Tyrosine kinase inhibitors and related compounds are well known in the art and described in U.S Patent Publication 2007/0254295, which is incorporated by reference herein in its entirety. It will be appreciated by one of skill in the art that a compound related to a tyrosine kinase inhibitor will recapitulate the effect of the tyrosine kinase inhibitor, e.g., the related compound will act on a different member of the tyrosine kinase signaling pathway to produce the same effect as would a tyrosine kinase inhibitor of that tyrosine kinase. Examples of tyrosine kinase inhibitors and related compounds suitable for use in methods of embodiments of the present invention include, but are not limited to Erlotinib, sunitinib (Sutent; SU11248), dasatinib (BMS-354825), PP2, BEZ235, saracatinib, gefitinib (Iressa), erlotinib (Tarceva; OSI-1774), lapatinib (GW572016; GW2016), canertinib (CI 1033), semaxinib (SU5416), vatalanib (PTK787/ZK222584), sorafenib (BAY 43-9006), imatinib (Gleevec; STI571), leflunomide (SU101), vandetanib (Zactima; ZD6474), MK-2206 (8-[4-aminocyclobutyl)phenyl]-9-phenyl-1,2,4-triazolo[3,4-f][1,6]naphthyridin-3(2H)-one hydrochloride) derivatives thereof, analogs thereof, and combinations thereof. Additional tyrosine kinase inhibitors and related compounds suitable for use in the present invention are described in, for example, U.S Patent Publication 2007/0254295, U.S. Pat. Nos. 5,618,829, 5,639,757, 5,728,868, 5,804,396, 6,100,254, 6,127,374, 6,245,759, 6,306,874, 6,313,138, 6,316,444, 6,329,380, 6,344,459, 6,420,382, 6,479,512, 6,498,165, 6,544,988, 6,562,818, 6,586,423, 6,586,424, 6,740,665, 6,794,393,

6,875,767, 6,927,293, and 6,958,340, all of which are incorporated by reference herein in their entirety. In certain embodiments, the tyrosine kinase inhibitor is a small molecule kinase inhibitor that has been orally administered and that has been the subject of at least one Phase I clinical trial, more preferably at least one Phase II clinical, even more preferably at least one Phase III clinical trial, and most preferably approved by the FDA for at least one hematological or oncological indication. Examples of such inhibitors include, but are not limited to Erlotinib, Gefitinib, Lapatinib, Canertinib, BMS-599626 (AC-480), Neratinib, KRN-633, CEP-11981, Imatinib, Nilotinib, Dasatinib, AZM-475271, CP-724714, TAK-165, Sunitinib, Vatalanib, CP-547632, Vandetanib, Bosutinib, Lestaurtinib, Tandutinib, Midostaurin, Enzastaurin, AEE-788, Pazopanib, Axitinib, Motasenib, OSI-930, Cediranib, KRN-951, Dovitinib, Seliciclib, SNS-032, PD-0332991, MKC-I (Ro-317453; R-440), Sorafenib, ABT-869, Brivanib (BMS-582664), SU-14813, Telatinib, SU-6668, (TSU-68), L-21649, MLN-8054, AEW-541, and PD-0325901.

EGFR tyrosine kinase inhibitors as used herein include, but are not limited to compounds selected from the group consisting of but not limited to Erlotinib, lapatinib, Rociletinib (CO-1686), gefitinib, Dacomitinib (PF-00299804), Afatanib, Brigatinib (AP26113), WJTOG3405, NEJ002, AZD9291, HM61713, EGF816, ASP 8273, AC 0010. Examples of antibody EGFR inhibitors include Cetuximab, panitumumab, matuzumab, zalutumumab, nimotuzumab, necitumumab, Imgatuzumab (GA201, RO5083945), and ABT-806.

In some embodiments, the MNP and the combination of the present invention is administered sequentially or concomitantly with one or more therapeutic active agent such as chemotherapeutic or radiotherapeutic.

In some embodiments, the MNP and the combination of the present invention is administered with a chemotherapeutic agent. The term "chemotherapeutic agent" refers to chemical compounds that are effective in inhibiting tumor growth. Examples of chemotherapeutic agents include alkylating agents such as thiotepa and cyclosphosphamide; alkyl sulfonates such as busulfan, improsulfan and piposulfan; aziridines such as benzodopa, carboquone, meturedopa, and uredopa; ethylenimines and methylamelamines including altretamine, triethylenemelamine, trietylenephosphoramide, triethylenethiophosphaorarnide and trimethylolomelamine; acetogenins (especially bullatacin and bullatacinone); a carnptothecin (including the synthetic analogue topotecan); bryostatin; callystatin; CC-1065 (including its adozelesin, carzelesin and bizelesin synthetic analogues); cryptophycins (particularly cryptophycin 1 and cryptophycin 8); dolastatin; duocarmycin (including the

synthetic analogues, KW-2189 and CBI-TMI); eleutherobin; pancratistatin; a sarcodictyin; spongistatin; nitrogen mustards such as chlorambucil, chlornaphazine, cholophosphamide, estrarnustine, ifosfamide, mechlorethamine, mechlorethamine oxide hydrochloride, melphalan, novembichin, phenesterine, prednimustine, trofosfamide, uracil mustard; nitrosureas such as carmustine, chlorozotocin, fotemustine, lomustine, nimustine, ranimustine; antibiotics such as the enediyne antibiotics (e.g. calicheamicin, especially calicheamicin (11 and calicheamicin 211, see, e.g., Agnew Chem Intl. Ed. Engl. 33:183-186 (1994); dynemicin, including dynemicin A; an esperamicin; as well as neocarzinostatin chromophore and related chromoprotein enediyne antiobiotic chromomophores), aclacinomysins, actinomycin, authramycin, azaserine, bleomycins, cactinomycin, carabicin, canninomycin, carzinophilin, chromomycins, dactinomycin, daunorubicin, detorubicin, 6-diazo-5-oxo-L-norleucine, doxorubicin (including morpholino-doxorubicin, cyanomorpholino-doxorubicin, 2-pyrrolino-doxorubicin and deoxydoxorubicin), epirubicin, esorubicin, idanrbicin, marcellomycin, mitomycins, mycophenolic acid, nogalarnycin, olivomycins, peplomycin, potfiromycin, puromycin, quelamycin, rodorubicin, streptomgrin, streptozocin, tubercidin, ubenimex, zinostatin, zorubicin; anti-metabolites such as methotrexate and 5-fluorouracil (5-FU); folic acid analogues such as denopterin, methotrexate, pteropterin, trimetrexate; purine analogs such as fludarabine, 6-mercaptopurine, thiamiprine, thioguanine; pyrimidine analogs such as ancitabine, azacitidine, 6-azauridine, carmofur, cytarabine, dideoxyuridine, doxifluridine, enocitabine, floxuridine, 5-FU; androgens such as calusterone, dromostanolone propionate, epitiostanol, mepitiostane, testolactone; anti-adrenals such as aminoglutethimide, mitotane, trilostane; folic acid replenisher such as frolinic acid; aceglatone; aldophospharnide glycoside; aminolevulinic acid; amsacrine; bestrabucil; bisantrene; edatraxate; defofamine; demecolcine; diaziquone; elfornithine; elliptinium acetate; an epothilone; etoglucid; gallium nitrate; hydroxyurea; lentinan; lonidamine; maytansinoids such as maytansine and ansamitocins; mitoguazone; mitoxantrone; mopidamol; nitracrine; pentostatin; phenamet; pirarubicin; podophyllinic acid; 2-ethylhydrazide; procarbazine; PSK®; razoxane; rhizoxin; sizofiran; spirogennanium; tenuazonic acid; triaziquone; 2,2',2"-trichlorotriethylarnine; trichothecenes (especially T-2 toxin, verracurin A, roridinA and anguidine); urethan; vindesine; dacarbazine; mannomustine; mitobromtol; mitolactol; pipobroman; gacytosine; arabinoside ("Ara-C"); cyclophosphamide; thiotepa; taxoids, e.g. paclitaxel (TAXOL®, Bristol-Myers Squibb Oncology, Princeton, N.].) and doxetaxel (TAXOTERE®, Rhone-Poulenc Rorer, Antony, France); chlorambucil; gemcitabine; 6-thioguanine; mercaptopurine; methotrexate; platinum analogs such as cisplatin and carboplatin; vinblastine; platinum; etoposide (VP-16); ifosfamide;

mitomycin C; mitoxantrone; vincristine; vinorelbine; navelbine; novantrone; teniposide; daunomycin; aminopterin; xeloda; ibandronate; CPT-1 1 ; topoisomerase inhibitor RFS 2000; difluoromethylornithine (DMFO); retinoic acid; capecitabine; and pharmaceutically acceptable salts, acids or derivatives of any of the above. Also included in this definition are antihormonal agents that act to regulate or inhibit hormone action on tumors such as anti-estrogens including for example tamoxifen, raloxifene, aromatase inhibiting 4(5)-imidazoles, 4-hydroxytamoxifen, trioxifene, keoxifene, LY117018, onapristone, and toremifene (Fareston); and anti-androgens such as flutamide, nilutamide, bicalutamide, leuprolide, and goserelin; and phannaceutically acceptable salts, acids or derivatives of any of the above.

In some embodiments, the MNP and the combination of the present invention is administered with a targeted cancer therapy. Targeted cancer therapies are drugs or other substances that block the growth and spread of cancer by interfering with specific molecules ("molecular targets") that are involved in the growth, progression, and spread of cancer. Targeted cancer therapies are sometimes called "molecularly targeted drugs", "molecularly targeted therapies", "precision medicines", or similar names. In some embodiments, the targeted therapy consists of administering the subject with a tyrosine kinase inhibitor as defined above.

In some embodiments, the MNP and the combination of the present invention is administered with an immunotherapeutic agent. The term "immunotherapeutic agent," as used herein, refers to a compound, composition or treatment that indirectly or directly enhances, stimulates or increases the body's immune response against cancer cells and/or that decreases the side effects of other anticancer therapies. Immunotherapy is thus a therapy that directly or indirectly stimulates or enhances the immune system's responses to cancer cells and/or lessens the side effects that may have been caused by other anti-cancer agents. Immunotherapy is also referred to in the art as immunologic therapy, biological therapy biological response modifier therapy and biotherapy. Examples of common immunotherapeutic agents known in the art include, but are not limited to, cytokines, cancer vaccines, monoclonal antibodies and non-cytokine adjuvants. Alternatively the immunotherapeutic treatment may consist of administering the subject with an amount of immune cells (T cells, NK, cells, dendritic cells, B cells…). Immunotherapeutic agents can be non-specific, i.e. boost the immune system generally so that the human body becomes more effective in fighting the growth and/or spread of cancer cells, or they can be specific, i.e. targeted to the cancer cells themselves immunotherapy regimens may combine the use of non-specific and specific immunotherapeutic agents. Non-specific immunotherapeutic agents are substances that stimulate or indirectly improve the immune system. Non-specific immunotherapeutic agents have been used alone as a main

therapy for the treatment of cancer, as well as in addition to a main therapy, in which case the non-specific immunotherapeutic agent functions as an adjuvant to enhance the effectiveness of other therapies (e.g. cancer vaccines). Non-specific immunotherapeutic agents can also function in this latter context to reduce the side effects of other therapies, for example, bone marrow suppression induced by certain chemotherapeutic agents. Non-specific immunotherapeutic agents can act on key immune system cells and cause secondary responses, such as increased production of cytokines and immunoglobulins. Alternatively, the agents can themselves comprise cytokines. Non-specific immunotherapeutic agents are generally classified as cytokines or non-cytokine adjuvants. A number of cytokines have found application in the treatment of cancer either as general non-specific immunotherapies designed to boost the immune system, or as adjuvants provided with other therapies. Suitable cytokines include, but are not limited to, interferons, interleukins and colony-stimulating factors. Interferons (IFNs) contemplated by the present invention include the common types of IFNs, IFN-alpha (IFN-α), IFN-beta (IFN-β) and IFN-gamma (IFN-γ). IFNs can act directly on cancer cells, for example, by slowing their growth, promoting their development into cells with more normal behaviour and/or increasing their production of antigens thus making the cancer cells easier for the immune system to recognise and destroy. IFNs can also act indirectly on cancer cells, for example, by slowing down angiogenesis, boosting the immune system and/or stimulating natural killer (NK) cells, T cells and macrophages. Recombinant IFN-alpha is available commercially as Roferon (Roche Pharmaceuticals) and Intron A (Schering Corporation). Interleukins contemplated by the present invention include IL-2, IL-4, IL-11 and IL-12. Examples of commercially available recombinant interleukins include Proleukin® (IL-2; Chiron Corporation) and Neumega® (IL-12; Wyeth Pharmaceuticals). Zymogenetics, Inc. (Seattle, Wash.) is currently testing a recombinant form of IL-21, which is also contemplated for use in the combinations of the present invention. Colony-stimulating factors (CSFs) contemplated by the present invention include granulocyte colony stimulating factor (G-CSF or filgrastim), granulocyte-macrophage colony stimulating factor (GM-CSF or sargramostim) and erythropoietin (epoetin alfa, darbepoietin). Treatment with one or more growth factors can help to stimulate the generation of new blood cells in subjects undergoing traditional chemotherapy. Accordingly, treatment with CSFs can be helpful in decreasing the side effects associated with chemotherapy and can allow for higher doses of chemotherapeutic agents to be used. Various-recombinant colony stimulating factors are available commercially, for example, Neupogen® (G-CSF; Amgen), Neulasta (pelfilgrastim; Amgen), Leukine (GM-CSF; Berlex), Procrit (erythropoietin; Ortho Biotech), Epogen (erythropoietin; Amgen), Arnesp

(erytropoietin). In addition to having specific or non-specific targets, immunotherapeutic agents can be active, i.e. stimulate the body's own immune response, or they can be passive, i.e. comprise immune system components that were generated external to the body. Passive specific immunotherapy typically involves the use of one or more monoclonal antibodies that are specific for a particular antigen found on the surface of a cancer cell or that are specific for a particular cell growth factor. Monoclonal antibodies may be used in the treatment of cancer in a number of ways, for example, to enhance a subject's immune response to a specific type of cancer, to interfere with the growth of cancer cells by targeting specific cell growth factors, such as those involved in angiogenesis, or by enhancing the delivery of other anticancer agents to cancer cells when linked or conjugated to agents such as chemotherapeutic agents, radioactive particles or toxins. Monoclonal antibodies currently used as cancer immunotherapeutic agents that are suitable for inclusion in the combinations of the present invention include, but are not limited to, rituximab (Rituxan®), trastuzumab (Herceptin®), ibritumomab tiuxetan (Zevalin®), tositumomab (Bexxar®), cetuximab (C-225, Erbitux®), bevacizumab (Avastin®), gemtuzumab ozogamicin (Mylotarg®), alemtuzumab (Campath®), and BL22. Other examples include anti-CTLA4 antibodies (e.g. Ipilimumab), anti-PD1 antibodies, anti-PDL1 antibodies, anti-TIMP3 antibodies, anti-LAG3 antibodies, anti-B7H3 antibodies, anti-B7H4 antibodies or anti-B7H6 antibodies. In some embodiments, antibodies include B cell depleting antibodies. Typical B cell depleting antibodies include but are not limited to anti-CD20 monoclonal antibodies [e.g. Rituximab (Roche), Ibritumomab tiuxetan (Bayer Schering), Tositumomab (GlaxoSmithKline), AME-133v (Applied Molecular Evolution), Ocrelizumab (Roche), Ofatumumab (HuMax-CD20, Gemnab), TRU-015 (Trubion) and IMMU-106 (Immunomedics)], an anti-CD22 antibody [e.g. Epratuzumab, Leonard et al., Clinical Cancer Research (Z004) 10: 53Z7-5334], anti-CD79a antibodies, anti-CD27 antibodies, or anti-CD19 antibodies (e.g. U.S. Pat. No. 7,109,304), anti-BAFF-R antibodies (e.g. Belimumab, GlaxoSmithKline), anti-APRIL antibodies (e.g. anti-human APRIL antibody, ProSci inc.), and anti-IL-6 antibodies [e.g. previously described by De Benedetti et al., J Immunol (2001) 166: 4334-4340 and by Suzuki et al., Europ J of Immunol (1992) 22 (8) 1989-1993, fully incorporated herein by reference]. The immunotherapeutic treatment may consist of allografting, in particular, allograft with hematopoietic stem cell HSC. The immunotherapeutic treatment may also consist in an adoptive immunotherapy as described by Nicholas P. Restifo, Mark E. Dudley and Steven A. Rosenberg “Adoptive immunotherapy for cancer: harnessing the T cell response, Nature Reviews Immunology, Volume 12, April 2012). In adoptive immunotherapy, the subject’s circulating lymphocytes, NK cells, are isolated

amplified in vitro and readministered to the subject. The activated lymphocytes or NK cells are most preferably be the subject's own cells that were earlier isolated from a blood or tumor sample and activated (or "expanded") in vitro.

Examples of chemotherapeutics include but are not limited to fludarabine, gemcitabine, capecitabine, methotrexate, mercaptopurine, thioguanine, hydroxyurea, cytarabine, cyclophosphamide, ifosfamide, nitrosoureas, platinum complexes such as cisplatin, carboplatin and oxaliplatin, mitomycin, dacarbazine, procarbazine, epipodophyllotoxins such as etoposide and teniposide, camptothecins such as irinotecan and topotecan, bleomycin, doxorubicin, idarubicin, dactinomycin, plicamycin, mitoxantrone, L-asparaginase, doxorubicin, epirubicin, 5-fluorouracil and 5-fluorouracil combined with leucovorin, taxanes such as docetaxel and paclitaxel, levamisole, estramustine, nitrogen mustards, nitrosoureas such as carmustine and lomustine, vinca alkaloids such as vinblastine, vincristine, vindesine and vinorelbine, imatinib mesylate, hexamethylmelamine, kinase inhibitors, phosphatase inhibitors, ATPase inhibitors, tyrphostins, protease inhibitors, inhibitors herbimycin A, genistein, erbstatin, and lavendustin A. In some embodiments, additional therapeutic active agents may be selected from, but are not limited to, one or a combination of the following class of agents: alkylating agents, plant alkaloids, DNA topoisomerase inhibitors, anti-folates, pyrimidine analogs, purine analogs, DNA antimetabolites, taxanes, podophyllotoxins, hormonal therapies, retinoids, photosensitizers or photodynamic therapies, angiogenesis inhibitors, antimitotic agents, isoprenylation inhibitors, cell cycle inhibitors, actinomycin, bleomycin, anthracyclines, MDR inhibitors and Ca2+ ATPase inhibitors.

Additional therapeutic active agents may be selected from, but are not limited to, cytokines, chemokines, growth factors, growth inhibitory factors, hormones, soluble receptors, decoy receptors, monoclonal or polyclonal antibodies, mono-specific, bi-specific or multi-specific antibodies, monobodies, polybodies.

Further therapeutic active agent can be an antiemetic agent. Suitable antiemetic agents include, but are not limited to, metoclopramide, domperidone, prochlorperazine, promethazine, chlorpromazine, trimethobenzamide, ondansetron, granisetron, hydroxyzine, acetylleucine, alizapride, azasetron, benzquinamide, bietanautine, bromopride, buclizine, clebopride, cyclizine, dimenhydrinate, diphenidol, dolasetron, meclizine, methallatal, metopimazine, nabilone, pipamazine, scopolamine, sulpiride, tetrahydrocannabinols, thiethylperazine, thioproperazine and tropisetron. In a preferred embodiment, the antiemetic agent is granisetron or ondansetron.

In another embodiment, the further therapeutic active agent can be a hematopoietic colony stimulating factor. Suitable hematopoietic colony stimulating factors include, but are not limited to, filgrastim, sargramostim, molgramostim and epoietin alpha.

In still another embodiment, the other therapeutic active agent can be an opioid or non-opioid analgesic agent. Suitable opioid analgesic agents include, but are not limited to, morphine, heroin, hydromorphone, hydrocodone, oxymorphone, oxycodone, metopon, apomorphine, buprenorphine, meperidine, loperamide, ethoheptazine, betaprodine, diphenoxylate, fentanyl, sufentanil, alfentanil, remifentanil, levorphanol, dextromethorphan, phenazone, pemazocine, cyclazocine, methadone, isomethadone and propoxyphene. Suitable non-opioid analgesic agents include, but are not limited to, aspirin, celecoxib, rofecoxib, diclofenac, diflunisal, etodolac, fenoprofen, flurbiprofen, ibuprofen, ketoprofen, indomethacin, ketorolac, meclofenamate, mefenamic acid, nabumetone, naproxen, piroxicam and sulindac.

In yet another embodiment, the further therapeutic active agent can be an anxiolytic agent. Suitable anxiolytic agents include, but are not limited to, buspirone, and benzodiazepines such as diazepam, lorazepam, oxazapam, clorazepate, clonazepam, chlordiazepoxide and alprazolam.

In some embodiments, the MNP and the combination of the present invention is administered with a radiotherapeutic agent. The term "radiotherapeutic agent" as used herein, is intended to refer to any radiotherapeutic agent known to one of skill in the art to be effective to treat or ameliorate cancer, without limitation. For instance, the radiotherapeutic agent can be an agent such as those administered in brachytherapy or radionuclide therapy. Such methods can optionally further comprise the administration of one or more additional cancer therapies, such as, but not limited to, chemotherapies, and/or another radiotherapy.

In one embodiment, said additional active compounds may be contained in the same composition or administrated separately.

Typically the MNP and the combination according to the invention as described above are administered to the subject in a therapeutically effective amount.

By a "therapeutically effective amount" of the MNP and the combination of the present invention as above described is meant a sufficient amount of the MNP and the combination for treating cancer at a reasonable benefit/risk ratio applicable to any medical treatment. It will be understood, however, that the total daily usage of the MNP and the combination of the present invention will be decided by the attending physician within the scope of sound medical judgment. The specific therapeutically effective dose level for any particular subject will depend upon a variety of factors including the disorder being treated and the severity of the

disorder; activity of the specific MNP and the combination employed; the specific composition employed, the age, body weight, general health, sex and diet of the subject; the time of administration, route of administration, and rate of excretion of the specific MNP and the combination employed; the duration of the treatment; drugs used in combination or coincidental with the specific MNP and the combination employed; and like factors well known in the medical arts. For example, it is well within the skill of the art to start doses of the MNP and the combination at levels lower than those required to achieve the desired therapeutic effect and to gradually increase the dosage until the desired effect is achieved. However, the daily dosage of the products may be varied over a wide range from 0.01 to 1,000 mg per adult per day. Typically, the compositions contain 0.01, 0.05, 0.1, 0.5, 1.0, 2.5, 5.0, 10.0, 15.0, 25.0, 50.0, 100, 250 and 500 mg of the MNP and the combination of the present invention for the symptomatic adjustment of the dosage to the subject to be treated. A medicament typically contains from about 0.01 mg to about 500 mg of the MNP and the combination of the present invention, preferably from 1 mg to about 100 mg of the MNP and the combination of the present invention. An effective amount of the drug is ordinarily supplied at a dosage level from 0.0002 mg/kg to about 20 mg/kg of body weight per day, especially from about 0.001 mg/kg to 7 mg/kg of body weight per day.

In a particular embodiment, the MNP and the combination according to the invention may be used in a concentration between 0.01 μM and 20 μM, particularly, the MNP and the combination of the invention may be used in a concentration of 0.01, 0.05, 0.1, 0.5, 1.0, 2.5, 5.0, 10.0, 15.0, 20.0 μM.

According to the invention, the MNP and the combination of the present invention is administered to the subject in the form of a pharmaceutical composition. Typically, the MNP and the combination of the present invention may be combined with pharmaceutically acceptable excipients, and optionally sustained-release matrices, such as biodegradable polymers, to form therapeutic compositions. "Pharmaceutically" or "pharmaceutically acceptable" refer to molecular entities and compositions that do not produce an adverse, allergic or other untoward reaction when administered to a mammal, especially a human, as appropriate. A pharmaceutically acceptable carrier or excipient refers to a non-toxic solid, semi-solid or liquid filler, diluent, encapsulating material or formulation auxiliary of any type.

In the pharmaceutical compositions of the present invention for oral, sublingual, subcutaneous, intramuscular, intravenous, transdermal, local or rectal administration, the active principle, alone or in combination with another active principle, can be administered in a unit administration form, as a mixture with conventional pharmaceutical supports, to animals and

human beings. Suitable unit administration forms comprise oral-route forms such as tablets, gel capsules, powders, granules and oral suspensions or solutions, sublingual and buccal administration forms, aerosols, implants, subcutaneous, transdermal, topical, intraperitoneal, intramuscular, intravenous, subdermal, transdermal, intrathecal and intranasal administration forms and rectal administration forms.

Typically, the pharmaceutical compositions contain vehicles which are pharmaceutically acceptable for a formulation capable of being injected. These may be in particular isotonic, sterile, saline solutions (monosodium or disodium phosphate, sodium, potassium, calcium or magnesium chloride and the like or mixtures of such salts), or dry, especially freeze-dried compositions which upon addition, depending on the case, of sterilized water or physiological saline, permit the constitution of injectable solutions. The pharmaceutical forms suitable for injectable use include sterile aqueous solutions or dispersions; formulations including sesame oil, peanut oil or aqueous propylene glycol; and sterile powders for the extemporaneous preparation of sterile injectable solutions or dispersions. In all cases, the form must be sterile and must be fluid to the extent that easy syringability exists. It must be stable under the conditions of manufacture and storage and must be preserved against the contaminating action of microorganisms, such as bacteria and fungi. Solutions comprising MNP and the combination of the invention as free base or pharmacologically acceptable salts can be prepared in water suitably mixed with a surfactant, such as hydroxypropylcellulose. Dispersions can also be prepared in glycerol, liquid polyethylene glycols, and mixtures thereof and in oils. Under ordinary conditions of storage and use, these preparations contain a preservative to prevent the growth of microorganisms. The MNP and the combination of the present invention can be formulated into a composition in a neutral or salt form. Pharmaceutically acceptable salts include the acid addition salts (formed with the free amino groups of the protein) and which are formed with inorganic acids such as, for example, hydrochloric or phosphoric acids, or such organic acids as acetic, oxalic, tartaric, mandelic, and the like. Salts formed with the free carboxyl groups can also be derived from inorganic bases such as, for example, sodium, potassium, ammonium, calcium, or ferric hydroxides, and such organic bases as isopropylamine, trimethylamine, histidine, procaine and the like. The carrier can also be a solvent or dispersion medium containing, for example, water, ethanol, polyol (for example, glycerol, propylene glycol, and liquid polyethylene glycol, and the like), suitable mixtures thereof, and vegetables oils. The proper fluidity can be maintained, for example, by the use of a coating, such as lecithin, by the maintenance of the required particle size in the case of dispersion and by the use of surfactants. The prevention of the action of microorganisms can

be brought about by various antibacterial and antifungal agents, for example, parabens, chlorobutanol, phenol, sorbic acid, thimerosal, and the like. In many cases, it will be preferable to include isotonic agents, for example, sugars or sodium chloride. Prolonged absorption of the injectable compositions can be brought about by the use in the compositions of agents delaying absorption, for example, aluminium monostearate and gelatin. Sterile injectable solutions are prepared by incorporating the active compounds in the required amount in the appropriate solvent with several of the other ingredients enumerated above, as required, followed by filtered sterilization. Generally, dispersions are prepared by incorporating the various sterilized agent of the present inventions into a sterile vehicle which contains the basic dispersion medium and the required other ingredients from those enumerated above. In the case of sterile powders for the preparation of sterile injectable solutions, the typical methods of preparation are vacuum-drying and freeze-drying techniques which yield a powder of the MNP and the combination of the present invention plus any additional desired ingredient from a previously sterile-filtered solution thereof. The preparation of more, or highly concentrated solutions for direct injection is also contemplated, where the use of DMSO as solvent is envisioned to result in extremely rapid penetration, delivering high concentrations of the active agents to a small tumor area. Upon formulation, solutions will be administered in a manner compatible with the dosage formulation and in such amount as is therapeutically effective. The formulations are easily administered in a variety of dosage forms, such as the type of injectable solutions described above, but drug release capsules and the like can also be employed. For parenteral administration in an aqueous solution, for example, the solution should be suitably buffered if necessary and the liquid diluent first rendered isotonic with sufficient saline or glucose. These particular aqueous solutions are especially suitable for intravenous, intramuscular, subcutaneous and intraperitoneal administration. In this connection, sterile aqueous media which can be employed will be known to those of skill in the art in light of the present disclosure. Some variation in dosage will necessarily occur depending on the condition of the subject being treated. The person responsible for administration will, in any event, determine the appropriate dose for the individual subject.

In another embodiment, the pharmaceutical composition of the invention relates to combined preparation for simultaneous, separate or sequential use in a method for inducing non-apoptotic signaling of cancer cell in a subject afflicted with cancer in need thereof.

In a further aspect, the present invention relates to a method for inducing non-apoptotic signaling of cancer cell in a subject afflicted with cancer in need thereof, comprising the steps

of administering to said subject the magnetic nanoparticle grafted with a tumor targeting agent, and application of a high frequency alternating magnetic field (AMF).

The term "high frequency alternating magnetic field (AMF)" has its general meaning in the art and refers to AMF frequency of 100 to 350 kHz and AMF amplitude of 20 to 60 mT. The term "high frequency alternating magnetic field (AMF)" also refers to AMF of frequency of 100, 150, 200, 250, 300 or 350 kHz and amplitude of 20, 30, 40, 50 or 60 mT. The term "high frequency alternating magnetic field (AMF)" also refers but not limited to AMF of frequency and amplitude of 275 kHz-52 mT, 275 kHz-50 mT, 275 kHz-40 mT and 300 kHz-53mT (Sanchez et al., 2014; Domenech et al., 2013; Creixell et al., 2011; Silva et al., 2011).

The invention also provides kits comprising the MNP and the combination of the invention. Kits containing the MNP and the combination of the invention find use in therapeutic methods.

The invention will be further illustrated by the following figures and examples. However, these examples and figures should not be interpreted in any way as limiting the scope of the present invention.

FIGURES:

Figure 1: Magnetic intra-lysosomal hyperthermia induces ROS generation. a) Schematic representation of targeted magnetic intra-lysosomal hyperthermia (MILH) approach. We previously showed that Gastrin-MNP are specifically internalized by the pancreatic endocrine tumoral cells INR1G9-CCK2R cells through a CCK2R-dependent physiological process, and are then trafficked to lysosomes where they accumulated. Upon AMF exposure, Gastrin-MNPs cause lysosome membrane permeabilization and the leakage of lysosomal enzymes into the cytosol including Cathepsins which trigger cell death. Subsequently, 19.9±1.5% or 32.3±2.7% of INR1G9-CCK2R cells were labeled by AnnexinV and propidium iodide or were killed 4h and 24h after AMF exposure. **b)** MILH increases cellular ROS production. AMF application to cells containing MNPs would generate a nanoscale temperature elevation and enhance ROS production within lysosomes. Lysosomes are well-known major sites of ROS production through the Fenton reaction ($Fe^{2+}+H_2O_2 \rightarrow Fe^{3+}+OH^-+OH^{\bullet}$) which catalyzes the transformation of hydrogen peroxide to hydroxyl radicals. INR1G9-CCK2R cells having or not internalized Gastrin-MNP were incubated in the presence or absence of 1 mM DFO, 1 nM BafA1, 20μM ART or 120 μM FeCl3, exposed or not to AMF and incubated with CellROX reagent. Quantification of ROS production was performed by analyzing the fluorescence intensity from confocal microscopy images. Results are expressed as fold change of fluorescence intensity over control cells (in absence of Gastrin-MNP and AMF) and **c)** MILH

increases lysosomal ROS production. INR1G9-CCK2R cells having or not internalized Gastrin-MNP were incubated in the presence or absence of 1 mM DFO, 1 nM BafA1, 20 μM ART or 120 μM FeCl3. Cells were incubated with CellROX reagent during the 30-min of AMF exposure. Quantification of ROS production colocalizing with Gastrin-MNP was performed by analyzing the % of relative fluorescence intensities of ROS production over Gastrin-MNP from confocal microscopy images. **d)** Absence of Gastrin-MNP degradation after AMF exposure. INR1G9-CCK2R cells were incubated with Gastrin-MNP for 24h and exposed or not to AMF for 2h. Fe contained in superparamagnetic MNPs of cells exposed or not to AMF was measured by particle electron paramagnetic resonance. **e)** Temperature analysis at MNP surface and lysosome membrane during MILH experiments. INR1G9-CCK2R cells transiently expressing YFP-Lamp1 were incubated with Gastrin-MNP-DY549 for 24h. AMF (275 kHz, 50 mT) was applied using a miniaturized electromagnet and temperature at MNPs surface and lysosome membrane was analyzed respectively using the molecular thermometers DY549 and YFP-Lamp1 by measuring the decrease of their fluorescence intensity. As a control, no significant changes of the MNP surface or lysosome membrane temperatures were observed in cells not exposed to AMF. Results are the mean ± SEM of at least 3 separate experiments.

Figure 2: MILH-induced ROS generation causes lysosome lipid peroxydation, lysosome membrane permeabilization and cell death. a) MILH causes lysosome lipid peroxidation. INR1G9-CCK2R cells having or not internalized Gastrin-MNP were incubated in the presence or absence of 1 mM DFO or 1 nM BafA1 and incubated with Image-IT® lipid peroxidation reagent during the 30-min of AMF exposure. Quantification was performed by measuring the % of fluorescence intensity of lipid peroxidation over that of Gastrin-MNP from confocal microscopy images. **b)** LMP induced by MILH is dependent on ROS production. INR1G9-CCK2R transiently expressing GFP-CathB and RFP-Lamp1 were incubated with Gastrin-MNP and exposed to AMF in the presence or not of NAC. LMP was evaluated by analyzing the colocalization between GFP-CathB and RFP-Lamp1 on confocal microscopy images using Pearson's coefficient (left panel) and quantified by measuring the % of fluorescence intensity of GFP-CathB over that of RFP-Lamp1 from confocal microscopy images (right panel). **c)** Monitoring of LMP during AMF exposure. INR1G9-CCK2R transiently expressing GFP-CathB and RFP-Lamp1 were incubated with Gastrin-MNP and exposed or not to AMF. Different positions were marked inside (+AMF) and outside (-AMF) the gap of the electromagnet allowing to visualize the effects of AMF under a confocal microscope. Before and during AMF application for 60-min, LMP was analyzed by measuring the % of GFP-CathB colocalized with RFP-Lamp1. Results are expressed as % of

CathB/Lamp1 colocalization over control cells (in absence of Gastrin-MNP and AMF). **d)** MILH-induced cell death is dependent on lysosomal ROS production. INR1G9-CCK2R cells were incubated with Gastrin-MNP, exposed to AMF in presence or not of 5 mM NAC, 1 mM DFO, 1 nM BafA1, 20 μM ART or 120 μM FeCl3. Dead cells were counted 4h after AMF exposure by confocal microscopy analysis of cells labeled with annexinV and/or propidium iodide. Results are expressed as fold change of death rate over control cells (in absence of Gastrin-MNP and AMF). The % of dead cells are indicated above the histogram. Results are the mean ± SEM of at least 3 separate experiments.

Figure 3: Cell death induced by MILH is dependent on CathB activity. a) INR1G9-CCK2R cells having or not internalized Gastrin-MNP were incubated with or without 10 μM CathB inhibitor CA-074-Me and exposed or not to AMF. Dead cells were counted 4h after the end of AMF exposure by confocal microscopy analysis of cells labeled with annexinV and/or propidium iodide. Results are expressed as fold change of death rate over control cells (in absence of Gastrin-MNP and AMF). The % of dead cells are indicated above the histograms. **b-c)** INR1G9-CCK2R transiently expressing GFP-CathB-C29A enzymatically inactive mutant (B) or GFP-CathB wild-type enzyme (C) were incubated with Gastrin-MNP and exposed or not to AMF. Dead cells were counted 4h after the end of AMF exposure by confocal microscopy analysis and expressed as the % of cells labeled with annexinV among transfected and non-transfected cells. Results are expressed as fold change of death rate over control cells (in absence of Gastrin-MNP and AMF). The % of dead cells are indicated above the histograms. Results are the mean ± SEM of at least 4 separate experiments.

Figure 4: Cell death induced by MILH is mediated through a non-apoptotic Caspase-1 signaling pathway which is dependent on CathB activity. a) MILH-induced cell death is independent of Caspase-3. INR1G9-CCK2R cells having or not internalized Gastrin-MNP were exposed or not to AMF in the presence of 10 μM Caspase-3 inhibitor. Dead cells were counted 4h after the end of AMF exposure by confocal microscopy analysis of cells labeled with annexinV and/or propidium iodide. As a positive control, INR1G9-CCK2R cells were incubated with 1 μM staurosporine for 4h. Results are expressed as fold change of death rate over control cells (in absence of Gastrin-MNP and AMF). The % of dead cells is indicated above the histogram. **b)** MILH does not induce Caspase-3 activation. Cells having or not internalized Gastrin-MNP were exposed or not to AMF in the presence or absence of 10 μM Caspase-3 inhibitor. As positive and negative controls of Caspase-3 activation, INR1G9-CCK2R cells were stimulated with 1 μM staurosporine in the absence or in the presence of Caspase-3 inhibitor. 4h after AMF exposure or staurosporine treatment, Caspase-3 activation

was analyzed by confocal microscopy of cells labeled with FAM-FLICA-Casp3. Results are expressed as the % of total cells labeled with fluorescent Caspase substrate. **c)** MILH does not induce mitochondrial outer membrane permeabilization (MOMP). INR1G9-CCK2R cells having or not internalized Gastrin-MNP were exposed or not to AMF. As a positive control, INR1G9-CCK2R cells were stimulated with 1 µM staurosporine. 4h after AMF exposure or staurosporine treatment, Cells were incubated with JC-10 reagent and were analyzed by confocal microscopy. Quantification of MOMP was performed by analyzing the ratio of green/red JC-10 fluorescence from confocal microscopy images. **d)** MILH-induced cell death is dependent of Caspase-1. INR1G9-CCK2R cells having or not internalized Gastrin-MNP were exposed or not to AMF in presence of 2.5 µM Caspase-1 inhibitor. Dead cells were counted 4h after the end of AMF exposure by confocal microscopy analysis of cells labeled with annexinV and/or propidium iodide. Results are expressed as fold change of death rate over control cells (in the absence of Gastrin-MNP and AMF). The % of dead cells is indicated above the histogram. **e)** INR1G9-CCK2R transiently expressing GFP-Casp1-C284A enzymatically inactive mutant were incubated with Gastrin-MNP and exposed or not to AMF. Dead cells were counted 4h after AMF exposure by confocal microscopy analysis of cells labeled with annexinV and/or propidium iodide. Results are expressed as fold change of death rate over control cells (in absence of Gastrin-MNP and AMF). The % of dead cells is indicated above the histogram. **f)** MILH induces Caspase-1 activation. Cells having or not internalized Gastrin-MNP were exposed or not to AMF in the presence or absence of 2.5 µM Caspase-1 inhibitor. 4h after AMF exposure, Caspase-1 activation was analyzed by confocal microscopy of cells labeled with FAM-FLICA-Casp1. Results are expressed in % of total cells labeled with fluorescent Caspase substrate. Results are the mean ± SEM of at least 4 separate experiments.

Figure 5: MILH triggers a non-apoptotic cell death mechanism related to pyroptosis. a) MILH does not induce Il1β secretion. INR1G9-CCK2R cells were treated or not with 500 ng/ml of LPS, Gastrin-MNP and exposed or not to AMF. As a positive control, Thp1 macrophages were treated with 500 ng/ml LPS. Il1β release in culture supernatant was assayed with an ELISA kit. **b)** MILH induces DNA fragmentation. INR1G9-CCK2R cells having or not internalized Gastrin-MNP were exposed or not to AMF. As controls of apoptotis and necrosis, cells were respectively treated with 1 µM of staurosporine (6h) or incubated at 45°C in a water-bath (30-min). DNA fragmentation was detected by TUNEL assay, 6h after AMF exposure. Cells presenting DNA fragmentation were counted by confocal microscopy analysis and expressed as % of total cells labeled with fluorescent dUTP. Results are the mean ± SEM of at least 5 separate experiments.

Figure 6: MILH induces the death and activates Caspase-1 in different cancer cells. INR1G9-CCK2R, AR4-2J and AGS-CCK2R cells were incubated or not with Gastrin-MNP and exposed or not to AMF. **a)** Cell survival was determined by MTT assay 24h after the end of AMF exposure. Results are expressed as the % of inhibition of cell survival over control cells (in absence of Gastrin-MNP and AMF) for each cell line. **b)** Dead cells were counted 4h after the end of AMF exposure by confocal microscopy analysis of cells labeled with annexinV and/or propidium iodide. Results are expressed as fold change of death rate over control cells (in absence of Gastrin-MNP and AMF) for each cell line. The % of dead cells is indicated above the histogram. **c)** Gastrin-MNP uptake was measured by colorimetric assay (total Fe) or by pEPR (Fe contained in superparamagnetic MNPs). **d)** Caspase-1 activation was analyzed by confocal microscopy of cells labeled with FAM-FLICA-Casp1, 4h after AMF exposure. Results are expressed in % of total cells labeled with fluorescent Caspase substrate. Results are the mean ± SEM of at least 4 separate experiments. **e)** Schematic representation of cell death mechanism induced by MILH. Application oh high frequency magnetic field to Gastrin-MNP specifically delivered to lysosomes of cancer cells increases the temperature at the nanoparticle periphery which enhances ROS production through the lysosomal Fenton reaction. Subsequently, ROS cause lipid peroxidation of lysosome membrane, lysosomal membrane permeabilization and the leakage of lysosomal enzymes into the cytosol, including CathB. Then, cytosolic CathB activates Caspase-1, but not the apoptotic Caspase-3, to induce the death of cancer cells.

Figure 7: a) Cellular ROS production in the absence of AMF exposure. INR1G9-CCK2R cells having or not internalized Gastrin-MNP were incubated in the presence or absence of 1mM DFO, 1nM BafA1 or 120µM $FeCl_3$ and incubated with CellROX Green reagent. Quantification of ROS production was performed by analyzing the fluorescence intensity from confocal microscopy images. Results are expressed as fold change of fluorescence intensity over control cells (in absence of Gastrin-MNP) and are the mean ± SEM of at least 3 separate experiments. **b) Analysis of lysosomal acidity.** INR1G9-CCK2R cells were incubated with 1 nM BafA1 or 20 µM ART for 3h, then with 5 µM acridine orange for 15-min at 37°C and washed before microscope observation. Quantitative analysis of red fluorescence of acridine orange from microscope images of 2-3000 cells. Results are expressed as the % of Red fluorescence relative to control cells and are the mean ± SEM of at least 3 separate experiments.

Figure 8: MILH induces ROS production through NADPH oxidases, but not through mitochondrial complex of respiratory chain. INR1G9-CCK2R cells having or not

internalized Gastrin-MNP were incubated or not in the presence of 1 μM rotenone (inhibitor of mitochondrial complex of respiratory chain) or DPI (inhibitor of NAPDH oxidases) and exposed or not to AMF for 2h. After AMF application, cells were incubated with CellROX Green reagent. Quantification of ROS production was performed by analyzing the intensity of CellROX Green reagent labeling of confocal microscopy images. Results are expressed as fold change of basal fluorescence intensity over control cells (in the absence of Gastrin-MNP and AMF) and are the mean ± SEM of at least 4 separate experiments.

Figure 9: Fluorescence intensity of Gastrin-MNP-DY549 and YFP-lamp1 is dependent on temperature. INR1G9-CCK2R cells transiently expressing YFP-Lamp1 were incubated with Gastrin-MNP-DY549 for 24h. Cells were slowly heated in the incubator chamber of the confocal microscope. Fluorescence intensity of fluorophores was analyzed from confocal microscopy images, normalized to $\Delta T=0$ and expressed as the mean ± SEM of at least 4 separate experiments.

Figure 10: MILH-induced cellular ROS production is inhibited by NAC. INR1G9-CCK2 cells having or not internalized Gastrin-MNP were incubated in the presence or absence of 5mM NAC, exposed or not to AMF for 2h and incubated with CellROX Green reagent. Quantification of ROS production was performed by analyzing the fluorescence intensity of confocal microscopy images. Results are expressed as fold change of fluorescence intensity over control cells (in absence of Gastrin-MNP and AMF) and are the mean ± SEM of at least 3 separate experiments.

Figure 11: Cell death determination in the presence of drugs modifying ROS production. INR1G9-CCK2R cells were incubated with Gastrin-MNP for 24h and then with 5 mM NAC, 1 mM DFO, 1 nM BafA1 or 120 μM $FeCl_3$ for 7-10h. Dead cells were counted by confocal microscopy analysis of cells labeled with annexinV and/or propidium iodide. Results are expressed as fold change of death rate over control cells (in absence of Gastrin-MNP and AMF) and are the mean ± SEM of at least 3 separate experiments. The % of dead cells are indicated above the histograms.

Figure 12: Analysis of MILH-induced cell death in presence of rotenone or DPI. INR1G9-CCK2R cells having or not internalized Gastrin-MNP were incubated or not in the presence of 1 μM rotenone (inhibitor of mitochondrial complex of respiratory chain) or DPI (inhibitor of NAPDH oxidases) and exposed or not to AMF for 2h. Dead cells were counted by confocal microscopy analysis of cells labeled with annexinV and/or propidium iodide. Results are expressed as fold change of death rate over control cells (in absence of Gastrin-MNP and

AMF) and are the mean ± SEM of at least 3 separate experiments. The % of dead cells are indicated above the histograms.

Figure 13: MILH induces lysosomal rupture and CathB leakage from lysosomes. INR1G9-CCK2R transiently expressing GFP-CathB and RFP-Lamp1 were incubated with Gastrin-MNP for 24h and exposed to AMF. Fluorescence intensity of GFP-CathB and RFP-Lamp1 were measured in cells exposed or not to AMF for 60-min from confocal images. Results are expressed as % of fluorescence intensity relative to t=0 and are the mean ± SEM of at least 4 separate experiments.

Figure 14: MILH does not induce Pro-Caspase-3 maturation. INR1G9-CCK2R cells having internalized Gastrin-MNP were exposed or not to AMF. As a positive control, INR1G9-CCK2R cells were treated with 1 µM staurosporine. Pro-Caspase-3 expression was analyzed by Western blot of total cell lysates. Results of quantification of pro-Caspase-3 expression represent mean ± SEM of 4 independent experiments and are expressed as fold control with control expression set to 1.

Figure 15: MILH does not induce mitochondrial outer membrane permeabilization (MOMP). INR1G9-CCK2R cells having or not internalized Gastrin-MNP were exposed or not to AMF. As a positive control, INR1G9-CCK2R cells were stimulated with 1 µM staurosporine for 4h. 24h after AMF exposure or staurosporine treatment, Cells were incubated with JC-10 reagent and were analyzed by confocal microscopy. Quantification of MOMP was performed by analyzing the green/red fluorescence ratio of confocal microscopy images. Results are the mean ± SEM of 3 separate experiments.

Figure 16: MILH-induced Caspase-1 activation is dependent on CathB activity. INR1G9-CCK2R cells having or not internalized Gastrin-MNP were exposed or not to AMF in the presence or absence of 2.5 µM Caspase-1. 1, 4 and 18h after AMF exposure, Caspase-1 activation was analyzed by confocal microscopy of cells labeled with FAM-FLICA-Casp1. Results are expressed as % of total cells labeled with fluorescent Caspase substrate and are the mean ± SEM of 4 separate experiments.

Figure 17: MILH induces the death of HEK-CCK2R cells and activates Caspase-1. HEK-CCK2R were incubated or not with Gastrin-MNP for 24h. **a)** Cells were exposed or not to AMF for 2h at 37°C. Cell survival was determined by MTT assay 24h after AMF exposure. Results are expressed as the % of cell survival relative to control cells (in absence of Gastrin-MNP and AMF) and are the mean ± SEM of at least 5 separate experiments. **b)** Cells were exposed or not to AMF. Dead cells were counted 4h after AMF exposure by confocal microscopy analysis of cells labeled with annexinV and/or propidium iodide. Results are

expressed as fold change of death rate over control cells (in absence of Gastrin-MNP and AMF) and are the mean ± SEM of at least 4 separate experiments. The % of dead cells are indicated above the histograms. **c)** Gastrin-MNP uptake was measured by colorimetric assay (total Fe) or by particle electron paramagnetic resonance (magnetic Fe) and expressed as the mean ± SEM of at least 4 separate experiments. **d-e)** 4h after AMF exposure, Caspase-3 and -1 activation was analyzed by confocal microscopy of cells labeled with FAM-FLICA-Casp3 or FAM-FLICA-Casp1. As positive control of Caspase-3 activation, INR1G9-CCK2R cells were stimulated with 1 μM staurosporine. Results are expressed in % of total cells labeled with fluorescent Caspase substrate and are the mean ± SEM of 4 separate experiments.

Figure 18: Absence of Caspase-3 activation following MILH treatment of different cancer cells. INR1G9-CCK2R, AGS-CCK2R and AR4-2J cells were incubated with Gastrin-MNP for 24h and exposed to AMF. 4h after AMF exposure, Caspase-3 activation was analyzed by confocal microscopy of cells labeled with FAM-FLICA-Casp3. As positive control of Caspase-3 activation, INR1G9-CCK2R cells were stimulated with 1 μM staurosporine. Results are expressed in % of total cells labeled with fluorescent Caspase substrate and are the mean ± SEM of 4 separate experiments.

Figure 19. Effect of combination of magnetic intra-lysosomal hyperthermia and doxorubicin treatment on cell death. INR1G9-CCK2R cells were pre-incubated with Gastrin-MNPs ([Fe] = 16 μg/ml) for 24 hours, allowing their internalization and lysosome accumulation, washed to eliminate unbound and non-internalized nanoparticles, before the addition of different concentrations of doxorubicin for another 24 hours and exposed or not to AMF (40 mT, 275 kHz). The impact of the treatments was determined 4 hours after AMF exposure by counting cells labeled with FITC-tagged annexin V (AnnV) and/or propidium iodide (IP) which identified dead cells. The % of induction of cell death are indicated above the histogram. Significant difference compared to the control condition corresponding to cells devoid of Gastrin-MNPs in absence of AMF exposure and doxorubicin treatment was indicated above histogram bar. Statistical significances between other conditions are also indicated. 2,000-3,000 cells/experiments were analyzed and results are the mean ± SEM of five separate experiments.

Figure 20: Effect of combination of magnetic intra-lysosomal hyperthermia with HSP70 inhibition on cell death. INR1G9-CCK2R cells were pre-incubated with 16 μg/ml Gastrin-MNP for 24 hours, allowing their internalization and lysosome accumulation, washed to eliminate unbound and non-internalized nanoparticles, before the addition of different concentrations of HSP70 inhibitor, PES, for 1 hour and submitted or not to a high frequency

alternating magnetic field (40 mT, 275 kHz). The impact of the treatments was determined 4 or 24 hours after magnetic field application by counting cells labeled with FITC-tagged annexin V (AnnV) and/or propidium iodide (PI), which identified dead cells using flow cytometry. Results represent the mean ± sem of eight independent experiments. a) Analysis of cell death in presence of 5 µM of PES 4 hours after AMF exposure. b) Analysis of cell death in presence of 7.55 µM of PES 4 hours after AMF exposure. c) Analysis of cell death in presence of 5 µM of PES 24 hours after AMF exposure.

Figure 21: Effect of combination of magnetic intra-lysosomal hyperthermia with HSP70 down-regulation on cell death. INR1G9-CCK2R cells were transfected or not with SiRNA directed against rat HSP70 (Dharmacon)for 48 hours, incubated or not with 16 µg/ml Gastrin-MNP for 24 hours, allowing their internalization and lysosome accumulation, washed to eliminate unbound and non-internalized nanoparticles, and exposed or not to a high frequency alternating magnetic field (40 mT, 275 kHz). The impact of the treatments was determined 4 hours after magnetic field application by counting cells labeled with FITC-tagged annexin V (AnnV) and/or propidium iodide (PI), which identified dead cells using flow cytometry. Results represent the mean ± sem of eight independent experiments.

Figure 22: Effect of combination of magnetic intra-lysosomal hyperthermia with HSP70 inhibition on lysosome membrane permeabilization. INR1G9-CCK2R cells having internalized Gastrin-MNP were exposed or not to AMF (40 mT, 275 kHz) for 2 hours in the presence or absence of 5 µM of HSP70 inhibitor PES. Cells were then incubated with RPMI 1640 0.5% FBS containing 75 nM LysoTraker Red (Molecular probes, excitation wavelength: 543 nm) for 15 minutes and rinsed with incubation medium. Lysosome membrane permeabilization was analyzed by flow cytometry by quantifying the fluorescence intensity of Lysotraker and normalized over control cells.

Figure 23: Effect of combination of magnetic intra-lysosomal hyperthermia with HSP70 inhibition on Caspase-1 (a) and Caspase-3 (b) activation. Cells having or not internalized Gastrin-MNP were exposed or not to AMF in the presence or absence of 5 µM of HSP70 inhibitor PES. 4h after AMF exposure, Caspase-1 or Capsase-3 activation was analyzed by flow cytometry of cells labeled with FAM-FLICA-Casp1 or FAM-FLICA-Casp3. Results are expressed as fold change of caspase-1 activation over control cells (in absence of Gastrin-MNP and AMF).

Treatment	Inhibition of cell viability (% control)	Combination Index (CI) value	Additivity Synergism effect	Induction of cell death (% total)	Combination Index ((CI) value	Additivity Synergism effect
Single drug						
Gastrin-MNP 16 µg/ml + AMF	26.1 ± 2.8			16.7 ± 1.0		
Gastrin-MNP 32 µg/ml + AMF	36.1 ± 4.3			61.5 ± 12.0		
Doxorubicin 1 µM	21.9 ± 3.0			13.4 ± 1.1		
Doxorubicin 3 µM	50.2 ± 3.8			18.2 ± 1.7		
Doxorubicin 5 µM	56.7 ± 4.4			21.0 ± 1.0		
Combination therapy (with amf)						
Gastrin-MNP + Doxorubicin 1 µM	46.5 ± 3.9	0.58	synergism	25.4 ± 2.4	0.10	synergism
Gastrin-MNP + Doxorubicin 3 µM	69.7 ± 3.1	0.94	additivity	28.6 ± 2.8	0.18	synergism
Gastrin-MNP + Doxorubicin 5 µM	77.7 ± 2.1	1.20	"	32.4 ± 0.8	0.20	synergism

Table 1: synergistic results with the doxorubicin.

EXAMPLES:

EXAMPLE 1:

Material & Methods

Nanoparticles and chemical materials

The synthesis method and characterization of the magnetic nanoplatform used in the present article have been previously described[4]. The nanoplatform (Gastrin-MNP) is composed of commercial iron oxide magnetic nanoparticles (MNPs) coated with PEG-Amine (Gecco Dots, Sweden) and decorated with 100 molecules of a synthetic replicate of gastrin (Covalab) plus 20 molecules of the fluorescent label DY647-PEG1 (Dyomics GmbH, Germany). The size of the nanoparticle core determined by transmission electron microscopy was 8.7±1.6 nm. The specific absorption rate of these MNPs is 13 W/g at 275kHz and 40mT. N-acetyl-cystein (NAC), Desferroxamine (DFO), bafilomycine A (BafA1), $FeCl_3$ and Doxorubicin were purchased from Sigma-Aldrich. CA-074-Me and Caspase-3 inhibitors were from ApexBio. Caspase-1 inhibitor was from Santa Cruz Biotechnologies.

Cell lines

The glucagon-producing Hamster tumoral cell line INR1G9 stably expressing CCK2R (INR1G9-CCK2R) obtained as previously described[15] was cultured in RPMI1640 medium containing 10% fetal bovine serum (FBS) and 100IU/ml penicillin/streptomycin (Life technologies). The HEK293 cells (Flp-In system, Invitrogen) stably expressing the CCK2R, named HEK-CCK2R, and the clone B13 of AR4-2J cells (kindly provided by Prof. Timo Otonkoski, University of Helsinki, Finland, with the permission of Dr Itaru Kojima, Gunma University, Maebashi, Japan) were cultured in DMEM medium containing 10% fetal bovine serum (FBS) and 100IU/ml penicillin/streptomycin (Life technologies). The AGS gastric adenocarcinoma cell line was permanently transfected with CCK2R (AGS-CCK2R) driven by the EF1-α promoter under puromycin selection and grown in DMEM/F-12 medium supplemented with 10% FBS and 100IU/ml penicillin/streptomycin[16]. The cells were grown in a humidified atmosphere at 95% air and 5% CO_2 at 37°C.

Quantification of Gastrin-MNP uptake by colorimetric assay

Cells were seeded onto 6-well plates at a density of 250 to $500x10^3$ cells/well and grown for 24h. Cells were incubated with Gastrin-MNP (16µg Fe_3O_4/ml) in medium buffered with 10mM HEPES buffer pH7.4 containing 0.5% FBS and 100IU/ml penicillin-streptomycin for 24h, at 37°C in a 5% CO_2 atmosphere, washed twice with ice-cold PBS. The number of cells was counted on an aliquot and cellular uptake of Gastrin-MNP was evaluated using a Prussian blue staining assay. Cells were digested in HCl 5N for 2h at 60°C, incubated for 30-min with

4% potassium ferrocyanide in 4% HCl (freshly prepared). Optical density was read at 690nm on a spectrophotometer.

Quantification of superparamagnetic Fe contained in Gastrin-MNP by electron paramagnetic resonance.

Cells were seeded onto 6-well plates at a density of 250 to 500x10^3 cells/well and grown for 24h. Cells were incubated with Gastrin-MNP (16µg Fe_3O_4/ml) in medium buffered with 10mM HEPES buffer pH7.4 containing 0.5% FBS and 100IU/ml penicillin-streptomycin for 24h, at 37°C in a 5% CO_2 atmosphere, washed twice with ice-cold PBS. The number of cells was counted on an aliquot and the electron paramagnetic resonance analysis was performed as described previously (17).

Gastrin-MNP localization in lysosomes by confocal microscopy

Cells were plated (60 to 120x10^3 cells/compartment) onto 4-compartment Cellview culture dishes (greiner Bio-One). After overnight growth, cells were incubated with Gastrin-MNP (16µg Fe_3O_4/mL) in medium that was buffered with 10mM HEPES buffer pH7.4 containing 0.5% FBS and 100IU/ml penicillin-streptomycin for 24h. For lysosome staining, cells were incubated for 30-min in the presence of 75nM LysoTracker Red DND-99 (excitation: 570nm, Life technologies). Gastrin-MNP (excitation: 633nm) and Lysotraker co-localisation was analyzed using LSM510 confocal microscope (Zeiss).

Cell treatment by alternating magnetic field

Cell treatment by alternalting magnetic field (AMF) was performed as follows. Cells were seeded onto 4-compartment Cellview dishes (Greiner Bio-One) at a density of 60 to 120x10^3 cells/compartment, grown overnight and incubated with Gastrin-MNP (16µg Fe_3O_4/ml) for 24h at 37°C in medium buffered with 10 mM HEPES buffer pH 7.4 containing 0.5% FBS and 100 IU/ml penicillin-streptomycin to allow Gastrin-MNP internalization and accumulation in lysosomes. Incubation medium was withdrawn and cells were rinsed twice with incubation medium and then incubated with 5mM NAC, 1mM DFO, 1nM BafA1, 10µM CA-074 Me, 2.5µM Caspase-1 inhibitor or 10µM Caspase-3 inhibitor for 1h or 120µM FeCl3 for 4h and exposed to AMF (275kHz, 40mT) for 2h using a commercial magnetic inductor (Fives Celes, Lautenback, France) as previously described (4). The temperature of the Cellview dish was maintained at 37.0±0.2°c and controlled using a thermal probe (Reflex, Neoptix, Canada) placed in the incubation medium of the cells. At the end of the experiments, cells were placed in a humidified atmosphere at 5% CO2 at 37°C.

Determination of cell death

The effects of AMF treatment were investigated as follows: first, cell survival was determined 24h post-AMF treatment using a MTT viability assay. Secondly, dead cells labeled with AnnexinV-iFluor488 and propidium iodide (excitation: 488and 540nm respectively, AAT Bioquest) were counted 4h after the end of AMF exposure as described before (4). To analyze cell death in INR1G9-CCK2R overexpressing GFP-CathB or –Casp1 fusion protein, INR1G9-CCK2R cells were seeded at a density of $250x10^3$ cells onto 35mm dishes and transfected with 3µg of pCathB-eGFP, pCathB-C29A-eGFP (given by Klaudia Brix, Jacobs University Bremen, Germany) or pMSCV2.2-IRES-GFP-Caspase-1-C284A (given by Petr Broz, University of Basel, Switzerland) using Lipofectamine 2000 reagent (Life technologies). 4h post-transfection, cells were seeded onto 4-compartment Cellview dishes (Greiner Bio-One) at a density of $60x10^3$ cells/compartment, grown overnight and incubated with Gastrin-MNP (16µg Fe_3O_4/ml) for 24h at 37°C in medium buffered with 10mM HEPES buffer pH7.4 containing 0.5% FBS and 100IU/ml penicillin-streptomycin. Cells were rinsed twice with incubation medium, exposed to AMF for 2 h, labeled with AnnexinV-iFluor555 (excitation: 540nm, AAT Bioquest) 4h after the end of AMF exposure and counted. Counting of labeled cells was carried out by analyzing confocal microscopy images (LSM510 confocal microscope, Zeiss) representing populations of 2-3000 cells/experiment using ImageJ software.

Analysis of ROS production

INR1G9-CCK2R cells were seeded 24 h before the experiments onto 4-compartment Cellview dishes (Greiner Bio-One) at a density of 60 to $120x10^3$ cells/compartment and incubated with Gastrin-MNP (16µg Fe_3O_4/ml) for 24h. Cells were rinsed twice with incubation medium and incubated with 5mM NAC, 1mM DFO, 1nM BafA1 for 1h or 120µM FeCl3 for 4h. For total ROS production analysis, cells were exposed to AMF for 2h, rinsed with incubation medium, incubated with CellROX Green reagent (Molecular probes, Excitation wavelegnth: 488nm) in incubation medium according to manufacturer's instructions and quantification of ROS production was performed by analyzing the intensity of CellROX Green reagent labeling of confocal microscopy images (LSM780 confocal microscope, Zeiss) using Image J software. 2000-3000 cells/experiments were analyzed in at least 4 independent experiments. For initial ROS production analysis, cells having or not internalized Gastrin-MNP were incubated in the presence or absence of 1mM DFO, 1nM BafA1, 20µM ART or 120µM FeCl3 and then with CellROX Green reagent (Molecular probes, Excitation: 488nm) in incubation medium according to manufacturer's instructions, exposed to AMF for 30-min, rinsed with incubation medium and ROS production was analyzed using confocal microscopy (LSM780 confocal microscope, Zeiss). Initial ROS production was quantified by fluorescence

intensity ratio of CellROX Green reagent to Gastrin-MNP labeling of confocal microscopy images (LSM780 confocal microscope, Zeiss) using Image J software. 20-30 cells/experiment were analyzed from at least 4 independent experiments.

Analysis of lipid peroxidation

INR1G9-CCK2R cells were seeded 24 h before the experiments onto 4-compartment Cellview dishes (Greiner Bio-One) at a density of 60 to 120x10^3 cells/compartment and incubated with Gastrin-MNP (16µg Fe_3O_4/ml) for 24h. Cells were rinsed twice with incubation medium and incubated with 1mM DFO or 1nM BafA1 for 1h. Cells were then incubated with Image-IT® lipid peroxidation reagent (Molecular probes, Excitation: 488nm) in medium according to manufacturer's instructions, during 30-min AMF exposure, rinsed and analyzed using confocal microscopy (LSM780 confocal microscope, Zeiss). Lysosomal lipid peroxidation were quantified by fluorescence intensity ratio of lipid peroxidation reagent to Gastrin-MNP labelings of confocal microscopy images (LSM780 confocal microscope, Zeiss) using Image J software. 20-30 cells/experiment were analyzed from at least 4 independent experiments.

Local heat quantification

INR1G9-CCK2R cells were seeded at a density of 250x10^3 cells onto 35-mm dishes and transfected with 0.1µg of YFP-Lamp1 (Addgene, plasmid #1816) and 2.9µg of pcDNA3 using Lipofectamine 2000 reagent (Life technologies). 24h post-transfection, cells were incubated with Gastrin-MNP-DY549 (16µg Fe_3O_4/ml) for 24h, included in 0.5% agarose gel, poured into the electromagnet placed in a CELLView dish and covered with RPMI containing 0.5% FBS, as previously described (18). Different positions were marked inside and outside the gap. Cells were exposed to the AMF (53mT, 300kHz). Before and during AMF application, fluorescence intensities of DY549 (excitation: 540nm) and YFP-Lamp1 (excitation: 510nm) were measured from confocal microscopy images LSM780 confocal microscope, Zeiss) using ImageJ software. Twenty to thirty cells/experiment were analyzed from 4 independent experiments.

CathB leakage from lysosome

INR1G9-CCK2R cells were seeded at a density of 250x10^3 cells onto 35-mm dishes and transfected with 0.1µg of RFP-Lamp1 (Addgene, plasmid#1816), pCathB-eGFP (given by Klaudia Brix, Jacobs University Bremen, Germany) and 2.9µg of pcDNA3 using Lipofectamine 2000 reagent (Life technologies). 4h post-transfection, cells were seeded onto 4-compartment Cellview dishes (Greiner Bio-One) at a density of 60x10^3 cells/compartment, grown overnight and incubated with Gastrin-MNP (16µg Fe_3O_4/ml) for 24h, rinsed twice with incubation medium and exposed to AMF for 2h. CathB leakage from lysosome was analyzed

by measuring the colocalization between the GFP-CathB and RFP-Lamp1 proteins and the fluorescence intensity ratio of GFP-CathB to RFP-Lamp1 labelings (excitation : 488 and 540nm respectively) of confocal microscopy images (LSM780 confocal microscope, Zeiss, ImageJ software). 200-300 cells/experiment were analyzed from 4 independent experiments.

For real-time analysis of CathB leakage, INR1G9-CCK2R cells were seeded at a density of $250x10^3$ cells onto 35-mm dishes and transfected with 0.1µg of pCathB-eGFP (given by Klaudia Brix, Jacobs University Bremen, Germany), 0.1µg RFP-Lamp1 (Addgene, plasmid #1817) and 2.8µg of pcDNA3 using Lipofectamine 2000 reagent (Life technologies). 24h post-transfection, cells were incubated with Gastrin-MNP (16µg Fe_3O_4/ml) for 24h. INR1G9-CCK2R cells expressing or not GFP-CathB and having or not internalized Gastrin-MNP were included in 0.5% agarose gel, poured into the electromagnet placed in a CELLView dish and covered with RPMI containing 0.5% FBS, as previously described {Conord, 2015 #200}. Different positions were marked inside and outside the gap. Cells were exposed to the AMF (53mT, 300kHz) for 60min. Before and during AMF application, CathB leakage from lysosome was analyzed by measuring the colocalization between the GFP-CathB and RFP-Lamp1 proteins labeling from confocal microscopy images of the marked positions by measuring the % of green pixels (GFP-CathB) colocalized with red pixels (RFP-Lamp1) (ImageJ software). Twenty to thirty cells/experiment were analyzed from 4 independent experiments.

Analysis of Caspase-1 and -3 activation

Cells were seeded 24h before the experiments onto 4-compartments Cellview dishes (Greiner Bio-One) at a density of 60 to $120x10^3$ cells/compartment and incubated with Gastrin-MNP (16 µg Fe_3O_4/ml) for 24h and exposed to AMF for 2h. Cells were incubated with Fluorochrome-Labeled Inhibitors of Caspase-1 (FLICA, FAM-YVAD-FMK, excitation: 488nm) or Caspase-3 (FLICA, FAM-DEVD-FMK, excitation: 488nm) reagent (Immunochemistry technologies) for 1h according to manufacturer's instructions. As a positive control for caspase-3 activation, INR1G9-CCK2R cells were incubated with 1 µM staurosporine for 4h. In some experiments, cells were pretreated with 2.5µM Caspase-1 inhibitor, 10µM Caspase-3 inhibitor or 10µM CA-074-Me CathB inhibitor for 1h. Inhibitors were washed from the cells before adding FLICA. Next, cells were washed and analyzed by confocal micrsocopy (LSM510 confocal microscope, Zeiss). After Caspase-1 staining, cells were labeled with AnnexinV-iFluor555 according to manufacturer's instruction (AAT Bioquest). Counting of labeled cells was carried out by analyzing confocal microscopy images representing populations of 2-3000 cells/experiment using ImageJ software.

Mitochondrial Membrane Potential Assay

For fluorometric measurement of mitochondrial outer membrane permeabilization (MOMP), INR1G9-CCK2R cells were seeded 24h before the experiments onto four-compartments Cellview dishes (Greiner Bio-One) at a density of $60x10^3$ cells/compartment and incubated with Gastrin-MNP (16µg Fe_3O_4/ml) for 24h, exposed to AMF for 2h and stained, 4 or 24h after AMF application, with 10µM JC10 for 30-min as manufacturer's instruction (AAT Bioquest). Next, 2-3000 cells/experiments were washed and analyzed by confocal micrsocopy (LSM780 confocal microscope, Zeiss). Quantification of MOMP was performed by analyzing the green/red fluorescence ratio of confocal microscopy images.

DNA fragmentation

INR1G9-CCK2R cells were seeded 24h before the experiments onto four-compartment Cellview dishes (Greiner Bio-One) at a density of $60x10^3$ cells/compartment and incubated with Gastrin-MNP (16µg Fe_3O_4/ml) for 24h, exposed or not to AMF for 2h and stained, 4 or 24h after AMF application. Then, the terminal deoxynucleotidyl transferase-mediated biotinylated UTP nick end labeling (TUNEL) assay was performed for adherent cells with Cell Meter TUNEL Apoptosis Assay kit (AAT Bioquest) according to the manufacturer's instructions. As controls of apoptotis and necrosis, cells were respectively treated with 1µM of staurosporine (6h) or incubated at 45°C in water-bath (30-min). After the TUNEL reaction, nuclei were counterstained with DAPI (4',6-diamidino-2-phenylindole). 2-3000 cells/experiments were analyzed under a fluorescence confocal microscope (LSM780 confocal microscope, Zeiss) using 550 or 385nm excitation filter, and 590 or 420nm band pass filter for TUNEL and DAPI assays, respectively. Images of 10 microscopic fields at 40-fold magnification were captured randomly, and the number of TUNEL-positive cells and DAPI-positive nuclei was counted manually to calculate the percentage of cells presenting DNA fragmentation.

$250x10^3$ INR1G9-CCK2R cells were seeded 24h before the experiments onto 35-mm dishes, incubated with Gastrin-MNP (16µg Fe_3O_4/ml) for 24h, exposed or not to AMF for 2h. Cells were scraped and centrifuged (1000xg, 5-min) in PBS at 4°C. The pellet was resuspended in 40µl phosphate-citrate buffer consisting of 192 parts of 0.2M Na_2HPO_4 and 8 parts of 0.1M citric acid (pH7.8), incubated at room temperature for at least 30-min and centrifuged 1000xg for 5 min. 3µl of 0.25% Nonidet NP-40 and 3µl of RNase (1 mg/ml) were added to the supernatant and incubated for 30-min at 37°C. Then, 3µl of proteinase K (1 mg/ml) was added and incubated for another 30-min at 37°C. Samples were loaded on a 1.5% agarose gel and electrophoresis was performed at 4V/cm for about 4h. DNA was detected by ethidium bromide under UV light.

Il-1β secretion

To evaluate Il-1 β secretion, INR1G9-CCK2R or Thp1 macrophages were seeded 24h before the experiments onto 35-mm dishes, primed or not with ultrapure lipopolysaccharide (LPS, 500 ng/mL) (Invivogen) for 24h, incubated with Gastrin-MNP (16µg Fe_3O_4/ml) for 24h, exposed or not to AMF for 2h. Supernatants were recovered and assayed for Il-1 β secretion with an ELISA kit according to the manufacturer's instructions (Becton Dickison).

Cell lysis and Western blotting

INR1G9-CCK2R or Thp1 macrophages were seeded 24h before the experiments onto 35-mm dishes, primed or not with ultrapure LPS (500 ng/mL) (Invivogen) for 4h, incubated with Gastrin-MNP (16µg Fe_3O_4/ml) for 24h, exposed or not to AMF for 2h. Cells were lysed in 10mM HEPES (pH7.5) buffer containing 10mM KCl, 0.1mM EDTA, 0.1mM EGTA, 1mM DTT, 2% Complete protease inhibitor cocktail® (Roche, 1 tablet/ml), 1mM Na_3VO_4 and 1% Nonidet P-40. Proteins were separated by SDS-PAGE followed by Western-blot assays using anti-Il-1β (1/500, sc-7884 Santa Cruz Biotechnologies), anti-Caspase-1 (1/200, sc-514 M20 Santa Cruz Biotechnologies) or anti-Caspase-3 (1/200, sc-271759 C6 Santa Cruz Biotechnologies) followed by reprobing with anti-GAPDH (1/1000, sc-25778 FL335, Santa Cruz Biotechnologies) for loading control. The protein expression signal was detected with Pierce SuperSignal Western blotting substrate.

Analysis of lysosomal acidity

INR1G9-CCK2R cells were seeded 24h before the experiments onto four-compartments Cellview dishes (Greiner Bio-One) at a density of $60x10^3$ cells/compartment and incubated with 1 nM BafA1 for 1h at 37°C, stained with 5 µg/ml acridine orange for 15-min and rinsed in complete medium. Cells were observed under a fluorescence confocal microscope (LSM780, Zeiss) using 550nm excitation filter and 590nm band pass filter. Measurements of lysosomal red AO-fluorescence were analyzed by determining the intensity of red fluorescence over that of control cells.

Statistical analysis

Results are expressed as the mean ± SEM of at least 3 independent experiments. Statistical analysis was performed using ANOVA test. Differences were considered significant when $p < 0.05$.

Results

Magnetic intra-lysosomal hyperthermia (MILH) enhances ROS production through the Fenton reaction within lysosomes

Over-expression of hormone receptors is a hallmark of neuroendocrine tumors which thus represent a perfect model for the experimentation of tumor cell targeting with ligand-

grafted MNPs. We previously showed that Gastrin-grafted iron oxide MNPs (termed Gastrin-MNP) are internalized specifically by the pancreatic endocrine tumoral cells INR1G9 overexpressing the CCK2R (INR1G9-CCK2R cells) through a CCK2R-dependent physiological process, and are then trafficked to lysosomes where they accumulated (Fig.1A). Upon AMF exposure, Gastrin-MNPs killed 32.3±2.7% of INR1G9-CCK2R tumoral cells by a phenomenon that we termed "Magnetic IntraLysosomal Hyperthermia" (MILH) (4) (Fig.1A). Four hours after MILH treatment, the rate of cell damage reached 19.9±1.5% (i.e. 3.5±0.3-fold basal) as indicated by AnnexinV and propidium iodide labelings (Fig.1A). Both annexinV and propidium iodide labelings, which constitute early features of MILH cell death, were thus used throughout our study to appreciate cell death.

So far, our current knowledge on the mechanism of cancer cell death caused by MILH treatment is still elusive, although we and others identified cellular ROS production and lysosome leakage as biological events accompanying cell death (4,5,15). To gain insight into cell death mechanisms, we hypothesized that AMF application to cells containing MNPs would generate a nanoscale temperature elevation and, inasmuch as MNPs are concentrated into lysosomes, heating of lysosome content would trigger a death signaling cascade initiated by the enhancement of ROS production within lysosomes. Indeed, in addition to being a major digestive compartment, lysosomes are well-known major sites of ROS production through the Fenton reaction ($Fe^{2+}+H_2O_2 \rightarrow Fe^{3+}+OH^-+OH^\bullet$) which catalyzes the transformation of hydrogen peroxide to hydroxyl radicals. This reaction is dependent on low-molecular-weight iron derived from degraded iron-containing proteins, lysosomal lumen acidity and temperature (16-18). It is also known that high levels of ROS cause lysosome membrane permeabilization (LMP) whereby lysosomal cathepsins, as well as other hydrolytic enzymes, are released from the lysosomal lumen to the cytosol and trigger cell death (Fig.1A-B) (19). In INR1G9-CCK2R cells, MILH increased ROS levels by 5.7±1.5-fold over the basal value (Fig.1B, 7A). Such effect is potentiated by the addition of FeCl3 which increased ROS levels to 7.5±0.7-fold. In contrast, intralysosomal chelation of iron by Desferrioxamine (DFO) (20) prevented MILH-increased cellular ROS production which returned nearly to the basal value (2.0±0.5-fold over basal). Also, the inhibition of the vacuolar H^+-ATPase pump by Bafilomicyne A (BafA1) treatment which caused intralysosomal pH rise (Fig.7B) decreased MILH-induced cellular ROS level to 2.7±0.4-fold over basal value (Fig.1B, 7A). Conversely, treatment of cells by Artesunate (ART), an activator of vacuolar H^+-ATPase pump decreasing intralysosomal pH (Fig.7B) (18), increased MILH-enhanced cellular ROS production from 5.7±1.5- to 8.3±0.3-fold over basal value (Fig.1B, 7A).

We previously showed that ROS production was significantly detectable after 30-min of AMF exposure (15). To precisely identify subcellular site(s) of ROS which are initially produced in MILH condition, a series of experiments combining confocal microscopy imaging and pharmacological agents were carried out. Firstly, analysis of confocal microscopy images indicated that fluorescent ROS sensor co-localized with Gastrin-MNPs in lysosomes after 30-min of AMF exposure (Fig.1C). Quantification of lysosomal ROS images showed that MILH enhanced ROS level in the vicinity of Gastrin-MNPs within lysosomes (% of relative fluorescence: 48.5±3.9% versus 24.8±1.1%). Moreover, addition of $FeCl_3$ augmented MILH-induced lysosomal ROS production by 1.3±0.1-fold (60.7±6.1% vs 48.5±3.9%), wheareas DFO inhibited it (37.8±5.8%). Variation of lysosomal pH also modified lysosmal ROS production. Indeed, while ART treatment increased MILH-induced lysosomal ROS production by 1.7±0.1-fold (80.9±8.5% vs 48.5±3.9%), BafA1 inhibited it (24.7±4.2%). Together, these results demonstrate that MILH initially generates ROS through the Fenton reaction within lysosomes where Gastrin-MNPs are accumulated.

However, as the ROS production can occur in other subcellular sites, we also determined whether MILH also generates ROS by activating, for instance, the mitochondrial respiratory chain complex or NADPH oxidases which are transmembrane proteins mostly present at the plasma membrane, in endosomes and in endoplasmic reticulum (21). We found that rotenone, an inhibitor of the mitochondrial respiratory chain complex, did not modify cellular ROS generation by MILH, whereas diphenyleneiodonium (DPI), an inhibitor of NADPH oxidases, decreased it (5.9±1.8- and 3.8±1.3-fold over basal value in the presence of rotenone or DPI, respectively versus 5.7±1.5-fold) (Fig.8). Hence, MILH initially triggers ROS production through the Fenton reaction within lysosomes and, likely secondary, through NADPH oxidases. Of note, no significant variation in ROS level was observed between the different conditions in the absence of AMF exposure (Fig.7A, 8).

We further investigated the mechanism whereby MILH enhanced the Fenton reaction in lysosomes. Firstly, we examined the possibility that Fe ions, participating in the Fenton reaction, could originate from MNPs dissolution in lysosomes during high frequency AMF exposure. Indeed, it has been reported that iron oxide MNPs, in the absence of AMF application, are degraded in vitro in an acidic buffer expected to mimic the lysosomal environment (22). On the other hand, another study performed at neutral pH, attributed ROS production to the catalytic reaction at the surface of MNPs rather than to being caused by dissolved iron from MNPs (23). Using particle electron paramagnetic resonance (pEPR) to determine cellular superparamagnetic iron content, we found that internalized Gastrin-MNPs were not degraded

following AMF application (0.94±0.06 vs 0.92±0.03 pg magnetic Fe/cell) (Fig.1D), indicating that MILH-induced ROS production was the result of enhanced Fenton reaction catalysis using cellular lysosomal iron rather than dissolved iron from MNPs.

Secondly, we evaluated the temperature rise during MILH experiments. So far, experimental data indicates that the death of cancer cells in MILH occurs without any perceptible temperature increase. The hypothesis that nanoscale heating occurs at proximity of MNPs has been supported by several experimental reports (24), but direct data accounting for such a phenomenon in MILH were still lacking. In particular, no intracellular or intra-lysosomal temperature measurement under magnetic hyperthermia has been reported so far in the literature. We therefore conducted such experiments, using fluorescent molecular thermometers and a previously described device which enables confocal fluorescence imaging of cells during MILH experiments15. Molecular thermometers were composed of the fluorescent moieties DY549 attached to MNPs via PolyEthyleneGlycol of 7nm-length or the Yellow Fluorescent Protein (YFP) linked to Lysosome-Associated Membrane Protein 1 (Lamp1) (4). Intensity of fluorescence emission of the two probes was previously shown to depend on the temperature (25). This relationship was confirmed by the calibration curve showing linearity of fluorescence intensity decrease as a function of temperature increase (Fig.9). Quantitative fluorescence imaging was then carried out on cells exposed to AMF for a limited duration (<10-min) and incubated with ROS scavenger NAC in order to preserve lysosome integrity and avoid possible chemical quenching of the fluorescent molecular thermometers by ROS. As shown on Fig.1E, fluorescence intensity of DY549 grafted to MNPs declined with the time of AMF exposure. According to the calibration curve (Fig.9), the percentage of decrease of fluorescence intensity observed after ~7-min of treatment corresponds to a temperature increase of 14.1±1.4°C, indicating that the temperature actually reached 51°C at 7nm-distance from the MNP core. However, fluorescence intensity of YFP-Lamp1 did not significantly change during MILH experiments (Fig.1E). These results strongly support that AMF exposure to MNPs that have been accumulated in lysosomes causes a significant temperature increase at the immediate vicinity of the MNPs since it is not detected at the outer surface of lysosomes.

MILH-enhanced ROS production within lysosomes causes lysosomal membrane permeabilization and cell death

We further assessed the relationship between ROS generation within lysosomes and cell damage. ROS can destabilize and permeabilize lysosome membranes through lipid and protein peroxidation (3). We performed experiments combining confocal microscopy imaging and pharmacological agents to analyze whether MILH induces the peroxidation of lysosomal lipids

(Fig.2A). Analysis of confocal microscopy images indicated that MILH enhanced the level of lipid peroxidation which was detectable from 30-min of AMF application, and co-localized with Gastrin-MNPs (% of relative fluorescence: 74.4±2.7% vs 41.5±5.6%). Moreover, intralysosomal chelation of iron by DFO or BafA1 treatment decreased MILH-induced lysosomal lipid peroxidation (54.4±3.1% and 48.7±15.1%). Together, these results demonstrate that MILH induces lysosomal lipid peroxidation concomitantly with lysosomal ROS production.

Since MILH stimulates lysosomal ROS production and lipid peroxydation, it appeared likely that LMP subsequently occurs. Previously, we documented that, in MILH circumstances, lysosomal integrity was affected as suggested by the decrease of lysosome labeling by LysoTracker. However, the criterium of LysoTracker labeling is insufficient to characterize LMP since it may account for leaking of low molecular weight components and not lysosomal enzymes which are key actors in lysosome functions. Herein, we determined whether ROS production in lysosomes truly triggered LMP. The decrease of CathB content in lysosomes (labeled with RFP-Lamp1) was chosen to represent lysosomal enzyme leakage (Fig.2B). In absence of AMF application, INR1G9-CCK2R cells having internalized Gastrin-MNPs presented a high level of GFP-CathB/RFP-Lamp1 colocalization which was reduced by the application of AMF (Pearson coefficient: 0.54±0.03 vs 0.69±0.02 in presence vs absence of AMF). The effect of MILH on GFP-CathB/RFP-Lamp1 colocalization was cancelled in the presence of the NAC scavenger (Pearson coefficient: 0.74±0.03, Fig. 2B, 10). Moreover, quantification of fluorescence intensity showed that MILH decreased lysosomal CathB levels by 19.2±3.7% (% of relative fluorescence: 30.7±3.9% vs 50.5±3.8%), whereas addition of NAC prevented it (50.3±5.8%). These results demonstrate that lysosomal leakage was entirely related to MILH-enhanced ROS production.

We then determined whether the leakage of CathB from lysosomes constituted an early event in the signaling cascade leading to cell death. During MILH experiments performed using a miniaturized electromagnet (AMF: 53mT, 300kHz) (15), we evaluated the decrease of the colocalization of GFP-CathB with RFP-Lamp1, a protein resident of lysosome membrane, in real time (Fig.2C). Before or after AMF exposure, INR1G9-CCK2R cells having internalized Gastrin-MNPs presented a high level of GFP-CathB/RFP-Lamp1 colocalization (Pearson coefficient>0.70). However, the lysosomal CathB level decreased significantly by 25.4±4.7% and 43.9±6.3% after 30 and 60-min of MILH treatment respectively, demonstrating that leakage of lysosome content is an early event occurring concomitantly with the generation of lysosomal ROS. Of note, RFP-Lamp1 and GFP-CathB fluorescence intensities, other LMP markers26,

decreased respectively by 20±2.4% and 16.5±6.6% from 30-min of AMF exposure, strongly suggesting that the changes in RFP-Lamp1 and GFP-CathB fluorescence represent respectively lysosomal rupture and CathB leakage from lysosome into the cytosol and that both events occur early in the signaling cascade leading to cell death.

Finally, we wished to establish the relationship between ROS generation within lysosomes and cell death MILH experiments. We found that the addition of $FeCl_3$ or ART, which enhance ROS production in the cell medium, augmented cell death induced by MILH (4.0±0.3- and 4.1±0.4-fold over basal value respectively vs 2.6±0.2-fold in presence of Gastrin-MNP alone, Fig.2D, 11). In contrast, NAC, DFO and BafA1 treatments which trapped ROS or inhibited their formation, prevented MILH-induced cell death (0.8±0.1, 1.4±0.1 and 1.3±0.1-fold over basal value respectively) (Fig.2D, 10, 11). Moreover, MILH-induced cell death was not inhibited by rotenone or DPI (Fig.12), indicating that neither the mitochondria respiratory chain complex nor NADPH oxidases were involved in cell death, further supporting the idea that ROS generated by NADPH oxidases are secondary to lysosomal stress caused by MILH treatment. All together, these results demonstrate that lysosomal ROS production, which is enhanced by MILH through the Fenton reaction, is at the origin of cancer cell death.

Cancer cell death induced by MILH is dependent on CathB activity

In a previous study, we showed that MILH-induced cell death depends on lysosomal cysteine cathepsins which include cathepsins B, C, H, K, L, S and X (4). Herein, we performed experiments to more precisely identify the enzyme(s) involved. A likely candidate is CathB which is involved in lysosomal cell death, abundant in lysosomes, overexpressed in cancers and maintains its activity at neutral pH (27-29). MILH experiments were performed in the presence of the selective inhibitor of CathB CA-074-Me (30) or by overexpressing the enzymatically inactive mutant GFP-CathB-C29A. As shown in Fig.3A-B, both the inhibitor CA-074-Me and the inactive mutant GFP-CathB-C29A prevented MILH-induced cell death (1.2±0.1 and 1.5±0.1-fold over basal value vs 2.5±0.1-fold). In contrast, overexpression of wild-type CathB (GFP-CathB-WT) augmented the efficiency of MILH to eradicate cancer cells (4.1±0.2 vs 3.0±0.3-fold over basal, Fig.3C) reaching 34.8% of dead cells comparatively to 17.3% of dead cells in the absence of CathB-WT overexpression. These results indicate that cell death induced by MILH is dependent on CathB activity.

MILH induces cell death through a Caspase-1-dependent but Caspase-3 independent mechanism.

So far, in most circumstances, partial LMP induce cell death through an apoptotic pathway, by triggering a cascade of regulated molecular events leading to activation of the

effector apoptotic enzyme Caspase-3 (3,14). We therefore investigated whether MILH also induces cell death through an apoptotic pathway. Surprisingly, the Caspase-3 inhibitor did not inhibit MILH-induced cell death (2.7±0.2% vs 2.8±0.2-fold over basal) whereas it prevented cell death induced by staurosporine used as a reference agent to stimulate apoptosis (Fig.4A). Moreover, Caspase-3 activation was not detected neither by confocal microscopy using a fluorescent substrate (Fig.4B), nor by western blot as shown by the absence of Pro-Caspase-3 cleavage (Fig.14). We also showed that MILH did not modify mitochondrial outer membrane permeabilization (MOMP), which critically relies on apoptotic cell death, as demonstrated with staurosporine treatment (Fig.4C, 15), 1h or 4h after AMF exposure (31). Hence, cell death induced by MILH does not involve an apoptotic pathway.

In some non-epithelial cells, especially in macrophages exposed to infectious agents, the release of lysosomal hydrolases such as CathB induced after LMP was shown to activate a non-apoptotic cell death pathway involving Caspase-1 activation (32). We therefore verified Caspase-1 expression in INR1G9-CCK2R cells (data not shown) and determined whether Caspase-1 was involved in MILH-induced tumor cell death. Incubation of INR1G9-CCK2R cells with Caspase-1 inhibitor prevented cell death induced by MILH (1.6±0.2- vs 2.8±0.2-fold over basal, Fig.4D). Likewise, overexpression of Caspase-1-C284A inactive mutant inhibited cell death (1.5±0.2 vs 3.0±0.2-fold over basal, Fig.4E). It was also noticed that overexpression of Caspase-1-C284A inactive mutant lowered basal rate of cell death (amount of dead cells: 1.2±0.4% vs 6.5±0.9%). Moreover, MILH increased Caspase-1 activation (3.5±0.4, 9.0±1.3 and 12.5±2.4-fold over basal 1h, 4h and 18h after AMF exposure) and this activation was inhibited by CathB inhibitor CA-074-Me (Fig.4F, 16). It is also important to note that 84.5±2.3% of cells presenting an upregulated Caspase-1 activity were labeled with AnnexinV (data not shown). Taken together, these results demonstrate that cell death induced by MILH does not involve an apoptotic pathway, but requires Caspase-1 and Cath-B activities.

An important function of Caspase-1 consists to process the precursor of the inflammatory cytokines, interleukine-1β (Il1β) and interleukine-18 (Il-18) into their active forms (33). Furthermore, activation of Caspase-1 in cells is a hallmark of pyroptosis, which is a form of regulated cell death, usually defined by several additional biochemical features such as independence of apoptotic caspases, Ann/PI positive labeling, DNA fragmentation (34). The current study demonstrates that MILH-induced cell death is dependent on Caspase-1 activation and featured by Ann/PI labeling. Owing to functions of Caspase-1 in immune cells, we first investigated whether MILH-induced Caspase-1 activation was associated with Il1β secretion (Fig.5A). Our results show that, in INR1G9-CCK2R cells which were LPS-primed or not,

MILH did not increase Il1β secretion relative to control cells. In contrast, in LPS-primed Thp1 macrophages, which were used as reference cells for Il1β processing and secretion, levels of Il1β secretion were increased by 27.7±3.2-fold over basal value. The levels of Il1β secretion by INR1G9-CCK2R cells were very low (<2pg/mg of cell proteins) as was that of Pro-Il1β expression, comparatively to macrophages cells (data not shown). Hence, MILH induces Caspase-1-dependent cell death without activating the Caspase-1 pro-inflammatory response in the endocrine tumoral INR1G9-CCK2R cells. However, we could not exclude that pro-inflammatory response could be activated by MILH in cancer cells expressing higher level of Pro-IL1β.

Then, we characterized DNA fragmentation caused by MILH using TUNEL analysis (Fig.5B). Results indicate that, after 6h of AMF exposure, DNA fragmentation increased by 3.4±0.5-fold relative to control cells (22.9±3.8% vs 8.5±1.4% of positive cells). Of note, DNA fragmentation induced by MILH was less abundant than that caused by staurosporine or by 42°C water bath (40.1±4.9% or 52.6±14.0% of positive cells, respectively). Secondly, we characterized the type of DNA fragmentation caused by MILH (data not shown). In contrast to staurosporine treatment which provoked regular inter-nucleosomic DNA fragmentation characterized by DNA ladder (34), MILH did not induce the formation of the characteristic laddering pattern associated with apoptosis. In conclusion, our results show that MILH induced a non-apoptotic Caspase-1 dependent cell death related to pyroptosis which occurred without Il1β secretion and which was characterized by the formation of TUNEL-positive cells without exhibiting a laddering pattern (34,35).

Gastrin-grafted MNPs induces the death of cells expressing the CCK2R by MILH.

The preceding experiments analyzed the effects and mechanisms of MILH applied to the pancreatic endocrine tumor cells INR1G9-CCK2R. Herein, we extended the experiments to two other tumor cell lines, the gastric cell line AGS and the pancreatic cell line AR4-2J, which express the CCK2R at low levels (~ 100 fmol/10^6 cells) (36). Cell survival data show that, 24h after AMF exposure, MILH has eradicated 22.0±4.5% of AGS-CCK2R cells and 23.1±1.3% of AR4-2J cells presenting Gastrin-MNPs mainly in their lysosomes (Fig.6A). In the same conditions, 56.6±4.0% and 42.7±6.4% of HEK-CCK2R cells were killed using 16µg/ml or 1µg/ml of Gastrin-MNP respectively (Fig.17A). Ann/PI labeling confirmed that MILH-induced cell death was detectable 4h post-AMF (Fig.6B) and dead cells were more often labeled with PI in AGS-CCK2R and AR4-2J cells than in INR1G9-CCK2R cells. MILH also triggered cell death in the non-tumoral embryonic kidney cell overexpressing the CCK2R (HEK-CCK2R:

2.0±0.2 pmol/10^6 cells) previously used to characterize uptake and cellular trafficking of Gastrin-MNP (Fig.17B) (4,37).

Determination of the uptake of Gastrin-MNPs by the different cells indicates that receptor-mediated uptake of MNPs by AGS-CCK2R, AR4-2J and INR1G9-CCK2R cells was 0.83±0.23, 0.60±0.13 and 3.38±0.74 pg of Fe/cell which corresponded to 0.52±0.22, 0.14±0.02 and 1.07±0.28 pg of magnetic Fe/cell, respectively, as measured by particle electron paramagnetic resonance, after 24h of intracellular accumulation (Fig.6C). Of note, in HEK-CCK2R cells, Gastrin-MNPs uptake was evaluated to be 4.01±0.40 and 1.48±0.22 pg of total and magnetic Fe/cell, respectively (Fig.17C).

We finally assessed that the signaling pathway involved in MILH-induced cell death in AGS-CCK2R, AR4-2J and HEK-CCK2R cells was similar to that identified in INR1G9-CCK2R. Firstly, no significant Caspase-3 activation could be detected in the 3 cell lines, similarly to INR1G9-CCK2R cells (Fig.17D, 18). Secondly, MILH increased Caspase-1 activation, 4h after AMF exposure, by 3.5-±0.1, 3.6-±0.2-fold and 6.2±0.6-fold in AGS-CCK2R, AR4-2J and HEK-CCK2R respectively, similarly to INR1G9-CCK2R cells (Fig.6D, 17E).

These above results demonstrate that MILH is effective in inducing the death of cancer cells from three different types of cancer (pancreatic endocrine, pancreatic exocrine and gastric) even if the targeted receptor, is expressed at low levels and if minute amounts of Gastrin-MNPs are internalized. Moreover, in the three cancers, as well as in HEK cells, MILH-induced cell death occurs through activation of Caspase-1 and without activation of Caspase-3, indicating that MILH triggers a non-apoptotic cell death pathway following lysosome damage which is dependent on Caspase-1 activation.

Discussion

Following the publication of the proof-of-concept of anti-cancer nanotherapy using ligand-grafted MNPs specifically internalized via cell surface receptor, this study gained insight into the mechanisms at the origin of cell death induced by MILH (Fig.6E). Using Gastrin-MNPs which specifically target lysosomes of tumoral cells expressing the CCK2R as a killing agent, we demonstrate that tumor cell death induced by MILH occurs through a Caspase-1-dependent mechanism, but not an apoptotic signaling pathway, since Caspase-3 was not activated. This mechanism of MILH-induced cell death was demonstrated in pancreatic endocrine tumor cells as well as in gastric and pancreatic exocrine tumor cells expressing the CCK2R.

MILH first upregulates the catalysis of ROS production through the Fenton-type reaction within lysosomes which subsequently causes lipid peroxidation, followed by LMP and

the leakage of lysosomal content into the cytosol. Among the lysosomal enzymes, CathB plays a critical role in cell death and activates Caspase-1. Thus, MILH-induced tumor cell death can be related to pyroptosis mainly described in macrophages, but rarely in epithelial cells (32,38,39). Indeed, we showed that dead cells present AnnexinV and/or propidium iodide positive labelings and irregular DNA fragmentation (TUNEL positive staining without laddering pattern) as previously observed in pyroptotic macrophages (34,35,40). However, whilst Caspase-1-dependent cell death by pyroptosis in macrophages is usually associated with pro-inflammatory responses resulting from Caspase-1 cleavage of Il-1β and -18, MILH did not increase Il-1β cleavage. These last results are in line with recent studies showing that Caspase-1 can induce pyroptotic cell death independently of Il1-β processing (41-43). On the other hand, Pro-Il1β is expressed at low levels in our tumor cell model. Thus, we cannot not exclude that pro-inflammatory response would be activated by MILH in cancer cells expressing higher level of Pro-IL-1β.

Our current knowledge about Caspase-1 indicates that Caspase-1 is synthesized as a cytosolic, inactive, monomeric zymogen (pro-Caspase-1) that is thought to be activated by dimerization and autoproteolytic processing, resulting in generation of large and small subunits (called p20 and p10) of the catalytically active enzyme (44,45). This activation step is preceded by recruitment of Pro-Caspase-1 into inflammasomes, which are multiprotein signaling complexes. Furthermore, a direct processing of Caspase-1 by CathB (46,47) or an indirect mechanism of activation through CathB-induced activation of inflammasome complexes (38,47-49) were reported. In the current study of MILH-induced cell death, CathB activation is critical for Caspase-1 activation and tumor cell death indicating that one of these two mechanisms may function, but this remains to be determined more precisely.

In conclusion, this study provides essential new data on the mechanism whereby targeted MNPs of low thermal power induce tumor cell death when exposed to a high frequency magnetic field. The central role of the Fenton reaction that produces ROS within lysosomes, together with that of CathB and Caspase-1, represent key elements which are the basis for optimization of MILH-induced tumor cell death and its future development as an anti-tumoral option.

EXAMPLE 2:

Magnetic intra-lysosomal hyperthermia (MILH)

The strategy developed in the team is in the field of targeted nanotherapy of cancers by magnetic hyperthermia. This strategy aims at developing a new therapeutic approach for cancer eradication by tumor targeting using magnetic iron oxide nanoparticles on which the ligand of

a receptor overexpressed in cancers is grafted. The ligand allows the specific binding of the nanoparticles to the receptors located on the surface of cancer cells and then the activation of these receptors triggers the process of internalisation of the "cargo" composed of the receptor, its ligand and the magnetic nanoparticles. This internalization is followed by intracellular transport within vesicles of endocytosis to the lysosomes, vesicles of degradation of "cellular waste". After the cells have accumulated the magnetic nanoparticles in their lysosomes, they are subjected to a high frequency alternating magnetic field which leads to cell death.

There are several important points to remember in this strategy:

• the high specificity of the targeting and the characterization of the cellular and molecular mechanisms governing the internalization of the vectorized nanoparticles,

• the fact that the application of a high frequency magnetic field causes the death of tumor cells having internalized very small quantities of nanoparticles (0.2-2 picograms per cell),

• The magnetic field has no effect on cells devoid of nanoparticles,

• Death occurs without any perceptible increase in the temperature of the environment, hence the name of the strategy: magnetic intra-lysosomal hyperthermia (MILH).

We have demonstrated that the application of the magnetic field causes a temperature increase at the surface of the nanoparticles which is detected using molecular thermometers. On the other hand, the temperature increase is no longer perceptible at the level of the external surface of the lysosome. We have introduced the term "Magnetic Intra-lysosomal Hyperthermia" (MILH) to name this type of hyperthermia.

MILH catalyzes ROS production by the Fenton reaction within the lysosomes. This reaction is at the origin of the signaling cascade leading to lysosome permeabilization and to cell death. We have demonstrated that an iron-complexing agent prevents these events and that, conversely, the culture of cells in an iron-ion enriched medium increases the treatment efficiency (death level increased by 40%) (Figure 2D). Similarly, a pH-neutralizing agent (bafilomycin A) of the lysosomes inhibits these effects, whereas an agent increasing the acidity of the lysosomal pH (Artesunate) increases them.

To date, MILH has been tested and validated by targeting the gastrin receptor (G-protein coupled transmembrane receptor, named CCK2R) overexpressed on the surface of pancreatic endocrine tumor cells, pancreatic exocrine or gastric cancer. Targeting of the iron oxide nanoparticles (size 10 nm) was obtained by grafting, on the surface of these nanoparticles, a peptide analogue of natural gastrin.

From a mechanistic point of view, we have also demonstrated that:

• Cysteine protease involved in MILH-induced death is Cathepsin-B.

• The mechanism of death induced by MILH is not apoptosis and does not involve Caspase-3. It is a mechanism involving Caspase-1 which could be related to cell death by pyroptosis, known to occur in cells of the immune system during inflammatory processes. In addition, activation of Caspase-1 occurs without proteolysis of pro-Caspase 1 and without secretion of interleukin-1β (IL1β) in the cell lines used in this study. However, Pro-Caspase-1 proteolysis and Il1β secretion may happen in other cell lines, depending on the level of their expression.

Lysosome permeabilization can be induced in apoptotic signaling initiated from death receptors or using lysosomotropic agents. To date, these agents do not specifically target tumor cells. Magnetic intra-lysosomal hyperthermia (MILH) induces cell death by a different mechanism, although initiated by permeabilization of the lysosome membrane. The leakage of lysosomal enzymes and more particularly of Cathepsin-B activates the pro-inflammatory and non-apoptotic Caspase-1 which then triggers a mechanism of cell death by pyroptosis.

MILH uses the newly emerging lysosomal death pathway and is described as a promising way to circumvent the apoptosis resistance phenomena that cancer cells develop before and during anti-cancer treatments (§1). On the other hand, this therapeutic strategy could also be used in combination with conventional treatments to increase the efficacy of eradication of tumor cells while decreasing the doses of the latter in order to limit their side effects (see Example 1 And §2).

§1 – Strategies to increase the effectiveness of HMIL

MILH-induced death pathway uses the Fenton reaction taking place within the lysosomes. Several approaches could be used to increase this one:

- in the presence of an excess of iron in solution (FeCl3, see figure 2D): iron enrichment could also be envisaged by a pretreatment with transferrin.

- by increasing the acidification of lysosomal pH, as we have shown with artesunate pretreatment, an activator of ATPase proton pump (see figures 2D and 7B with the artesunate (ART)).

- Catalysis of the Fenton reaction could also be increased by using nanoparticles with higher thermal power. Magnetic nanoparticles are capable of transforming electromagnetic energy into heat when exposed to a high frequency alternating magnetic field. The heating of the magnetic particles depends on their size and their magnetic properties.

- In addition, preliminary data obtained in the team show that MILH induced HSP70 expression protecting cancer cells from death (data not shown) and that overexpression of the

HSP70 heat shock protein inhibits lysosomal membrane permeabilization and MILH-induced cell death (data not shown). It is therefore not excluded that HSP70, localized in lysosomes, play a protective role in the efficiency of HMIL on the leakage of the lysosome membrane. It should be noted that HSP proteins are often overexpressed in tumor cells. Their activity is modulable by means of pharmacological inhibitors. Pretreatment with HSP70 inhibitors could increase the effectiveness of the HMIL strategy (see example 3: HMIL and HSP70 inhibitors).

After permeabilization of the lysosome membrane, lysosomal enzymes including Cathepsin-B are released into the cytosol. We showed that Cathepsin-B has a primordial role in the cell death triggered by MILH since it activates Caspase-1, the enzyme executing cell death.

According to most studies using death ligands or lysosomotropic agents (lysosome-attacking agents), the lysosomal death pathway is generally associated with death by apoptosis. However, our results show that MILH does not induce apoptosis but a Caspase-1-dependent pathway that could be related to pyroptosis. These data are an advantage because MILH could be an alternative to eradicate tumor cells resistant to conventional treatments and cell death by apoptosis. Moreover, cells dying by pyroptosis present a "porous" plasma membrane allowing the passage of pro-inflammatory molecules, such as ATP. Thus, unlike apoptosis which is considered immunologically silent, pyroptosis has the power to stimulate inflammation, which from the point of view of anti-cancer therapies is an advantage. Finally, the level of Pro-Caspase 1 (the pro-form of Caspase-1) can be stimulated by cytokines such as TNFα or interleukin 1α; it can therefore be envisaged to increase the effectiveness of an anti-cancer treatment by MILH by first administering a cytokine, such as TNFα, to the patients.

§2 – Strategies to increase the efficiency of tumor cell eradication: HMIL co-treatment and chemotherapy (see attached article, in the course of writing)

We observed that the combination of two treatments, MILH and doxorubicin (used for the treatment of endocrine tumors) increases the effectiveness of eradication of tumor cells. Doxorubicin treatment induces cell death by a Caspase-3-dependent apoptotic pathway without activating Caspase-1, while MILH activates the Caspase-1 dependent death pathway without inducing Caspase-3 activation (see figure 19 and table 1 which show synergistic results with the doxorubicin). The two treatments therefore stimulate different death pathways. The combination of these two treatments makes it possible to combine the efficacy of the two individual treatments and thus to increase the overall efficiency to eradicate tumor cells. Moreover, such strategies combining MILH with chemotherapeutic treatment could reduce the

doses of chemotherapeutic agents, reducing their side effects and improving their tolerance by patients.

In conclusion, MILH strategy has several advantages:

• Specific targeting of tumors; Possibility of personalized treatments depending on the target biomolecule expressed in the tumor to be treated, lower predictable doses in nanoparticles, less undesired effects. The proof of concept established with targeting of the CCK2 receptor on endocrine tumor cells can be extended to any type of cancers at the condition that a receptor overexpressed on the surface of the cancer cells and endowed with internalization property has been identified.

• Increased therapeutic potential by adding iron (a priori without significant toxicity), decreased lysosomal pH ...

• Potential for bypassing resistance linked to drug efflux and apoptosis

• Possibility of potentiating the treatment with a preliminary treatment with a cytokine

• Possibility of associating this treatment with chemotherapeutic treatment; Additive effect.

The inventors also investigate the MILH in a transgenic murine model of endocrine tumors (mouse MEN1 +/-).

EXAMPLE 3: HMIL and HSP70 inhibitors:

We performed experiments combining MILH with the HSP70 inhibitor PES (2-Phenylethynesulfonamide, Pifithrin-μ). All the experiments were made on the tumoral endocrine cell line INR1G9-CCK2R. As shown in the figure 20 (a, b and c), this combination increases the efficiency to kill cancer cells with synergy, comparatively to individual treatment.

We also performed experiments combining MILH with a SiRNA directed against HSP70 to inhibit its expression. This combination increases also the efficiency to kill cancer cells with synergy, comparatively to individual treatment (Figure 21).

We next analyzed the effect of such treatments on different mechanisms involved in cell death: lysosome membrane permeabilization, activation of Caspase-1 (induced by MILH) and Caspase-3 (apoptosis), autophagy.

First, we observed that MILH/HSP70 inhibition (with PES inhibitor) increases the lysosome membrane permeabilization with a higher efficiency than individual treatments (Figure 22).

Then, we analyzed the effect of MILH and/or PES treatments on the activation of Caspase-1 and 3. We observed that MILH/HSP70 inhibition (with PES inhibitor) increases the activation of both caspases with a higher efficiency than individual treatments (Figure 23a and

b), indicating that HSP70 inhibition potentiates the activation of Caspase-1 induced by MILH and that the MILH/HSP70 inhibition activates an additional cell death mechanism, apoptosis revealed by the activation of Caspase-3.

Finally, we analyzed the effect of MILH and/or PES treatments on the formation of autophagosome/autolysosome which can protect cancer cell to death (data not shown). We observed that MILH/HSP70 inhibition (with PES inhibitor) decreases autophagy with a higher efficiency than individual treatments.

EXAMPLE 4: others cancerous cells lines and parameters:

Most of the previous results were mostly obtained on the tumoral endocrine cell line INR1G9-CCK2R. Experiments are performed on other cells lines from different cancer type such as glioblastoma, pancreatic cancer, and gastric cancer. The effect of the combination of MILH with HSP70 inhibition (PES inhibitor or SiRNA) is analyzed on cell death and survival, as well as on different biological effects or mechanisms associated with the regulation of cell death or survival such as Caspases activation, lysosome membrane permeabilization, DNA fragmentation, cytoskeleton and microtubule disorganization. Other drug inhibiting HSP70 are also used; preliminary results show identical results. The effects of the MILH/HSP70 inhibition are analyzed in vivo on different murine models of cancer: tumor growth, cell death, cell survival and proliferation, study of signaling pathways associated with cell death and survival.

REFERENCES:

Throughout this application, various references describe the state of the art to which this invention pertains. The disclosures of these references are hereby incorporated by reference into the present disclosure.

1 Kachalaki, S., Ebrahimi, M., Mohamed Khosroshahi, L., Mohammadinejad, S. & Baradaran, B. Cancer chemoresistance; biochemical and molecular aspects: a brief overview. European journal of pharmaceutical sciences : official journal of the European Federation for Pharmaceutical Sciences 89, 20-30, doi:10.1016/j.ejps.2016.03.025 (2016).

2 Groth-Pedersen, L. & Jaattela, M. Combating apoptosis and multidrug resistant cancers by targeting lysosomes. Cancer letters 332, 265-274, doi:10.1016/j.canlet.2010.05.021 (2013).

3 Repnik, U., Hafner Cesen, M. & Turk, B. Lysosomal membrane permeabilization in cell death: concepts and challenges. Mitochondrion 19 Pt A, 49-57, doi:10.1016/j.mito.2014.06.006 (2014).

4 Sanchez, C. et al. Targeting a G-protein-coupled receptor overexpressed in endocrine tumors by magnetic nanoparticles to induce cell death. ACS nano 8, 1350-1363, doi:10.1021/nn404954s (2014).

5 Domenech, M., Marrero-Berrios, I., Torres-Lugo, M. & Rinaldi, C. Lysosomal membrane permeabilization by targeted magnetic nanoparticles in alternating magnetic fields. ACS nano 7, 5091-5101, doi:10.1021/nn4007048 (2013).

6 Creixell, M., Bohorquez, A. C., Torres-Lugo, M. & Rinaldi, C. EGFR-targeted magnetic nanoparticle heaters kill cancer cells without a perceptible temperature rise. ACS nano 5, 7124-7129, doi:10.1021/nn201822b (2011).

7 Fourmy, D., Carrey, J. & Gigoux, V. Targeted nanoscale magnetic hyperthermia: challenges and potentials of peptide-based targeting. Nanomedicine (Lond) 10, 893-896, doi:10.2217/nnm.14.236 (2015).

8 Reubi, J. C. Targeting CCK receptors in human cancers. Current topics in medicinal chemistry 7, 1239-1242 (2007).

9 Silva, A. C. et al. Application of hyperthermia induced by superparamagnetic iron oxide nanoparticles in glioma treatment. Int J Nanomedicine 6, 591-603, doi:10.2147/IJN.S14737 (2011).

10 Tan, R. P., Carrey, J. & Respaud, M. Magnetic hyperthermia properties of nanoparticles inside lysosomes using kinetic Monte Carlo simulations: Influence of key parameters and dipolar interactions, and evidence for strong spatial variation of heating power. Phys Rev B 90, doi:Artn 21442110.1103/Physrevb.90.214421 (2014).

11 Gewies, A. & Grimm, S. Cathepsin-B and cathepsin-L expression levels do not correlate with sensitivity of tumour cells to TNF-alpha-mediated apoptosis. Brit J Cancer 89, 1574-1580, doi:10.1038/sj.bjc.6601297 (2003).

12 Li, W. et al. Induction of cell death by the lysosomotropic detergent MSDH. FEBS letters 470, 35-39, doi:Doi 10.1016/S0014-5793(00)01286-2 (2000).

13 Uchimoto, T. et al. Mechanism of apoptosis induced by a lysosomotropic agent, L-Leucyl-L-leucine methyl ester. Apoptosis 4, 357-362, doi:Doi 10.1023/A:1009695221038 (1999).

14 Cirman, T. et al. Selective disruption of lysosomes in HeLa cells triggers apoptosis mediated by cleavage of Bid by multiple papain-like lysosomal cathepsins. The Journal of biological chemistry 279, 3578-3587, doi:10.1074/jbc.M308347200 (2004).

15 Connord, V. et al. Real-Time Analysis of Magnetic Hyperthermia Experiments on Living Cells under a Confocal Microscope. Small 11, 2437-2445, doi:10.1002/smll.201402669 (2015).

16 Kurz, T., Gustafsson, B. & Brunk, U. T. Intralysosomal iron chelation protects against oxidative stress-induced cellular damage. The FEBS journal 273, 3106-3117, doi:10.1111/j.1742-4658.2006.05321.x (2006).

17 Ghosh, P., Kumar, C., Samanta, A. N. & Ray, S. Comparison of a new immobilized Fe3+ catalyst with homogeneous Fe3+-H2O2 system for degradation of 2,4-dinitrophenol. J Chem Technol Biot 87, 914-923, doi:10.1002/jctb.3699 (2012).

18 Yang, N. D. et al. Artesunate Induces Cell Death in Human Cancer Cells via Enhancing Lysosomal Function and Lysosomal Degradation of Ferritin. Journal of Biological Chemistry 289, 33425-33441, doi:10.1074/jbc.M114.564567 (2014).

19 Boya, P. & Kroemer, G. Lysosomal membrane permeabilization in cell death. Oncogene 27, 6434-6451, doi:10.1038/onc.2008.310 (2008).

20 Cable, H. & Lloyd, J. B. Cellular uptake and release of two contrasting iron chelators. The Journal of pharmacy and pharmacology 51, 131-134 (1999).

21 Dikalov, S. Cross talk between mitochondria and NADPH oxidases. Free radical biology & medicine 51, 1289-1301, doi:10.1016/j.freeradbiomed.2011.06.033 (2011).

22 Lartigue, L. et al. Biodegradation of iron oxide nanocubes: high-resolution in situ monitoring. ACS nano 7, 3939-3952, doi:10.1021/nn305719y (2013).

23 Wydra, R. J. et al. The role of ROS generation from magnetic nanoparticles in an alternating magnetic field on cytotoxicity. Acta biomaterialia 25, 284-290, doi:10.1016/j.actbio.2015.06.037 (2015).

24 Riedinger, A. et al. Subnanometer local temperature probing and remotely controlled drug release based on azo-functionalized iron oxide nanoparticles. Nano letters 13, 2399-2406, doi:10.1021/nl400188q (2013).

25 Huang, H., Delikanli, S., Zeng, H., Ferkey, D. M. & Pralle, A. Remote control of ion channels and neurons through magnetic-field heating of nanoparticles. Nature nanotechnology 5, 602-606, doi:10.1038/nnano.2010.125 (2010).

26 Xu, Y. et al. Protective mechanisms of CA074-me (other than cathepsin-B inhibition) against programmed necrosis induced by global cerebral ischemia/reperfusion injury in rats. Brain research bulletin 120, 97-105, doi:10.1016/j.brainresbull.2015.11.007 (2016).

27 Nomura, T. & Katunuma, N. Involvement of cathepsins in the invasion, metastasis and proliferation of cancer cells. The journal of medical investigation : JMI 52, 1-9 (2005).

28 Turk, B. et al. Regulation of the activity of lysosomal cysteine proteinases by pH-induced inactivation and/or endogenous protein inhibitors, cystatins. Biological chemistry Hoppe-Seyler 376, 225-230 (1995).

29 Pillay, C. S. & Dennison, C. Cathepsin B stability, but not activity, is affected in cysteine:cystine redox buffers. Biological chemistry 383, 1199-1204, doi:10.1515/BC.2002.132 (2002).

30 Buttle, D. J., Murata, M., Knight, C. G. & Barrett, A. J. CA074 methyl ester: a proinhibitor for intracellular cathepsin B. Archives of biochemistry and biophysics 299, 377-380 (1992).

31 Galluzzi, L. et al. Essential versus accessory aspects of cell death: recommendations of the NCCD 2015. Cell death and differentiation 22, 58-73, doi:10.1038/cdd.2014.137 (2015).

32 Galluzzi, L. et al. Molecular definitions of cell death subroutines: recommendations of the Nomenclature Committee on Cell Death 2012. Cell death and differentiation 19, 107-120, doi:10.1038/cdd.2011.96 (2012).

33 Fantuzzi, G. & Dinarello, C. A. Interleukin-18 and interleukin-1 beta: two cytokine substrates for ICE (caspase-1). Journal of clinical immunology 19, 1-11 (1999).

34 Miao, E. A., Rajan, J. V. & Aderem, A. Caspase-1-induced pyroptotic cell death. Immunological reviews 243, 206-214, doi:10.1111/j.1600-065X.2011.01044.x (2011).

35 Watson, P. R. et al. Salmonella enterica serovars typhimurium and Dublin can lyse macrophages by a mechanism distinct from apoptosis. Infection and immunity 68, 3744-3747, doi:Doi 10.1128/Iai.68.6.3744-3747.2000 (2000).

36 Scemama, J. L. et al. Characterisation of gastrin receptors on a rat pancreatic acinar cell line (AR42J). A possible model for studying gastrin mediated cell growth and proliferation. Gut 28 Suppl, 233-236 (1987).

37 Magnan, R. et al. Regulation of membrane cholecystokinin-2 receptor by agonists enables classification of partial agonists as biased agonists. The Journal of biological chemistry 286, 6707-6719, doi:10.1074/jbc.M110.196048 (2011).

38 Tseng, W. A. et al. NLRP3 inflammasome activation in retinal pigment epithelial cells by lysosomal destabilization: implications for age-related macular degeneration. Investigative ophthalmology & visual science 54, 110-120, doi:10.1167/iovs.12-10655 (2013).

39 Derangere, V. et al. Liver X receptor beta activation induces pyroptosis of human and murine colon cancer cells. Cell death and differentiation 21, 1914-1924, doi:10.1038/cdd.2014.117 (2014).

40 Brennan, M. A. & Cookson, B. T. Salmonella induces macrophage death by caspase-1-dependent necrosis. Molecular microbiology 38, 31-40, doi:DOI 10.1046/j.1365-2958.2000.02103.x (2000).

41 Miao, E. A. et al. Caspase-1-induced pyroptosis is an innate immune effector mechanism against intracellular bacteria. Nature immunology 11, 1136-1142, doi:10.1038/ni.1960 (2010).

42 Broz, P., von Moltke, J., Jones, J. W., Vance, R. E. & Monack, D. M. Differential requirement for Caspase-1 autoproteolysis in pathogen-induced cell death and cytokine processing. Cell host & microbe 8, 471-483, doi:10.1016/j.chom.2010.11.007 (2010).

43 Guey, B., Bodnar, M., Manie, S. N., Tardivel, A. & Petrilli, V. Caspase-1 autoproteolysis is differentially required for NLRP1b and NLRP3 inflammasome function. Proceedings of the National Academy of Sciences of the United States of America 111, 17254-17259, doi:10.1073/pnas.1415756111 (2014).

44 Martinon, F., Mayor, A. & Tschopp, J. The inflammasomes: guardians of the body. Annual review of immunology 27, 229-265, doi:10.1146/annurev.immunol.021908.132715 (2009).

45 Thornberry, N. A. et al. A novel heterodimeric cysteine protease is required for interleukin-1 beta processing in monocytes. Nature 356, 768-774, doi:10.1038/356768a0 (1992).

46 Vancompernolle, K. et al. Atractyloside-induced release of cathepsin B, a protease with caspase-processing activity. FEBS letters 438, 150-158 (1998).

47 Hentze, H., Lin, X. Y., Choi, M. S. & Porter, A. G. Critical role for cathepsin B in mediating caspase-1-dependent interleukin-18 maturation and caspase-1-independent necrosis triggered by the microbial toxin nigericin. Cell death and differentiation 10, 956-968, doi:10.1038/sj.cdd.4401264 (2003).

48 Hornung, V. et al. Silica crystals and aluminum salts activate the NALP3 inflammasome through phagosomal destabilization. Nature immunology 9, 847-856, doi:10.1038/ni.1631 (2008).

49 Newman, Z. L., Leppla, S. H. & Moayeri, M. CA-074Me protection against anthrax lethal toxin. Infection and immunity 77, 4327-4336, doi:10.1128/IAI.00730-09 (2009).

50. Cole AJ, Yang VC, David AE. Cancer theranostics: the rise of targeted magnetic nanoparticles. Trends Biotechnol. 2011 Jul;29(7):323-32.

51. Kim JE, Shin JY, Cho MH. Magnetic nanoparticles: an update of application for drug delivery and possible toxic effects. Arch Toxicol. 2012 May;86(5):685-700.

52. Yang HW, Hua MY, Liu HL, Huang CY, Wei KC. Potential of magnetic nanoparticles for targeted drug delivery. Nanotechnol Sci Appl. 2012 Aug 27;5:73-86.

53. Liu J, Lu W, Reigada D, Nguyen J, Laties AM, Mitchell CH. Restoration of lysosomal pH in RPE cells from cultured human and ABCA4(-/-) mice: pharmacologic approaches and functional recovery. Invest Ophthalmol Vis Sci. 2008 Feb;49(2):772-80.

54. Li X, Shao H, Taylor IR, Gestwicki JE. Targeting Allosteric Control Mechanisms in Heat Shock Protein 70 (Hsp70). Curr Top Med Chem. 2016;16(25):2729-40.

55. Assimon VA, Gillies AT, Rauch JN, Gestwicki JE. Hsp70 protein complexes as drug targets. Curr Pharm Des. 2013;19(3):404-17.

56. Reikvam H, Brenner AK, Nepstad I, Sulen A, Bruserud Ø. Heat shock protein 70 - the next chaperone to target in the treatment of human acute myelogenous leukemia? Expert Opin Ther Targets. 2014 Aug;18(8):929-44.

57. Patury S, Miyata Y, Gestwicki JE. Pharmacological targeting of the Hsp70 chaperone. Curr Top Med Chem. 2009;9(15):1337-51.

58. Guo F, Rocha K, Bali P, Pranpat M, Fiskus W, Boyapalle S, Kumaraswamy S, Balasis M, Greedy B, Armitage ES, Lawrence N, Bhalla K. Abrogation of heat shock protein 70 induction as a strategy to increase antileukemia activity of heat shock protein 90 inhibitor 17-allylamino-demethoxy geldanamycin. Cancer Res. 2005 Nov 15;65(22):10536-44.

59. Aggarwal N, Sloane BF. Cathepsin B: multiple roles in cancer. Proteomics Clin Appl. 2014 Jun;8(5-6):427-37.

CLAIMS:

1. A magnetic nanoparticle grafted with a tumor targeting agent for use in a method for inducing non-apoptotic signaling of cancer cell in a subject afflicted with cancer in need thereof.

2. A magnetic nanoparticle grafted with a tumor targeting agent in combination with one or more compound selected from the group consisting of compound inducing iron excess or iron enrichment, compound increasing the acidification of the lysosomal pH, HSP70 inhibitor, Cathepsin-B activator, and Caspase-1 activator for use in a method for inducing non-apoptotic signaling and/or inducing a signaling death pathway of cancer cell in a subject afflicted with cancer in need thereof.

3. The magnetic nanoparticle for use according to claims 1 or 2, wherein the cancer cell is resistant cancer cell.

4. The magnetic nanoparticle for use according to claims 1 or 2, wherein the magnetic nanoparticle is selected from the group consisting of iron oxide magnetic nanoparticles, iron oxide magnetic nanoparticles coated with PEG-COOH and iron oxide magnetic nanoparticles coated with PEG-amine.

5. The magnetic nanoparticle for use according to claims 1 or 2 in combination with one or more anti-cancer compound.

6. The magnetic nanoparticle for use according to claim 5, wherein the anti-cancer compound is doxorubicin.

7. A method for inducing non-apoptotic signaling of cancer cell in a subject afflicted with cancer in need thereof, comprising the steps of administering to said subject the magnetic nanoparticle grafted with a tumor targeting agent, and application of a high frequency alternating magnetic field.

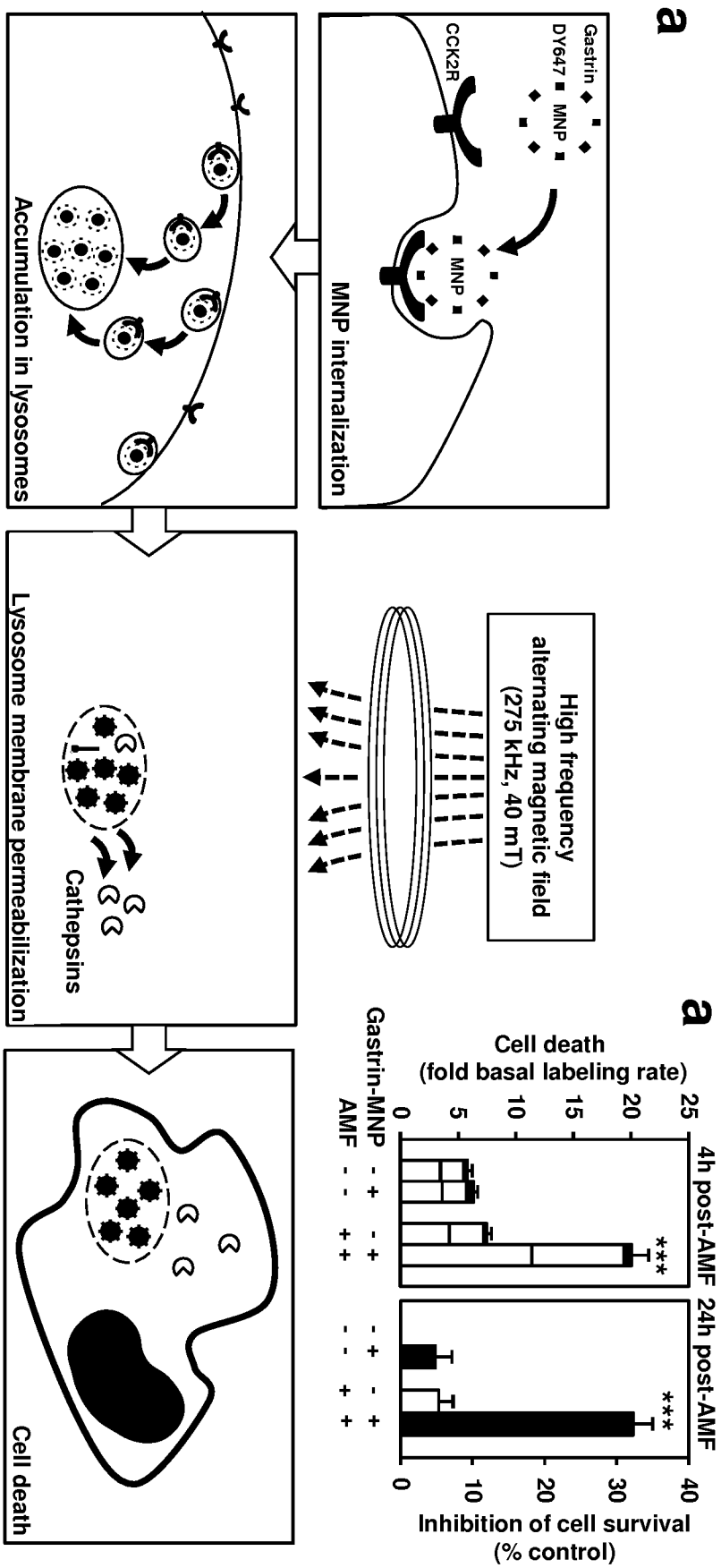
a
Gastrin
DY647
MNP
CCK2R
MNP
MNP internalization
Accumulation in lysosomes
High frequency
alternating magnetic field
(275 kHz, 40 mT)
Lysosome membrane permeabilization
Cathepsins
Cell death
a
Cell death
(fold basal labeling rate)
Gastrin-MNP
AMF
4h post-AMF
24h post-AMF
***
***
Inhibition of cell survival
(% control)

Figure 1a

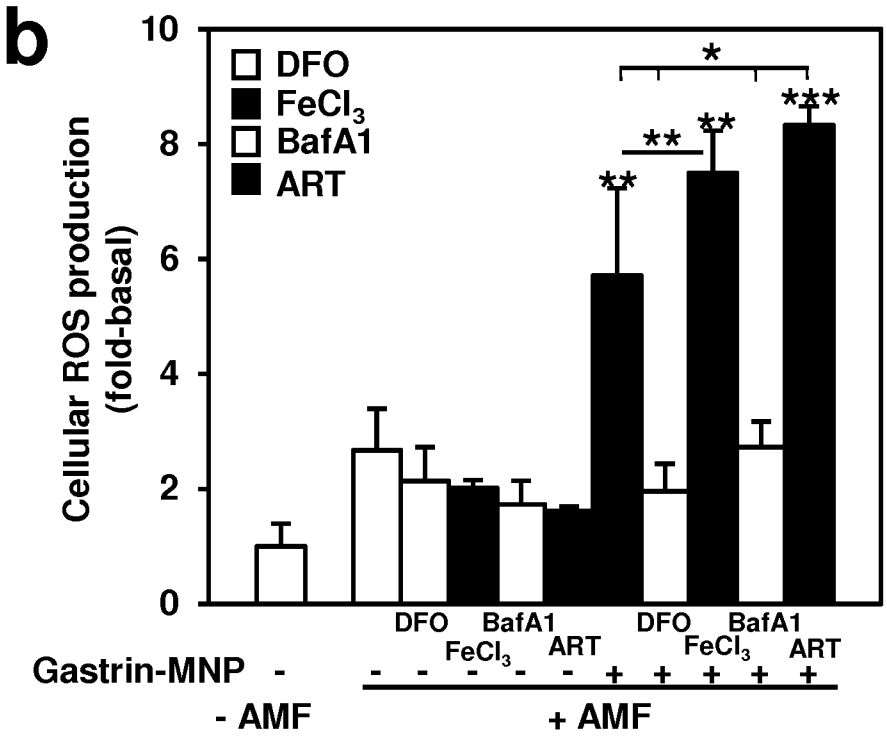

Figure 1b

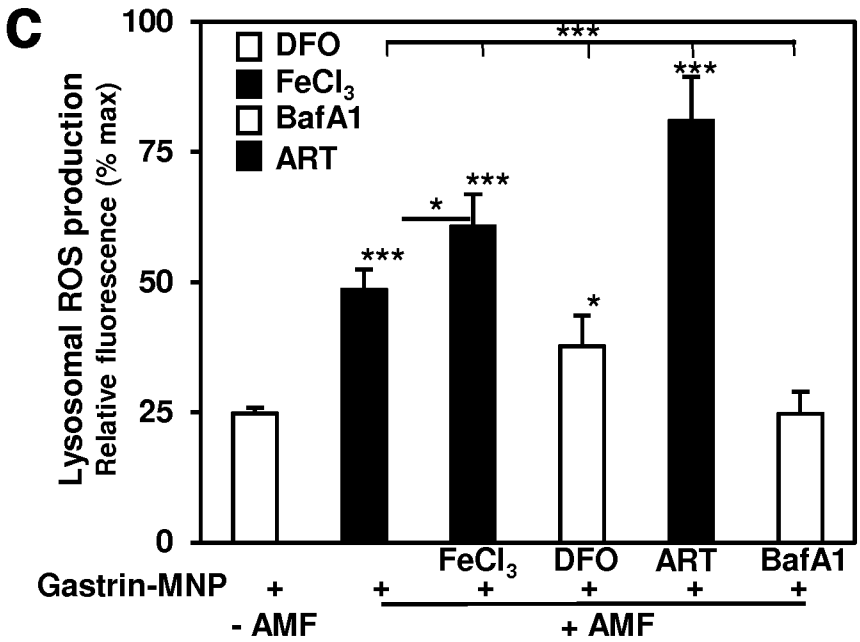

Figure 1c

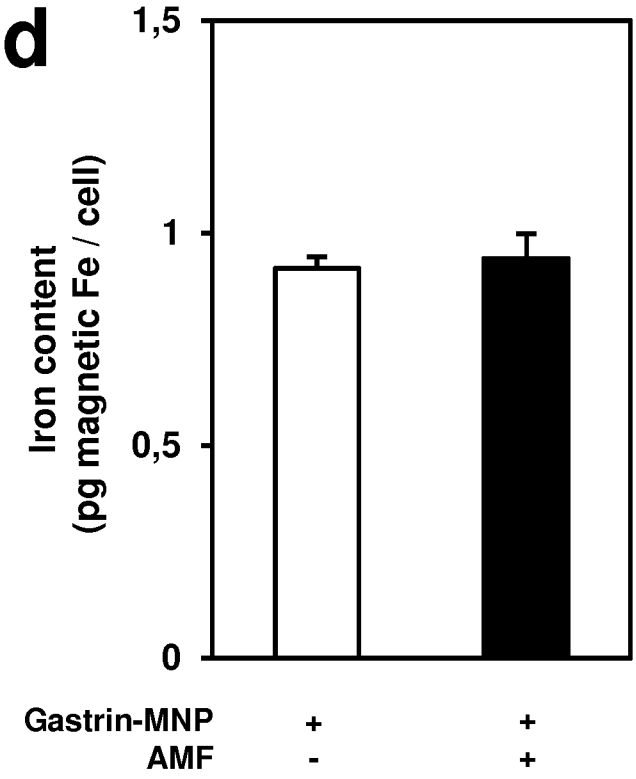

Figure 1d

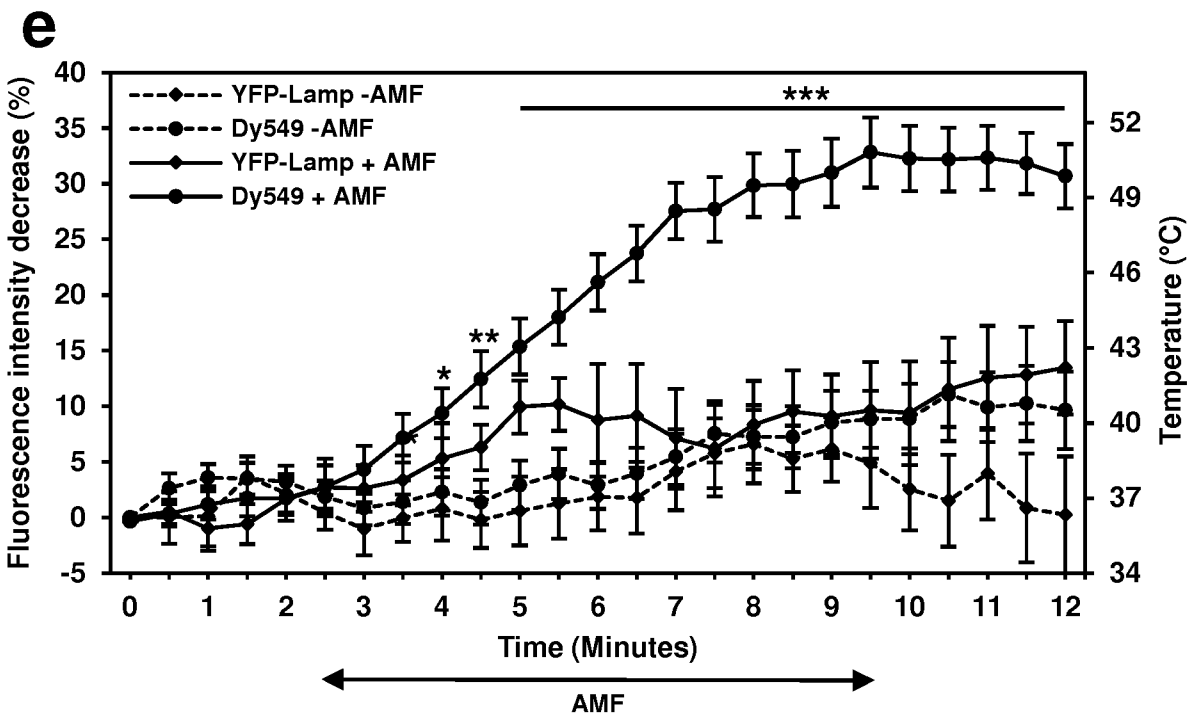

Figure 1e

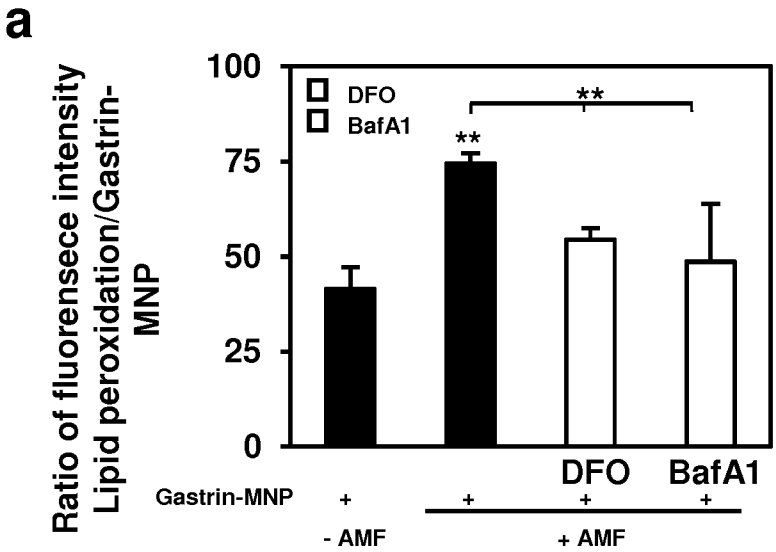

Figure 2a

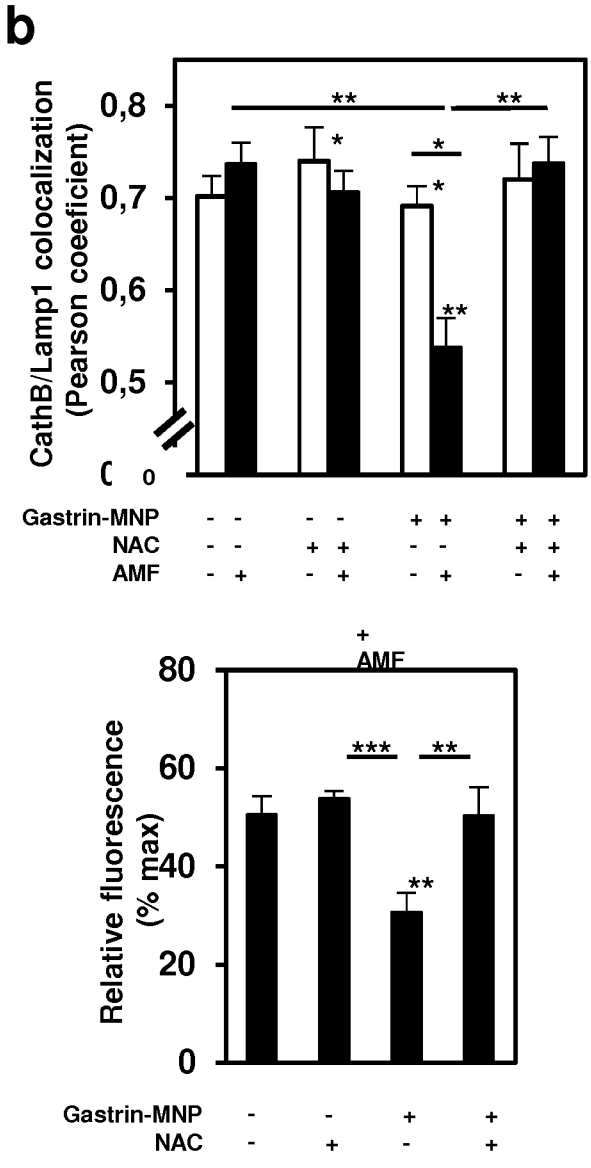

Figure 2b

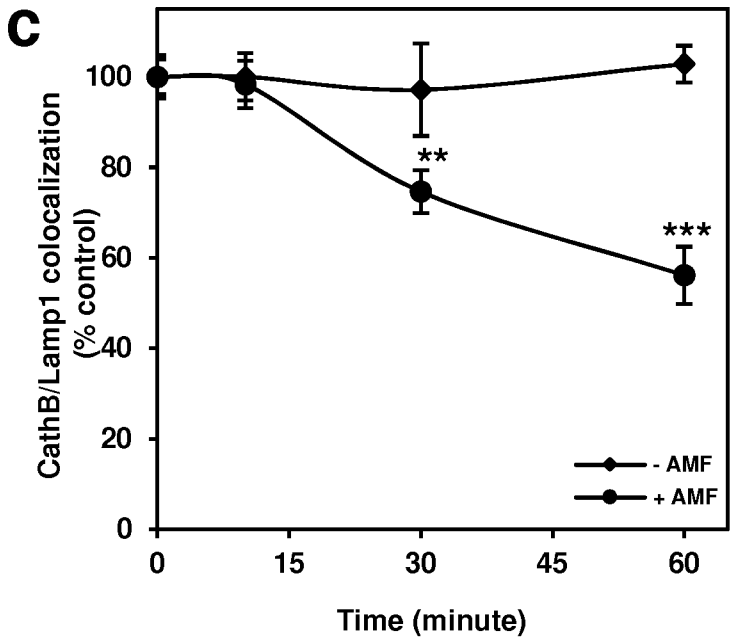

Figure 2c

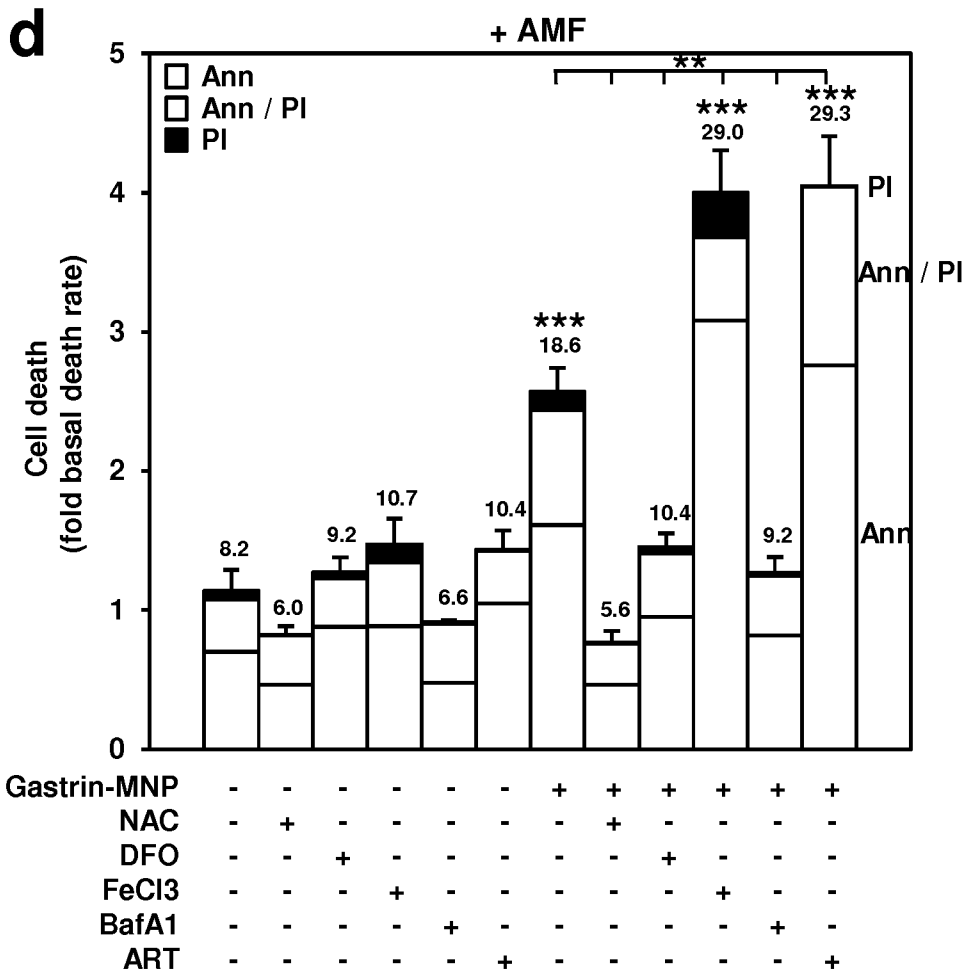

Figure 2d

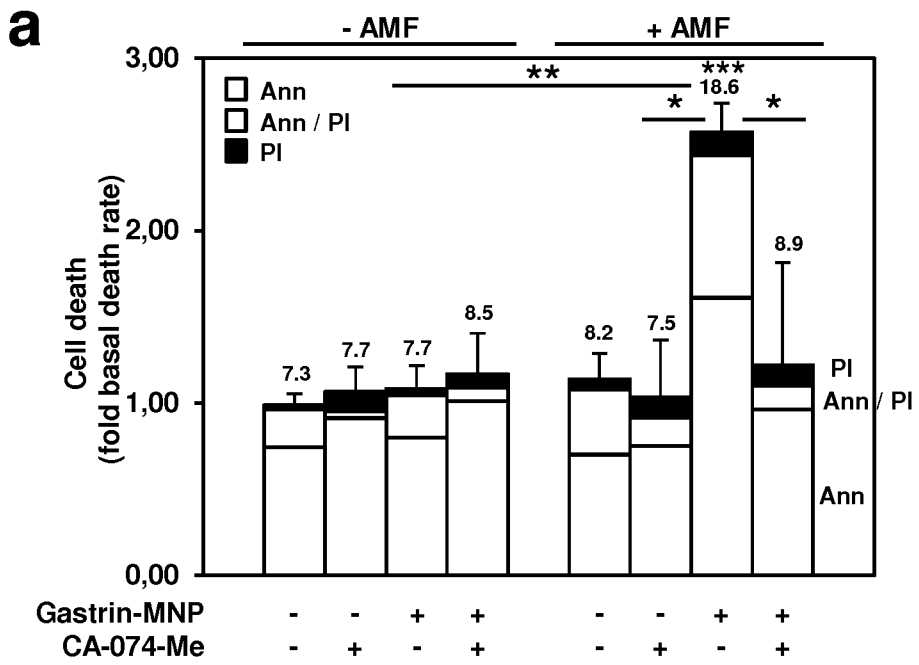

Figure 3a

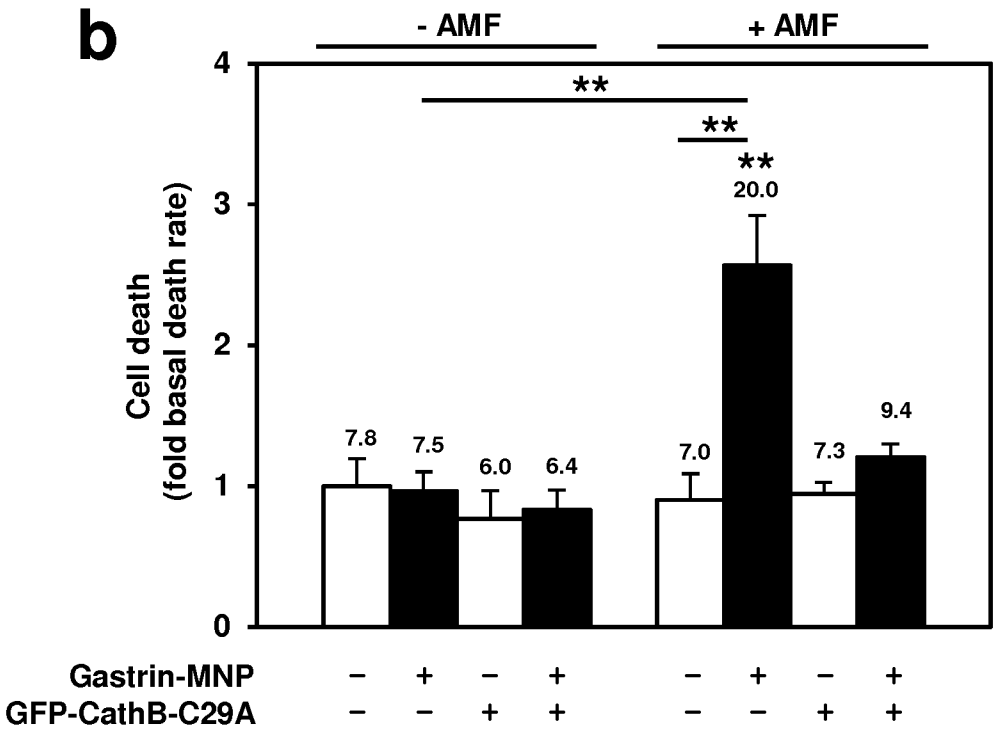

Figure 3b

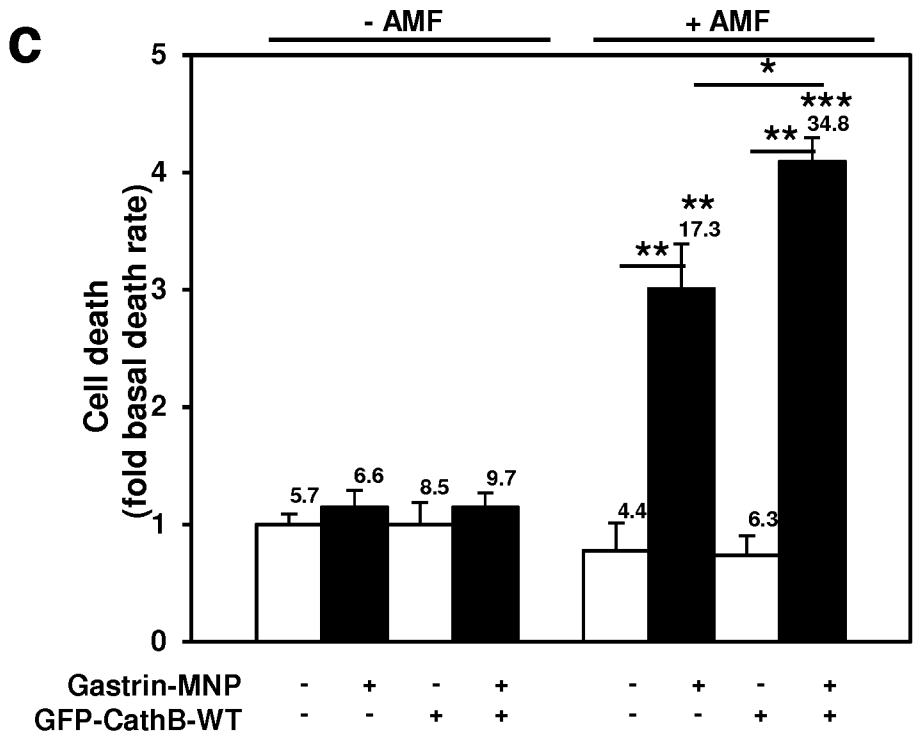

Figure 3c

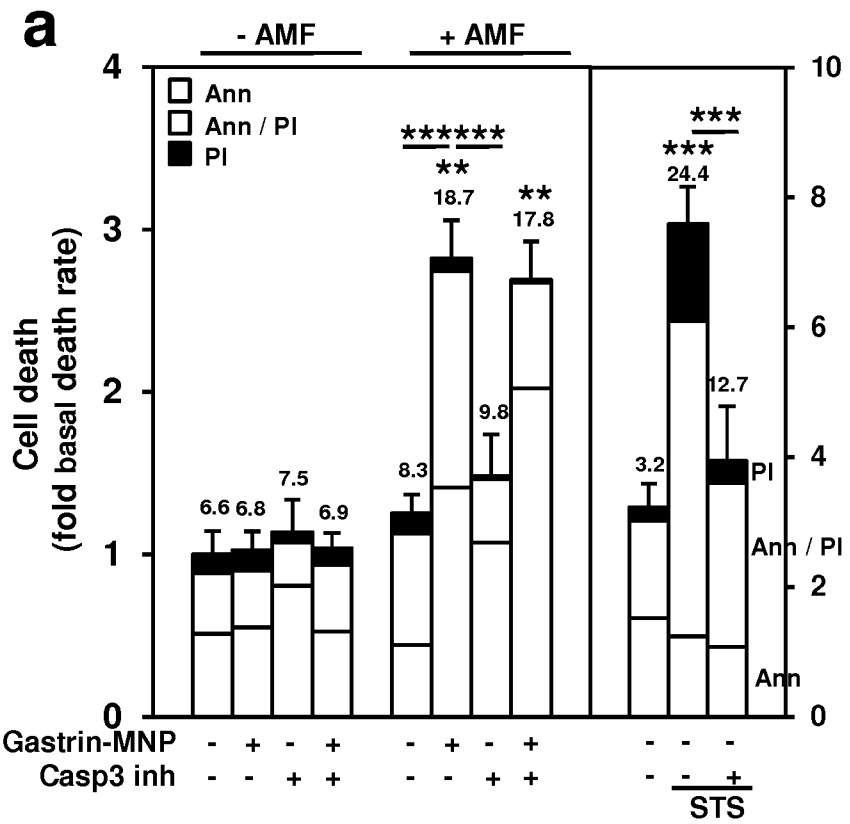

Figure 4a

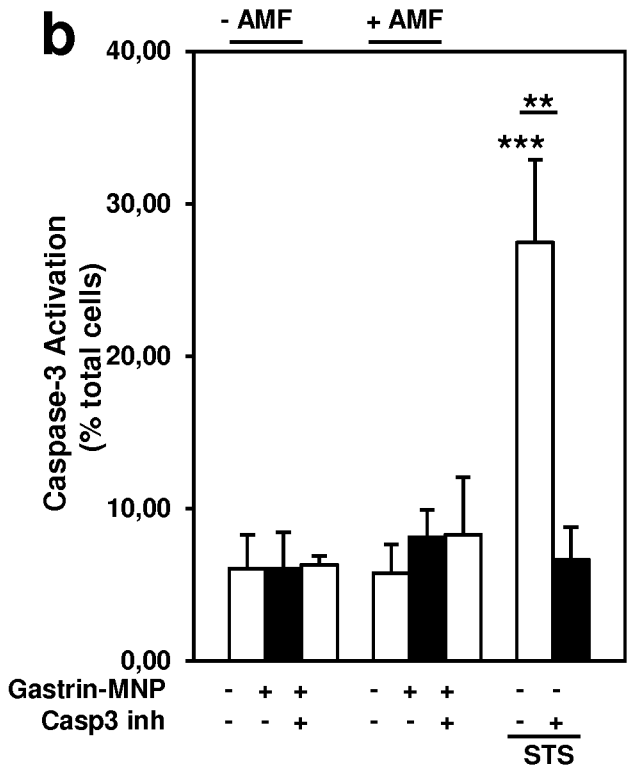

Figure 4b

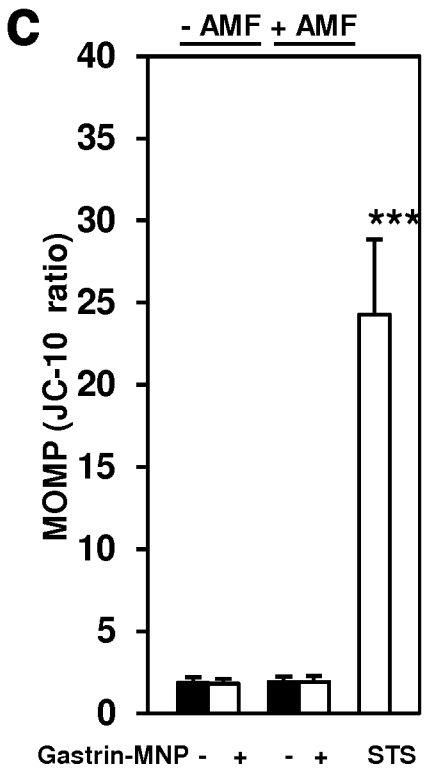

Figure 4c

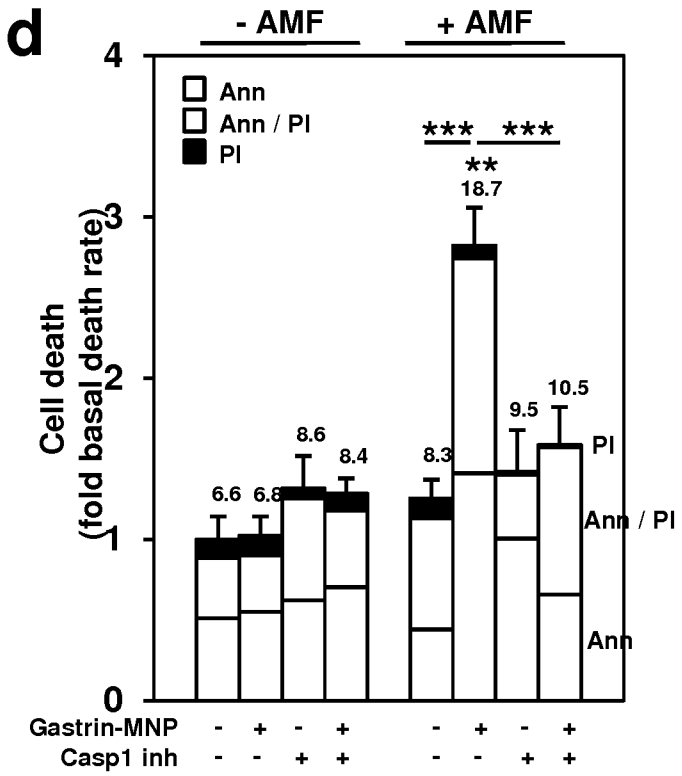

Figure 4d

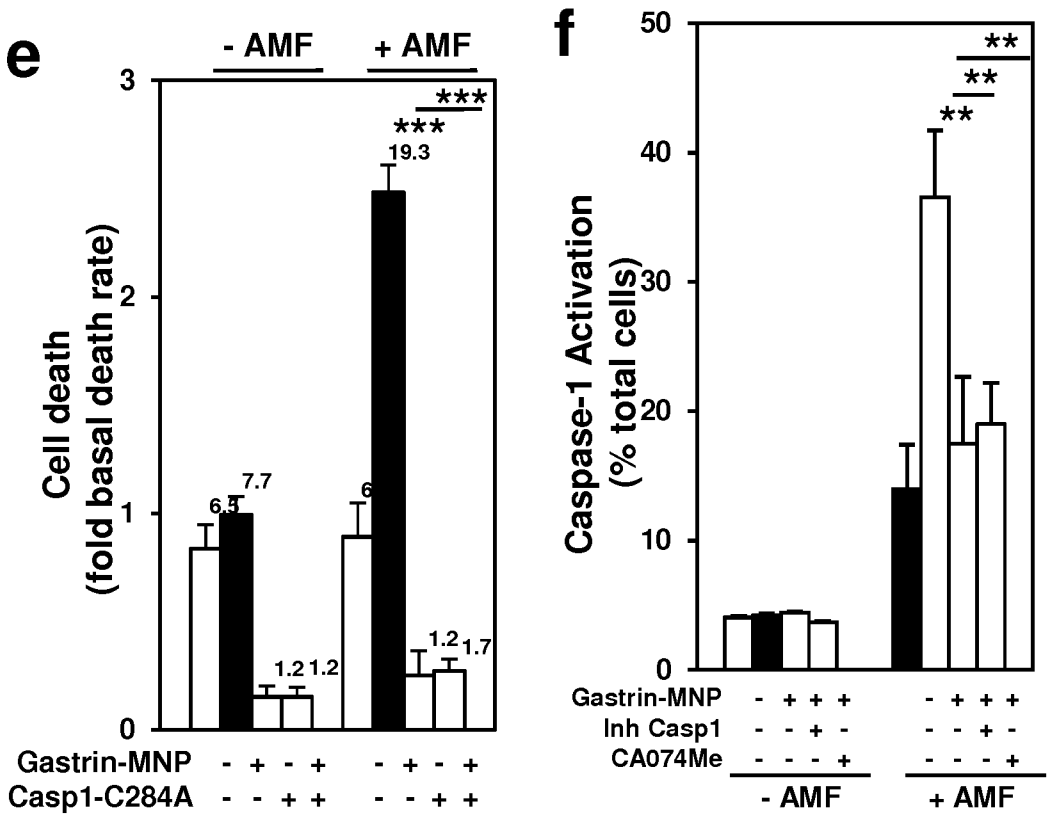

Figure 4 e-f

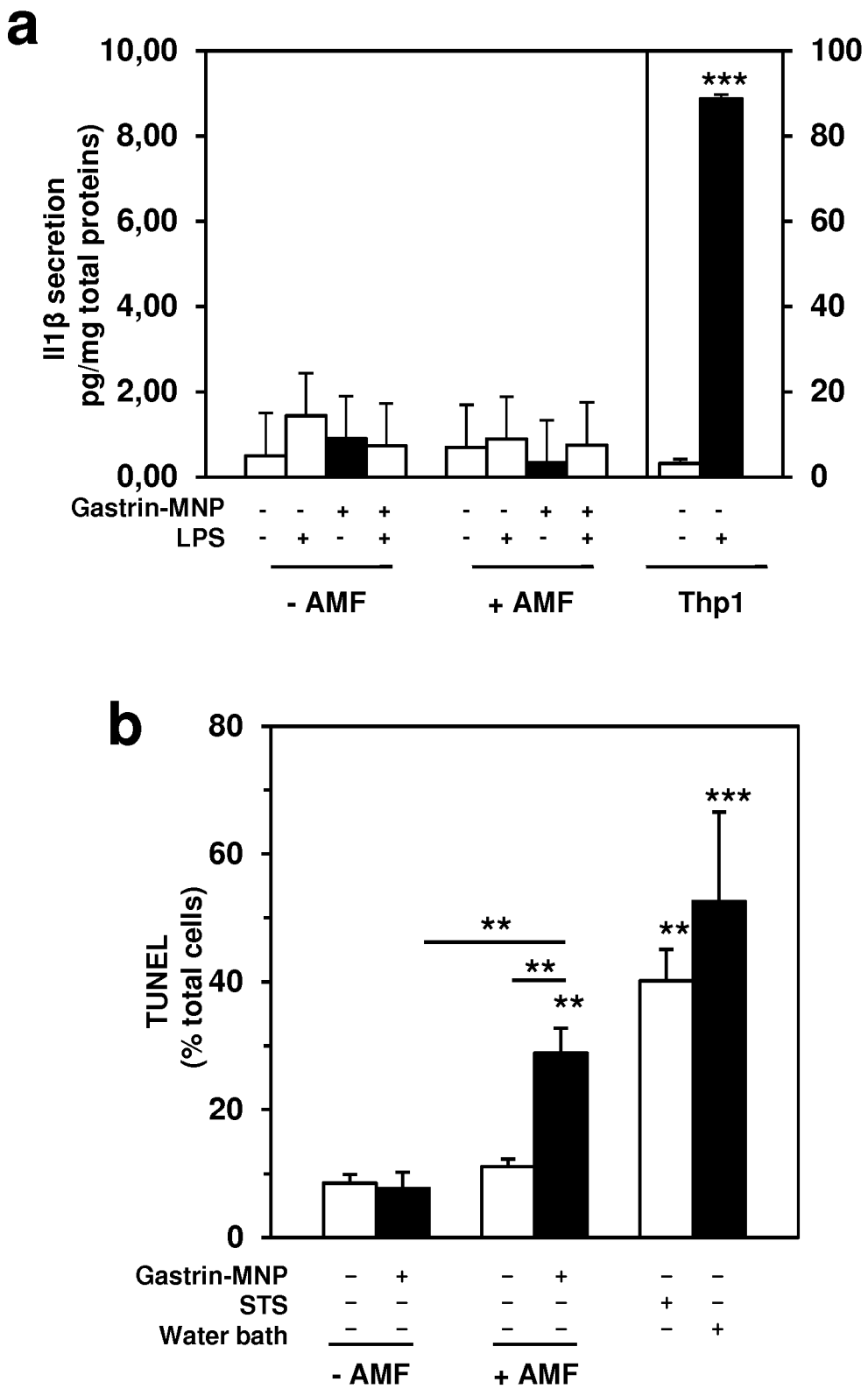

Figure 5 a and b

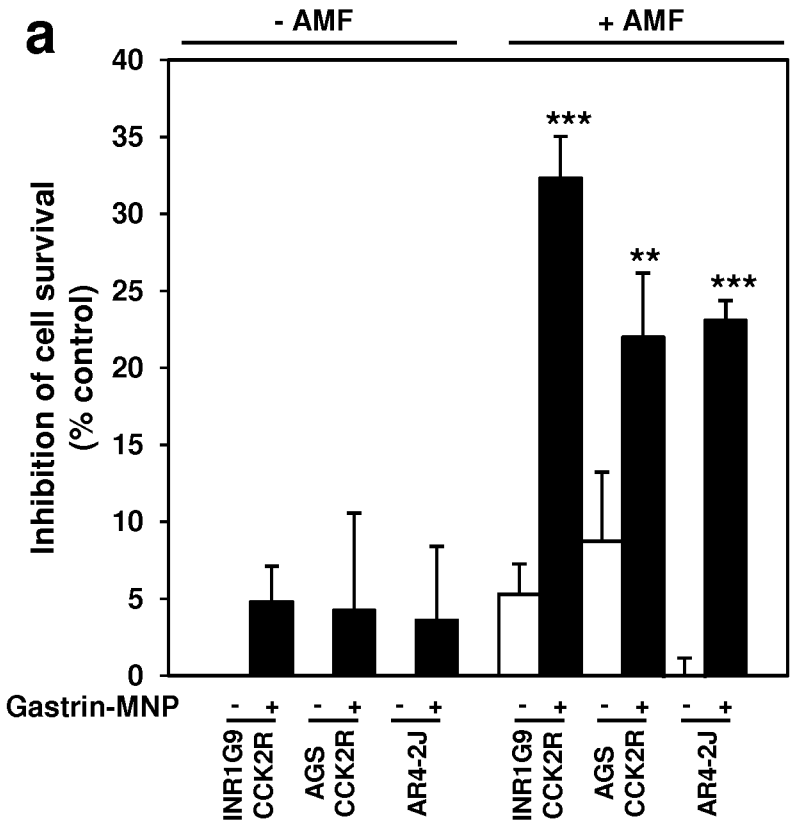

Figure 6a

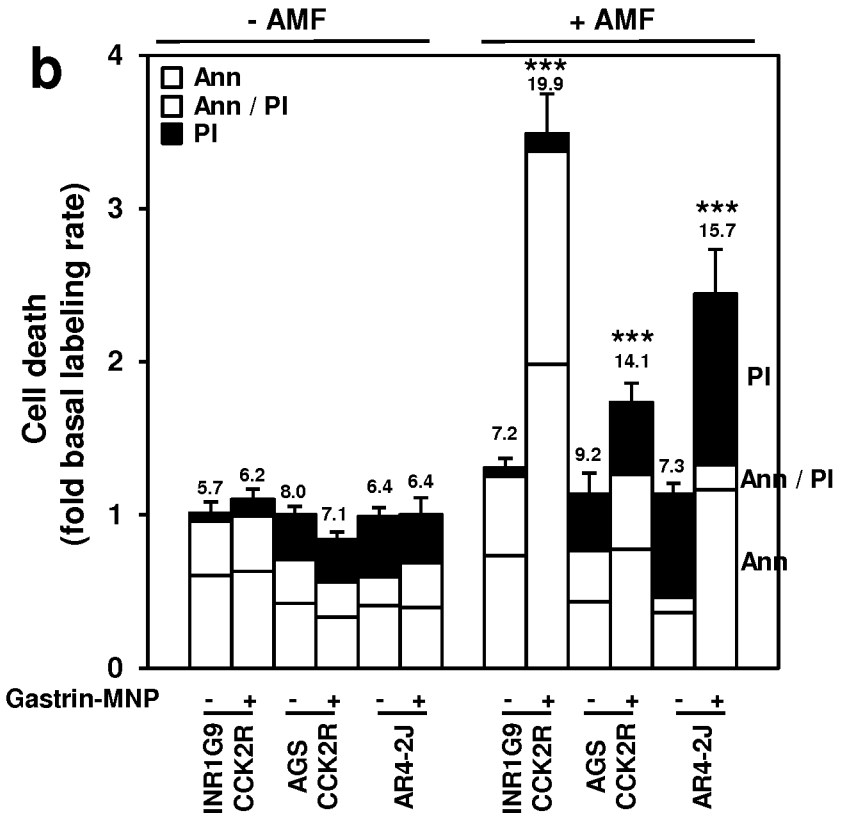

Figure 6b

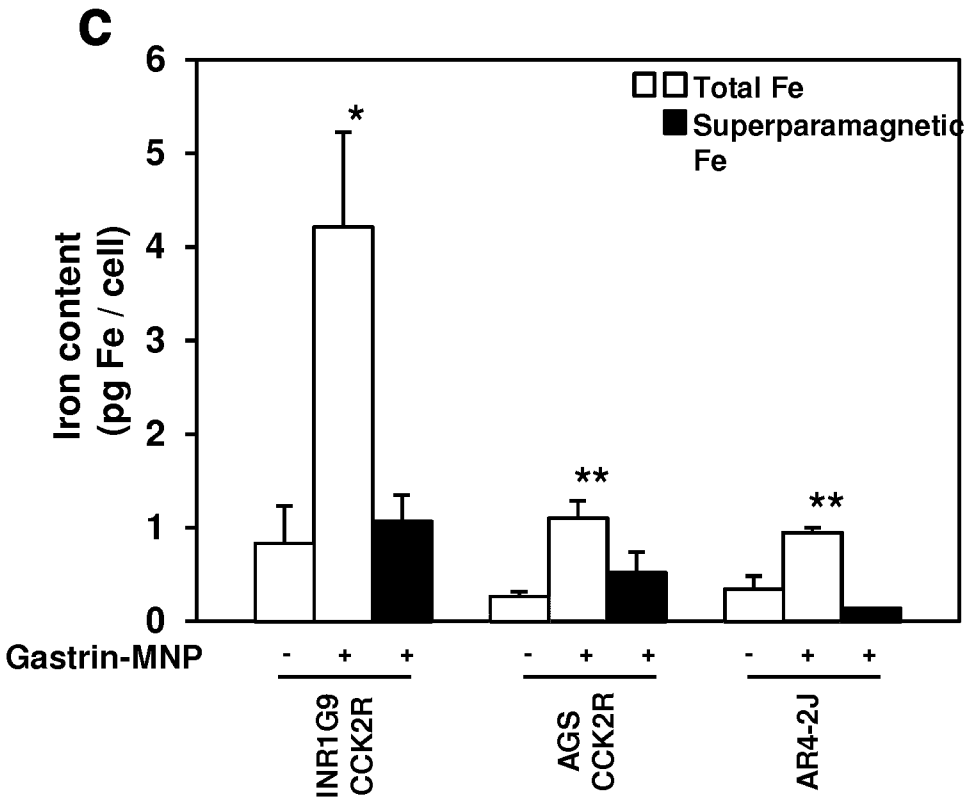

Figure 6c

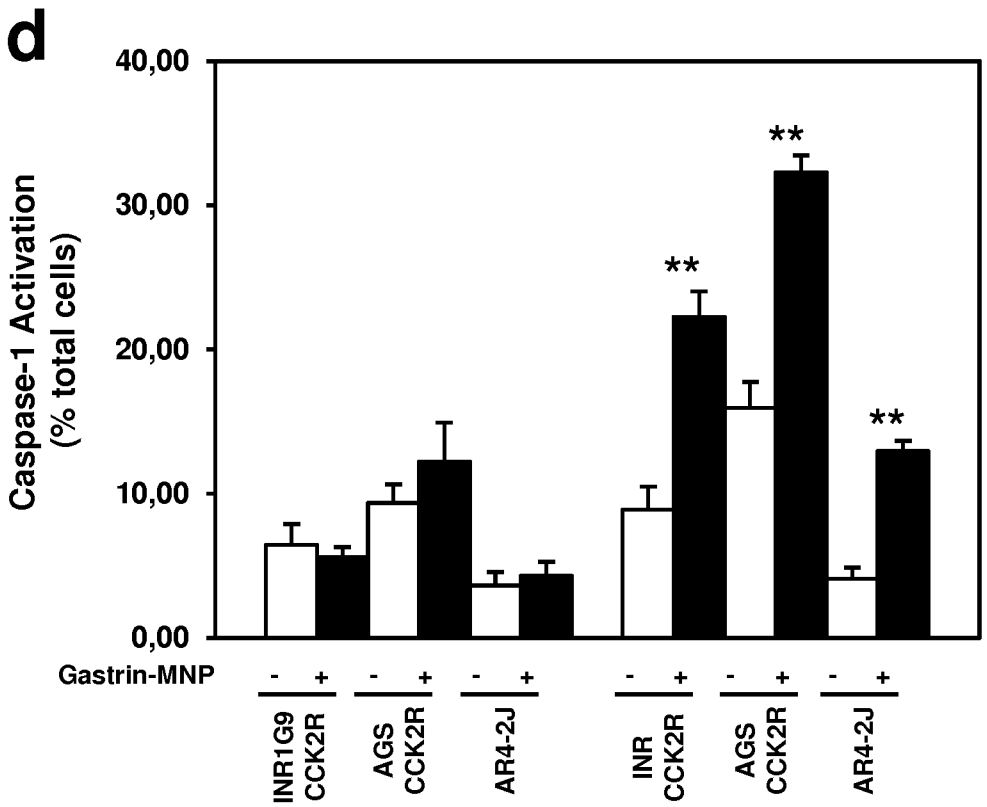

Figure 6d

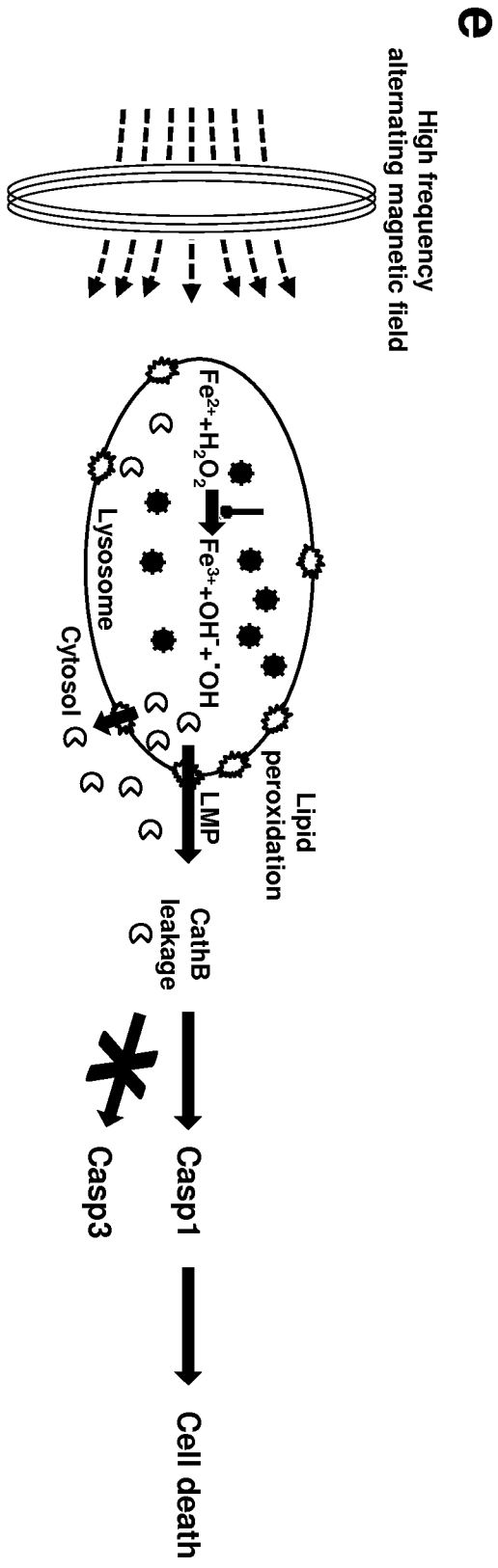
e
High frequency
alternating magnetic field
Fe2+ +H2O2
Fe3+ +OH- + •OH
Lysosome
Cytosol
LMP
Lipid
peroxidation
CathB
leakage
Casp3
Casp1
Cell death

Figure 6e

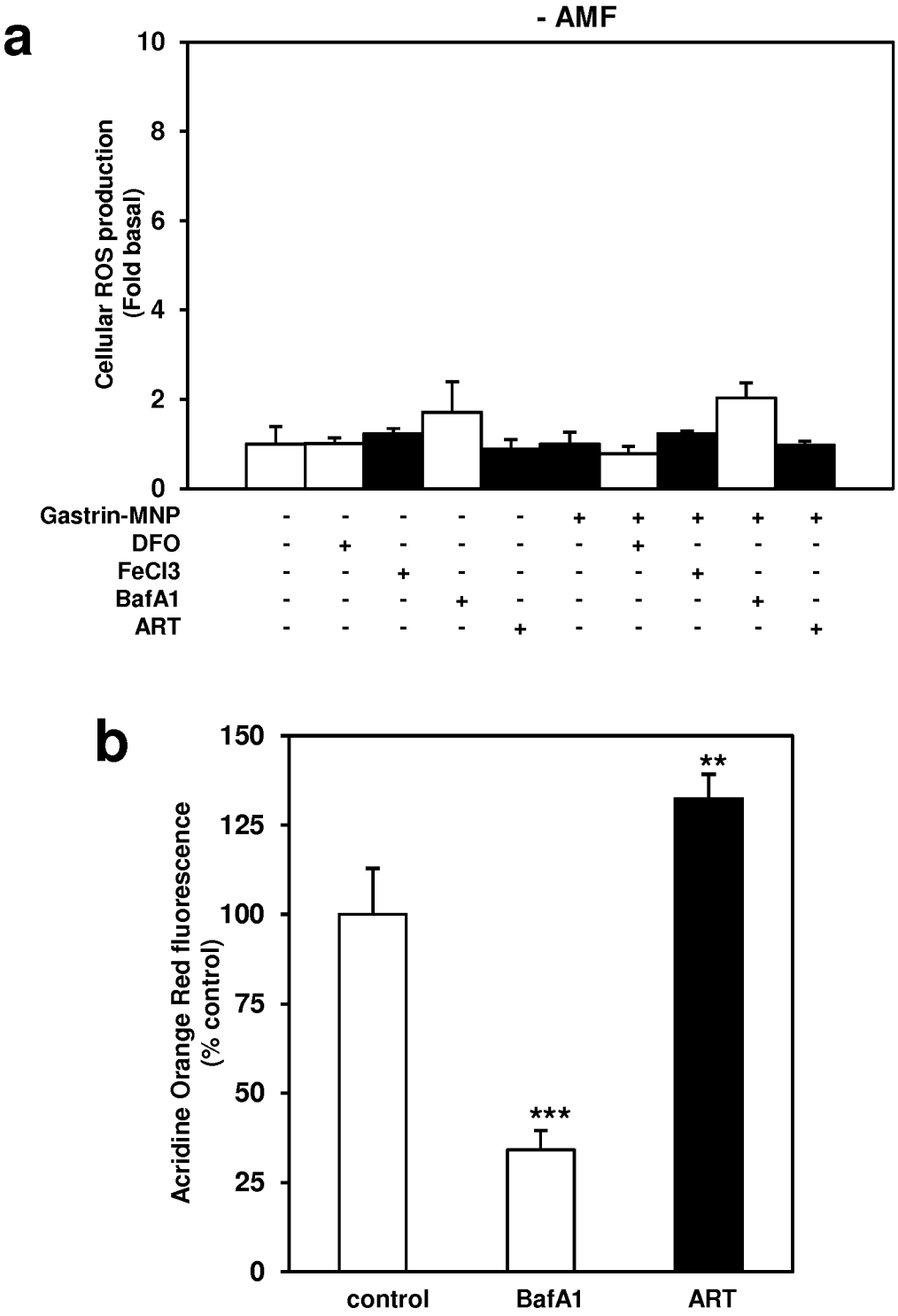

Figure 7 a and b

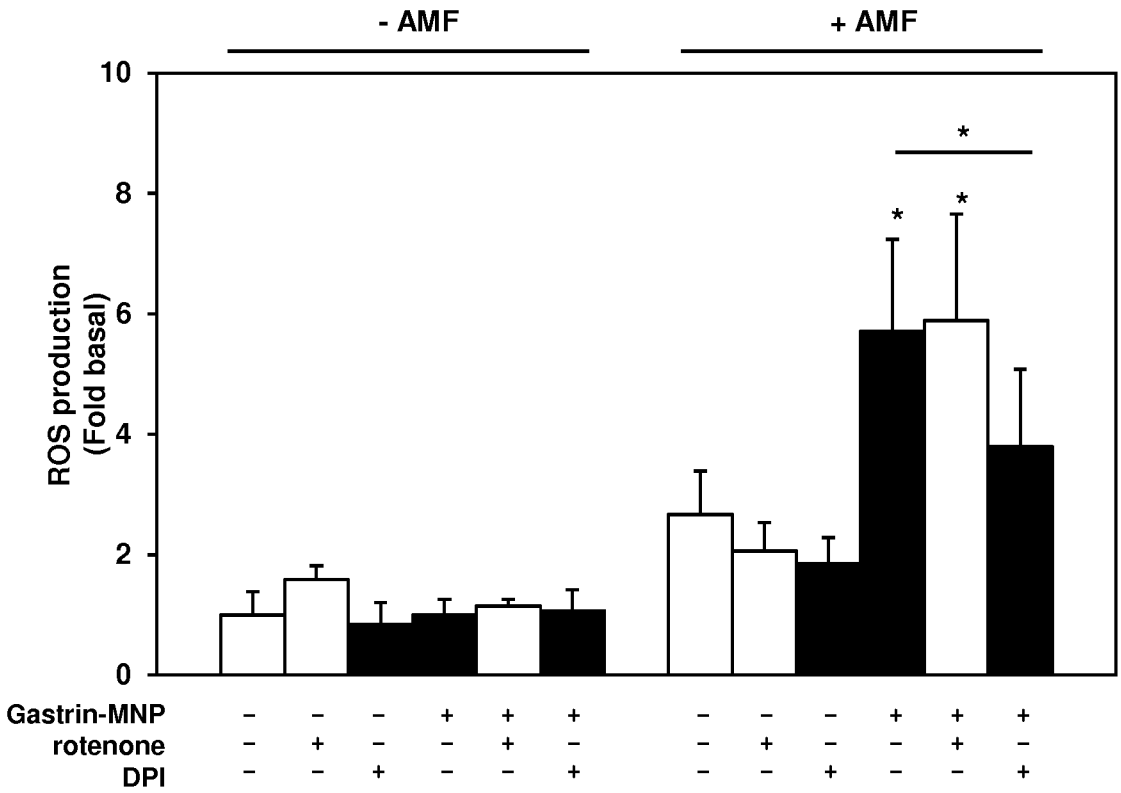

Figure 8

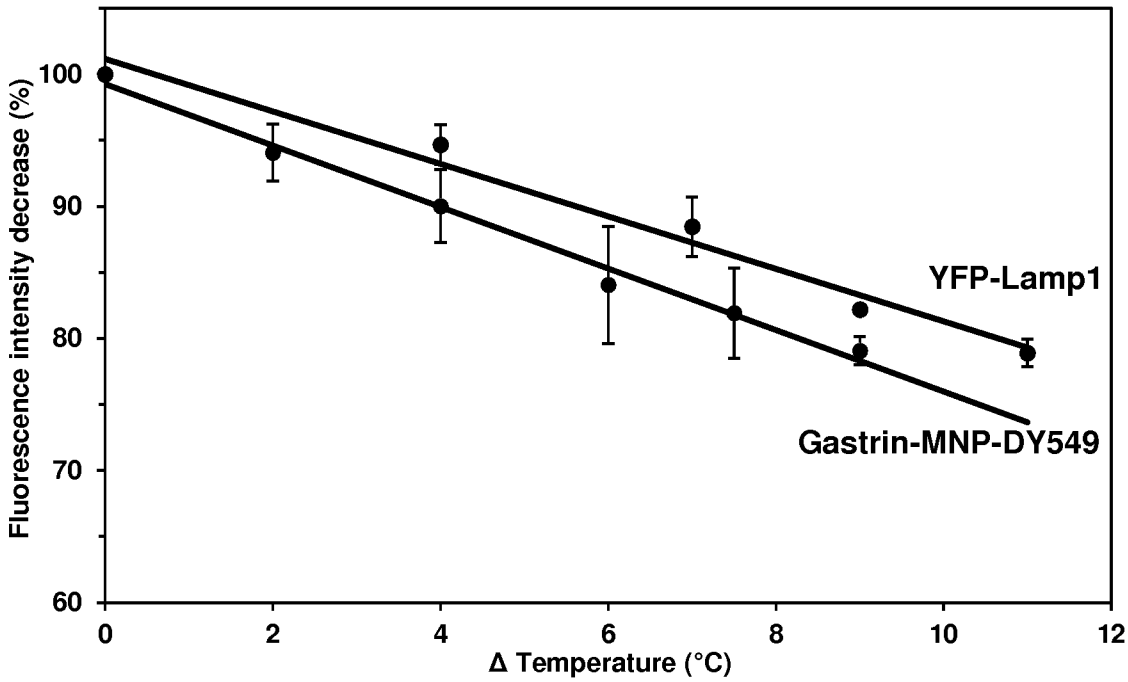

Figure 9

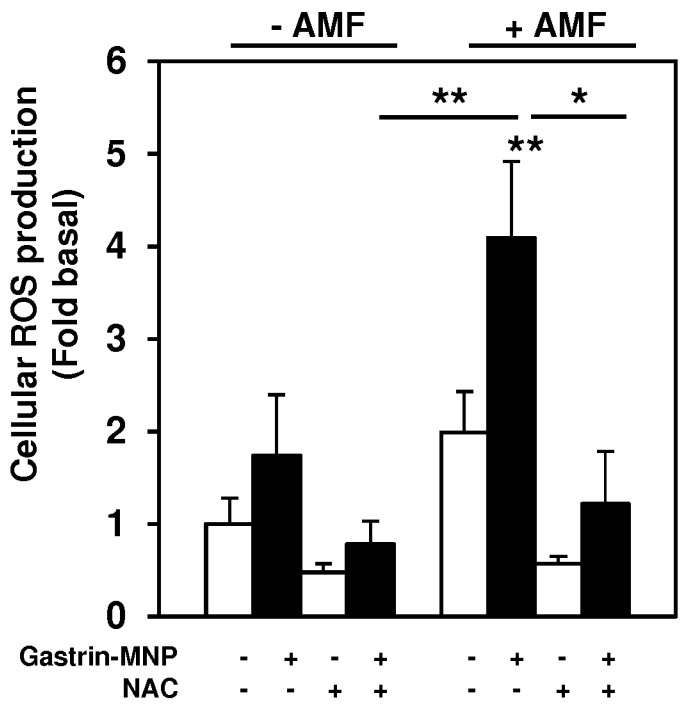

Figure 10

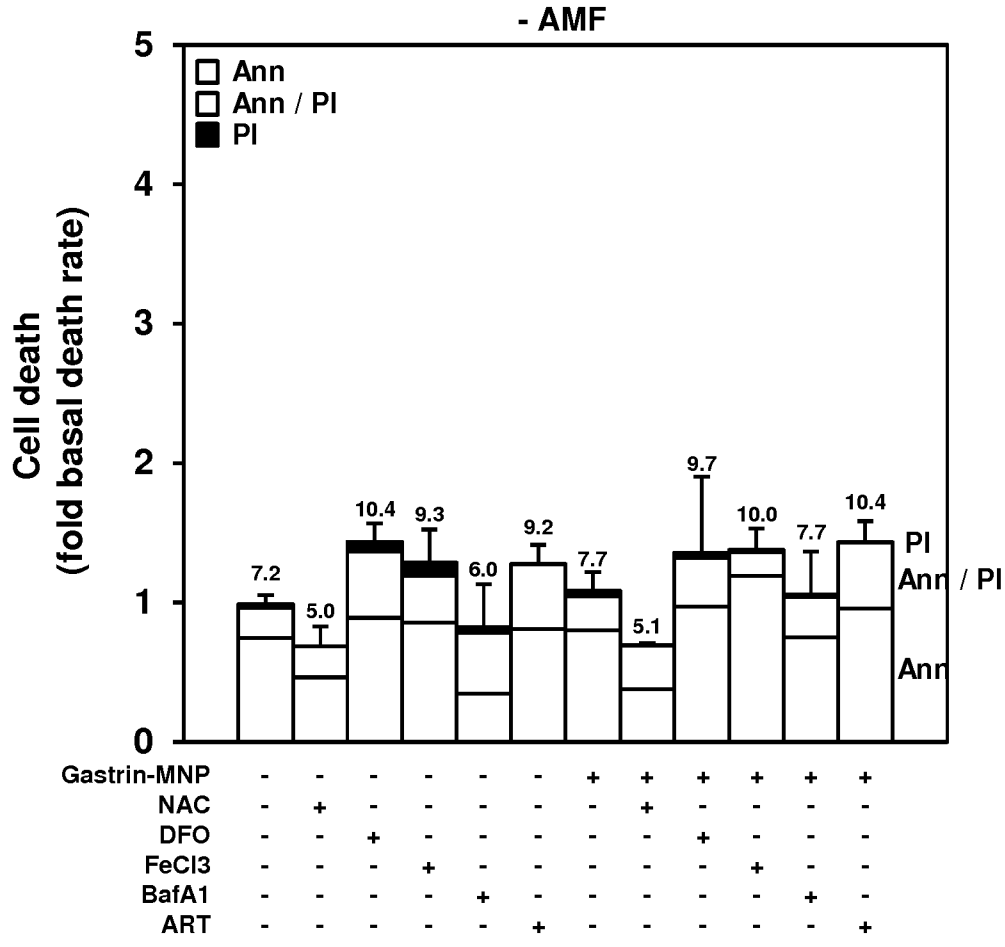

Figure 11

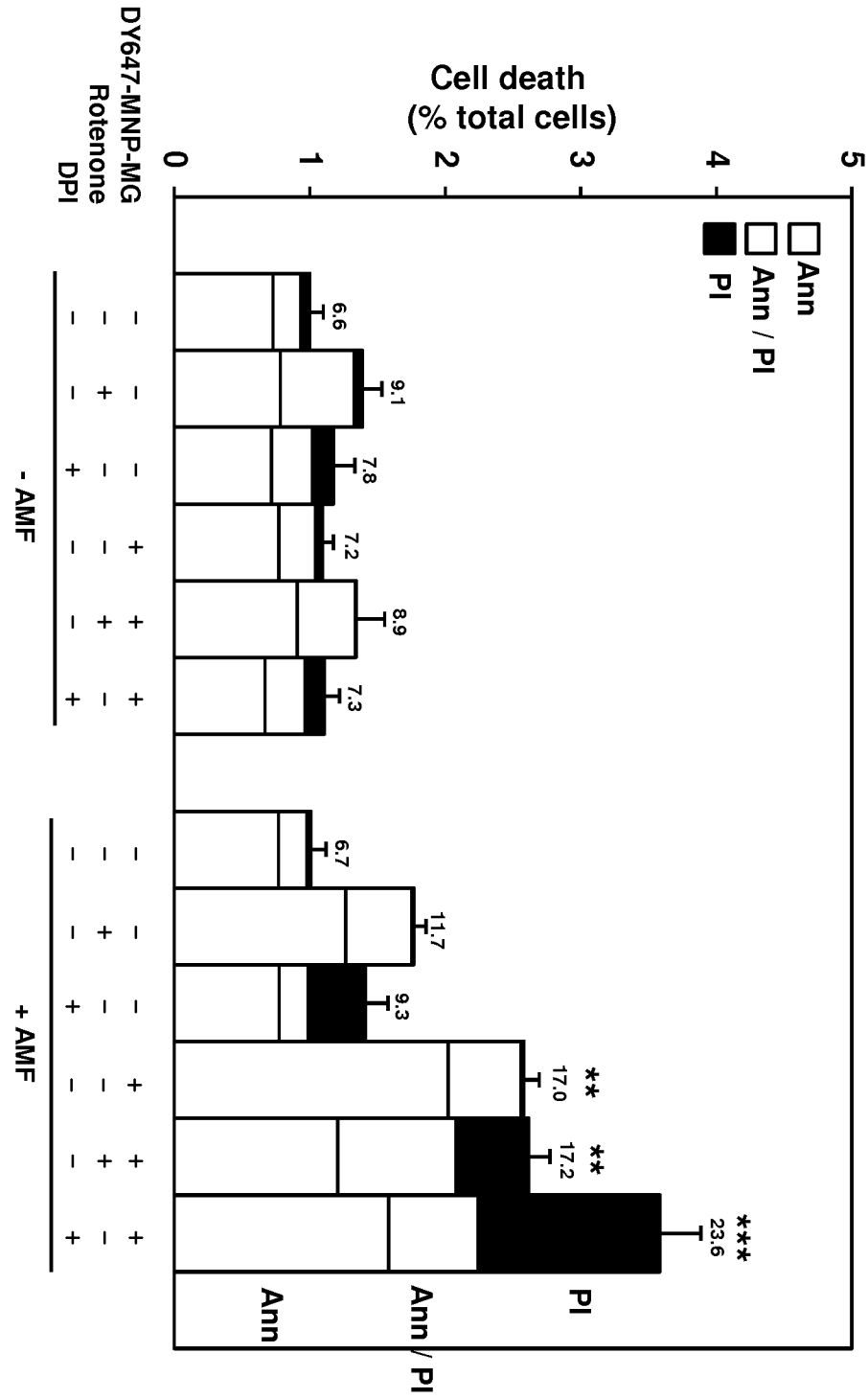
Cell death
(% total cells)
0
1
2
3
4
5
Ann
Ann / PI
PI
DY647-MNP-MG
Rotenone
DPI
- AMF
+ AMF
6.6
9.1
7.8
7.2
8.9
7.3
6.7
11.7
9.3
17.0
17.2
23.6
**
**
***
Ann
Ann / PI
PI

Figure 12

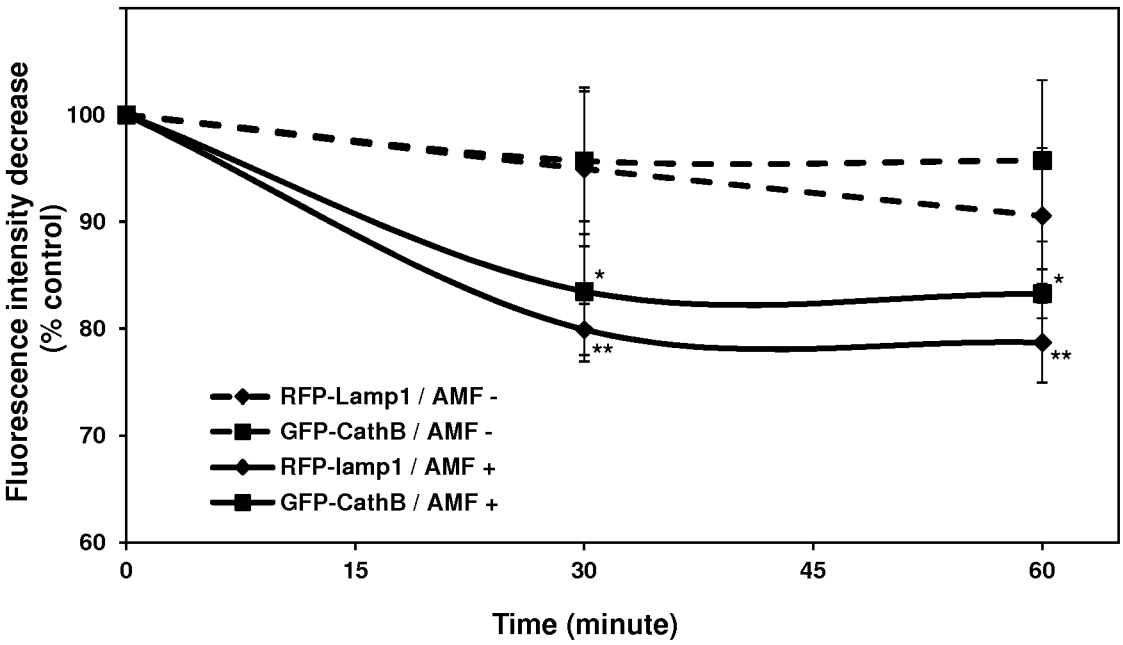

Figure 13

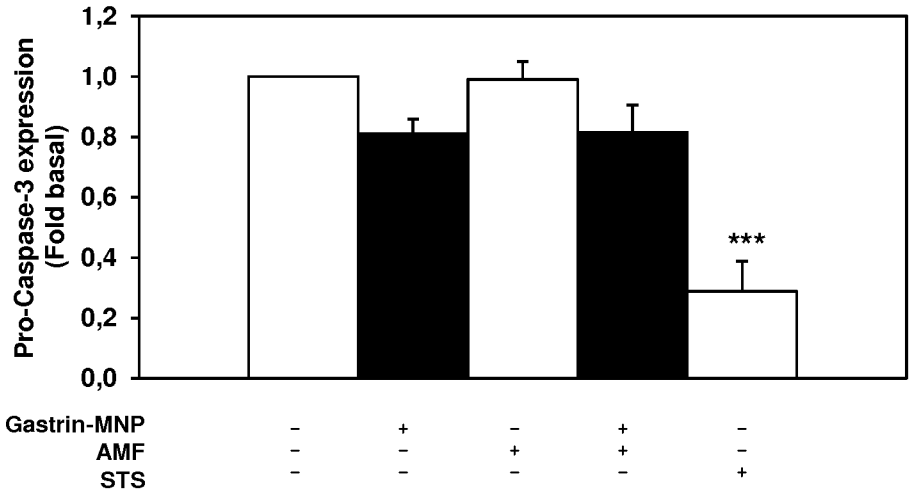

Figure 14

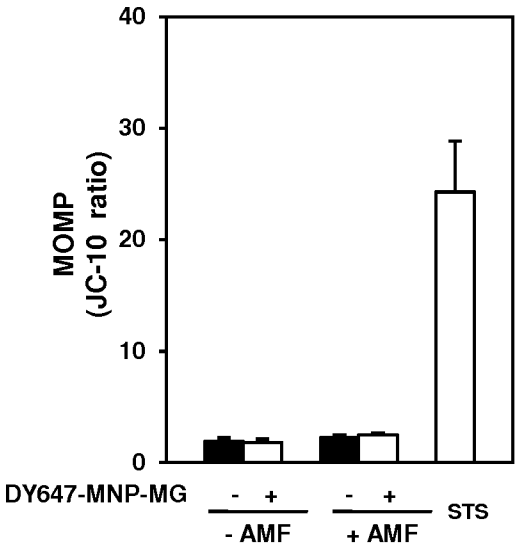

Figure 15

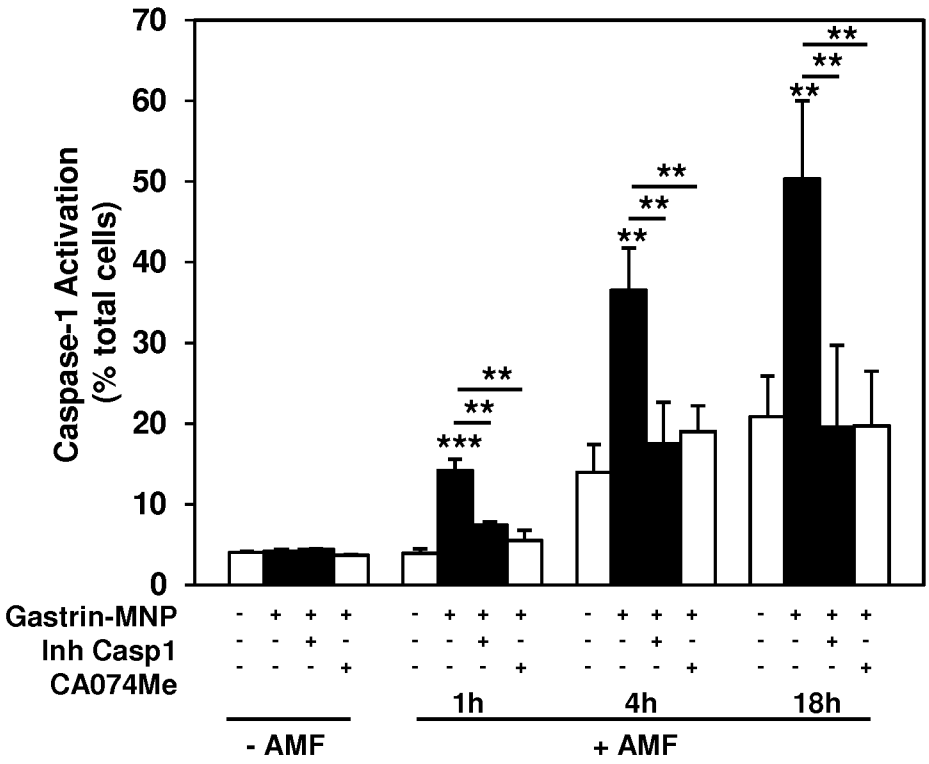

Figure 16

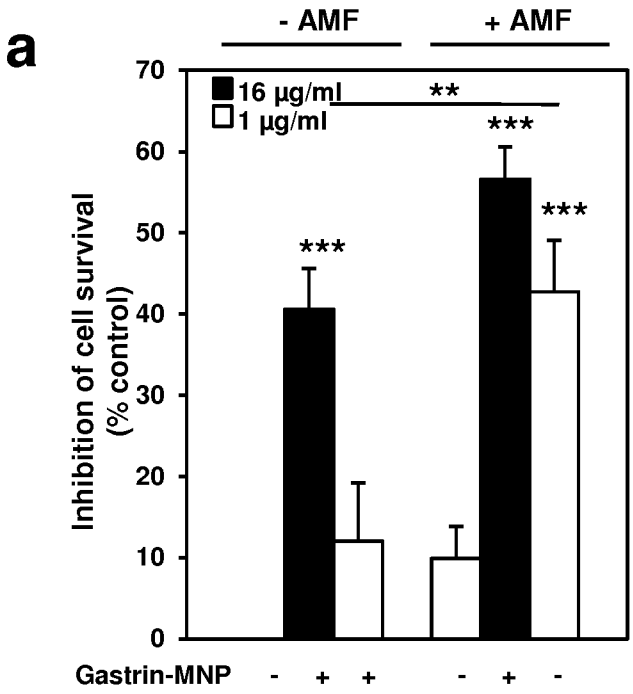

Figure 17a

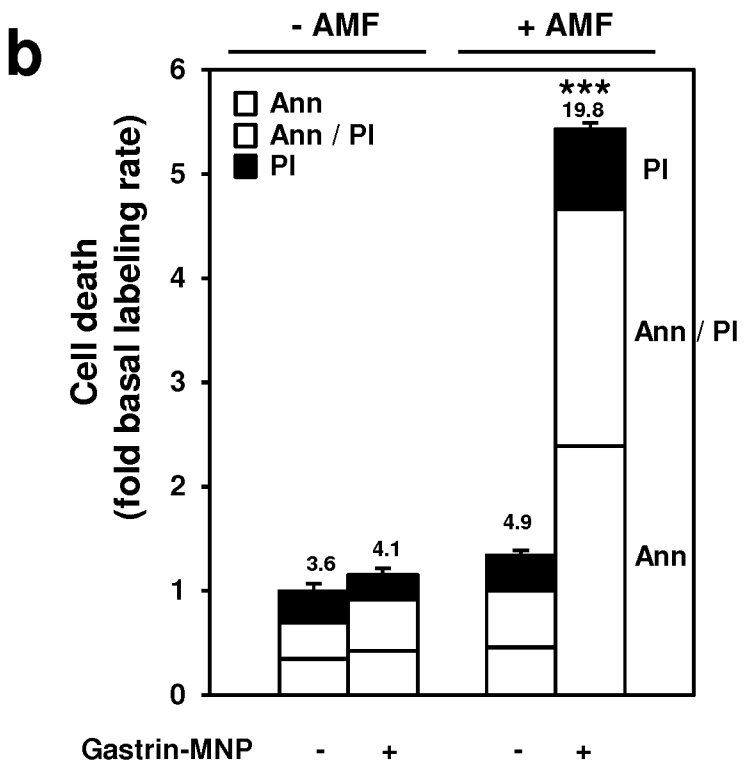

Figure 17b

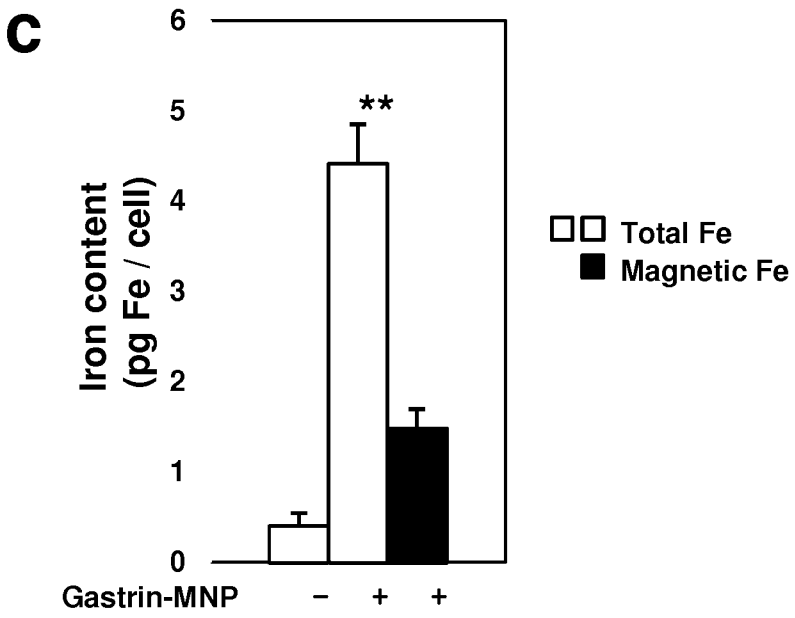

Figure 17c

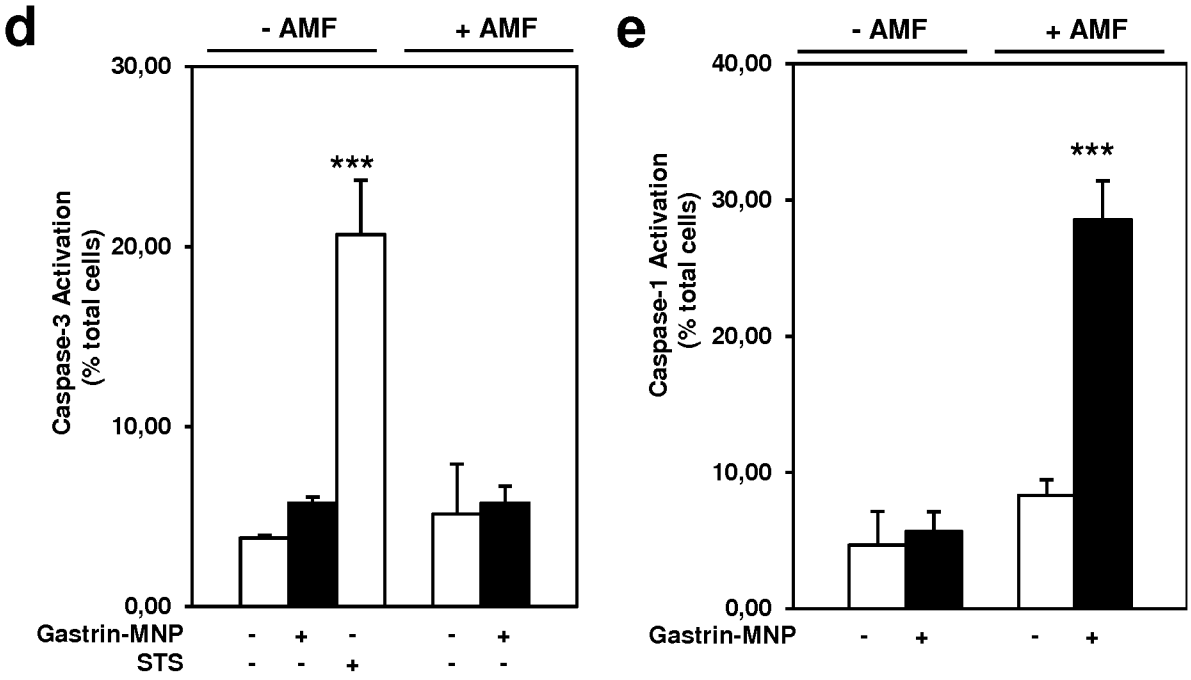

Figure 17 d and e

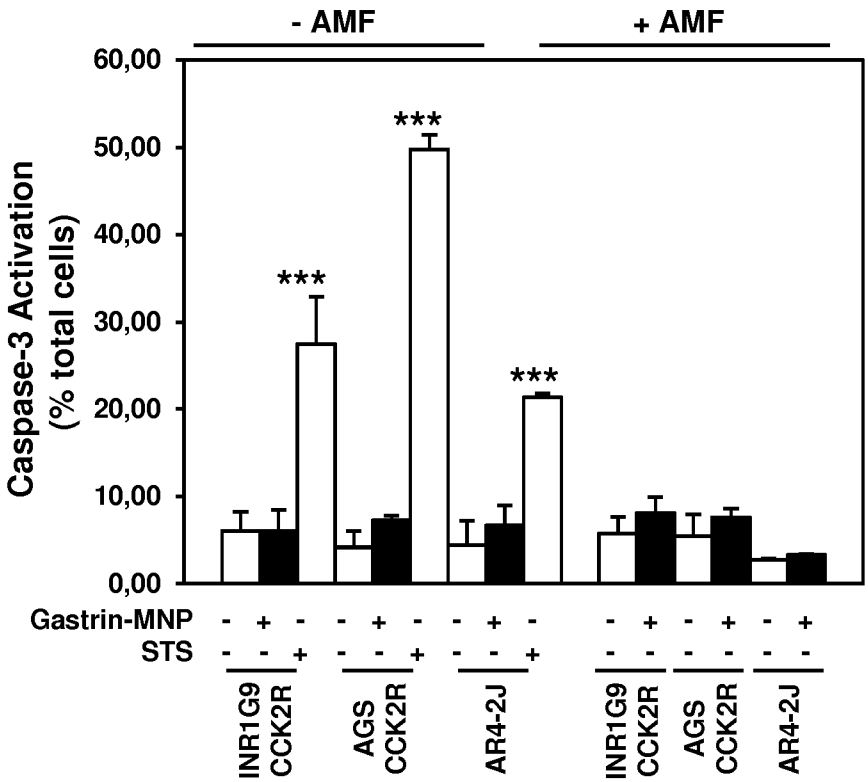

Figure 18

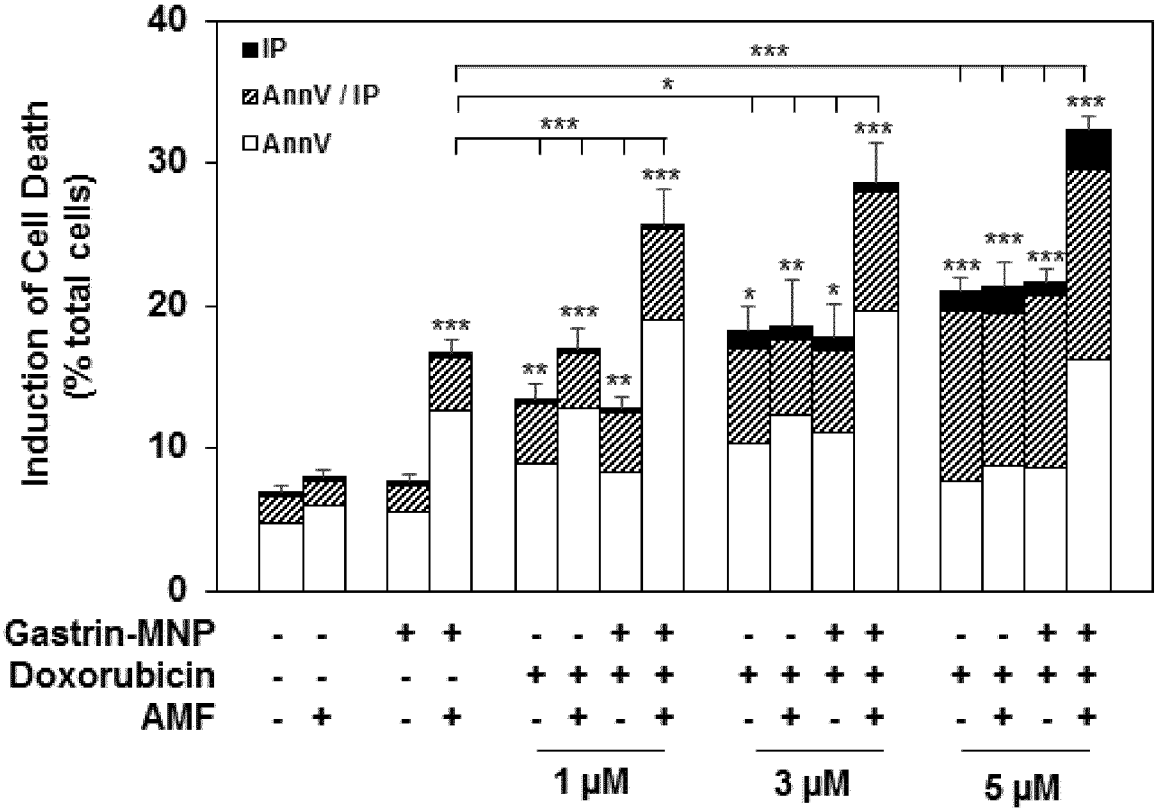

Figure 19

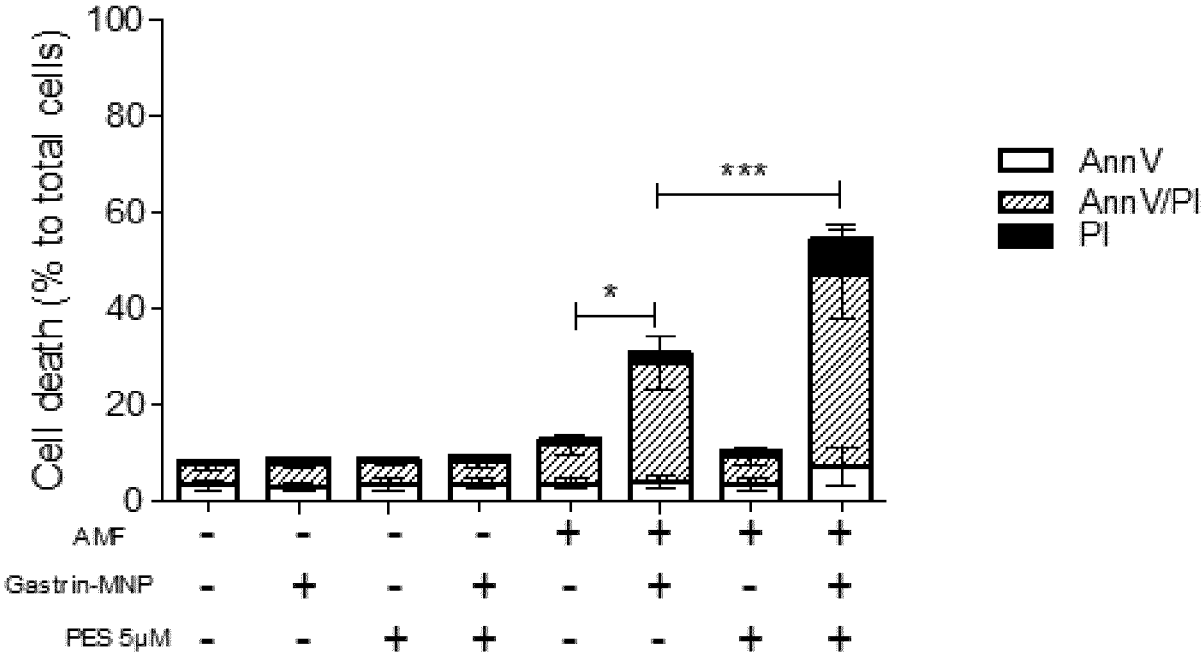

Figure 20a

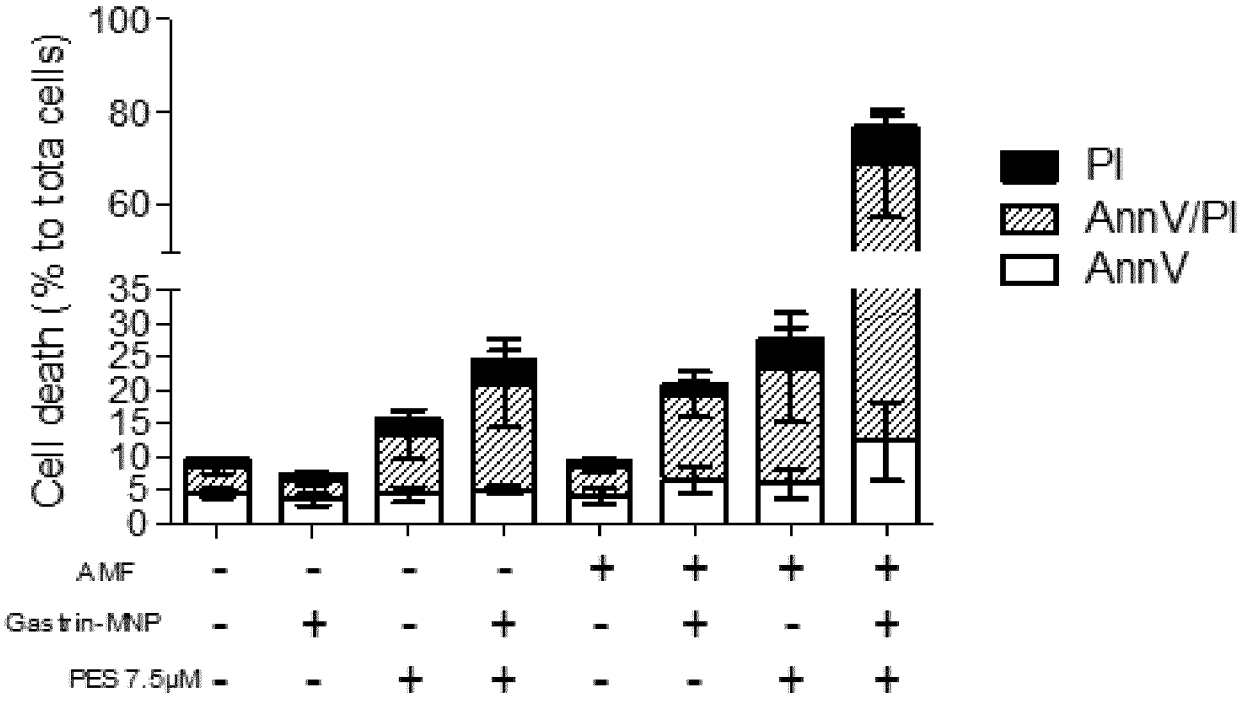

Figure 20b

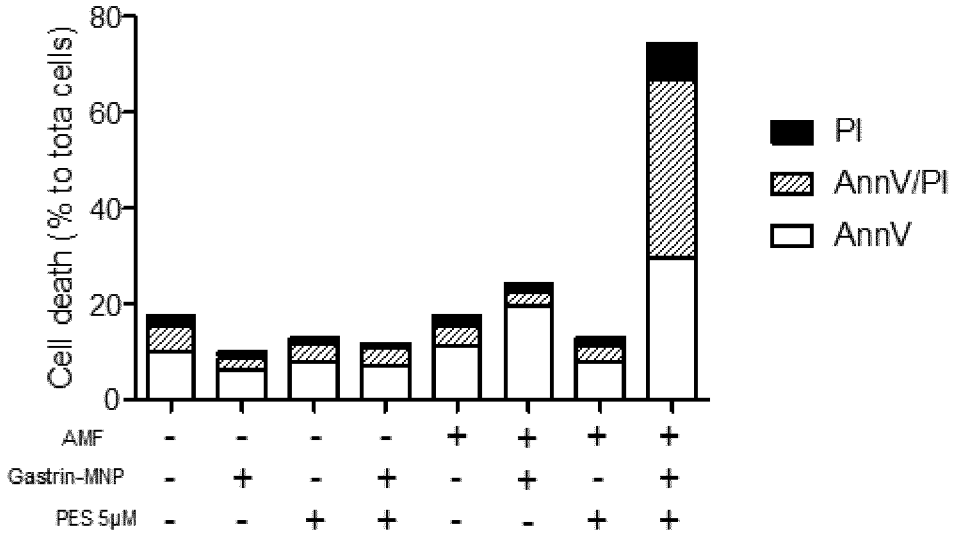

Figure 20c

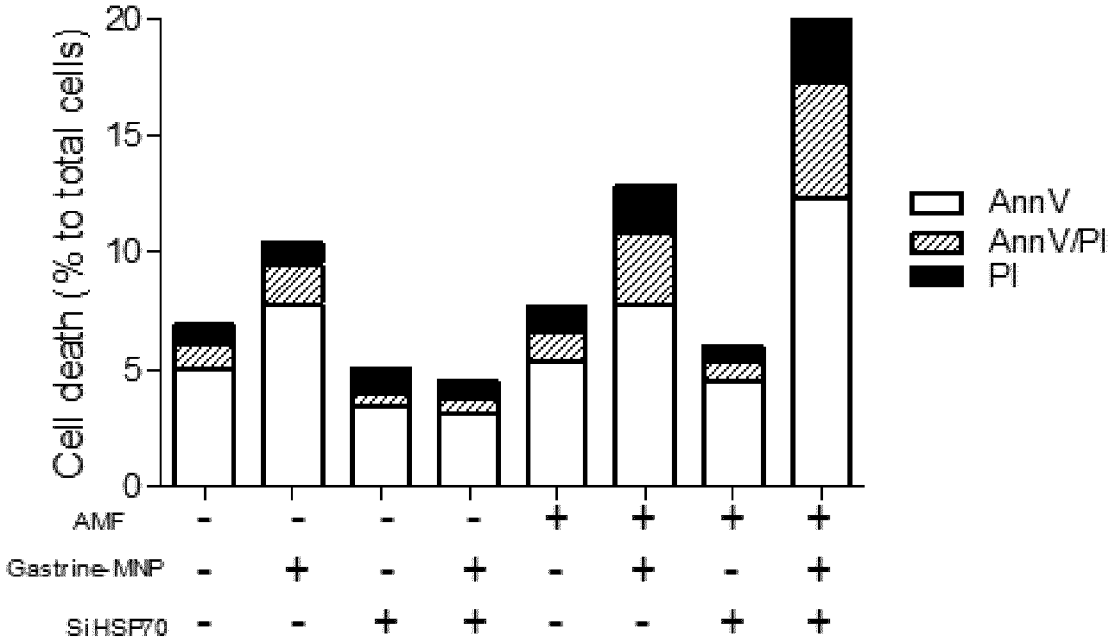

Figure 21

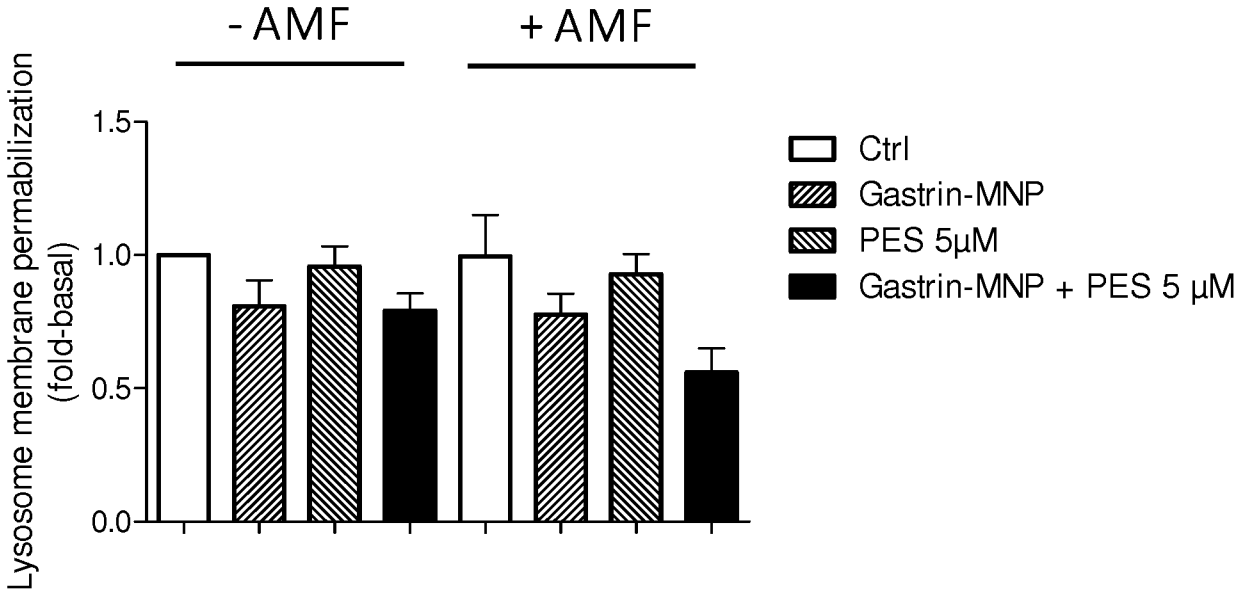

Figure 22

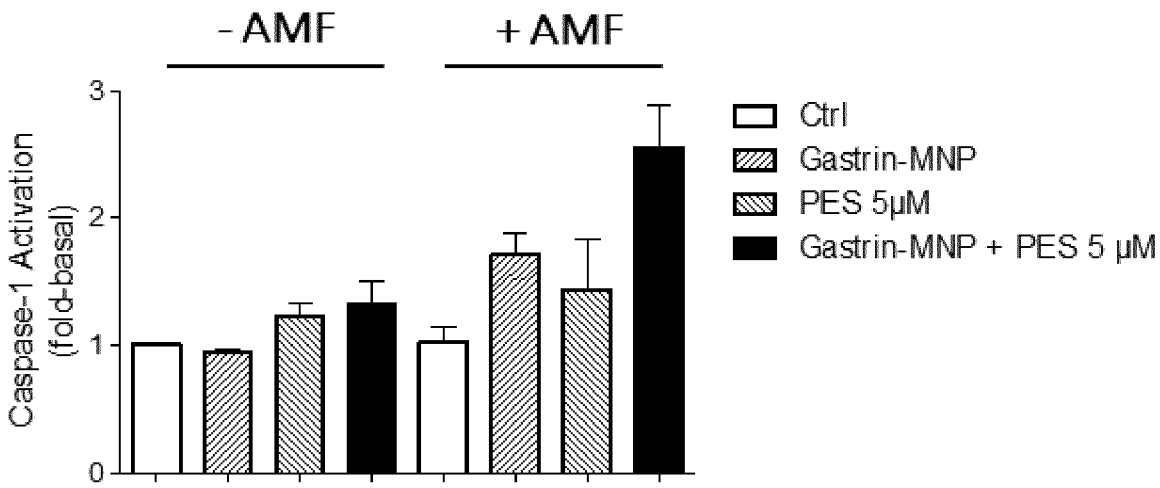

Figure 23a

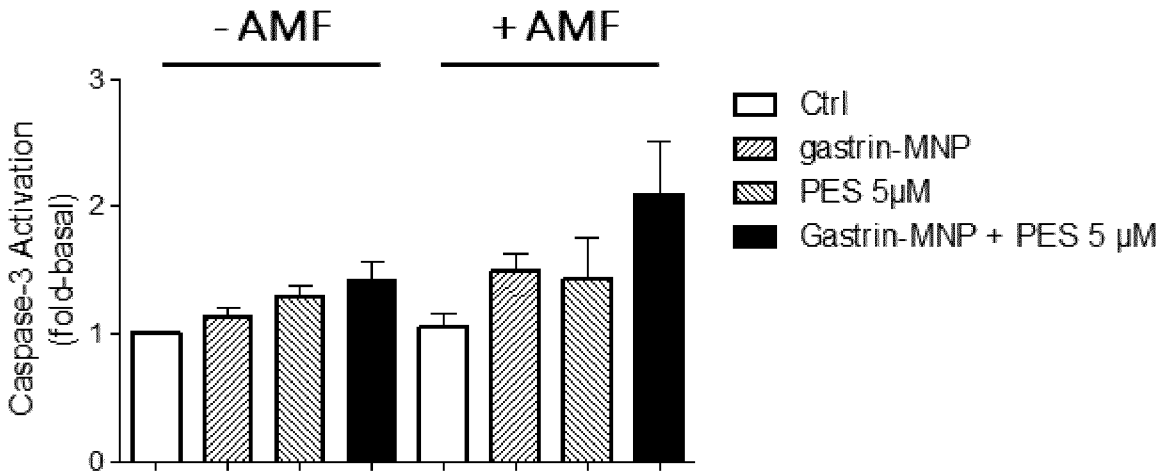

Figure 23b

INTERNATIONAL SEARCH REPORT

International application No
PCT/EP2018/077547

A. CLASSIFICATION OF SUBJECT MATTER
INV. A61K31/704 A61K45/06 A61K47/69 A61P35/00
ADD.

According to International Patent Classification (IPC) or to both national classification and IPC

B. FIELDS SEARCHED

Minimum documentation searched (classification system followed by classification symbols)
A61K

Documentation searched other than minimum documentation to the extent that such documents are included in the fields searched

Electronic data base consulted during the international search (name of data base and, where practicable, search terms used)
EPO-Internal, BIOSIS, CHEM ABS Data, EMBASE, WPI Data

C. DOCUMENTS CONSIDERED TO BE RELEVANT

Category*	Citation of document, with indication, where appropriate, of the relevant passages	Relevant to claim No.
X	KOWICHI JIMBOW ET AL: "Melanoma-Targeted Chemothermotherapy and In Situ Peptide Immunotherapy through HSP Production by Using Melanogenesis Substrate, NPrCAP, and Magnetite Nanoparticles", JOURNAL OF SKIN CANCER, vol. 2013, January 2013 (2013-01), pages 1-12, XP055445216, US ISSN: 2090-2905, DOI: 10.1155/2013/742925 the whole document, in particular chapters 3.2, 4 and 5.1; figures ----- -/--	1-7

[X] Further documents are listed in the continuation of Box C. [ ] See patent family annex.

* Special categories of cited documents :

"A" document defining the general state of the art which is not considered to be of particular relevance

"E" earlier application or patent but published on or after the international filing date

"L" document which may throw doubts on priority claim(s) or which is cited to establish the publication date of another citation or other special reason (as specified)

"O" document referring to an oral disclosure, use, exhibition or other means

"P" document published prior to the international filing date but later than the priority date claimed

"T" later document published after the international filing date or priority date and not in conflict with the application but cited to understand the principle or theory underlying the invention

"X" document of particular relevance; the claimed invention cannot be considered novel or cannot be considered to involve an inventive step when the document is taken alone

"Y" document of particular relevance; the claimed invention cannot be considered to involve an inventive step when the document is combined with one or more other such documents, such combination being obvious to a person skilled in the art

"&" document member of the same patent family

Date of the actual completion of the international search	Date of mailing of the international search report
7 January 2019	17/01/2019

Name and mailing address of the ISA/	Authorized officer
European Patent Office, P.B. 5818 Patentlaan 2 NL - 2280 HV Rijswijk Tel. (+31-70) 340-2040, Fax: (+31-70) 340-3016	Büttner, Ulf

1

Form PCT/ISA/210 (second sheet) (April 2005)

C(Continuation). DOCUMENTS CONSIDERED TO BE RELEVANT

Category*	Citation of document, with indication, where appropriate, of the relevant passages	Relevant to claim No.
X	BIAO LE ET AL: "Preparation of tumor-specific magnetoliposomes and their application for hyperthermia", JOURNAL OF CHEMICAL ENGINEERING OF JAPAN, SOCIETY OF CHEMICAL ENGINEERS, JP, vol. 34, no. 1, 26 April 2002 (2002-04-26) , pages 66-72, XP002375313, ISSN: 0021-9592 the whole document, in particular chapters 1.2, 1.8, 2.3. and 2.4.	1-7
X	HUIJUAN ZHANG ET AL: "An Intelligent and Tumor-Responsive Fe 2+ Donor and Fe 2+ -Dependent Drugs Cotransport System", ACS APPLIED MATERIALS & INTERFACES, vol. 8, no. 49, 30 November 2016 (2016-11-30), pages 33484-33498, XP055445419, US ISSN: 1944-8244, DOI: 10.1021/acsami.6b11839 the whole document, in particular chapters 3.4., 3.7. and figure 9	1-7
X	CLAIRE SANCHEZ ET AL: "Targeting a G-Protein-Coupled Receptor Overexpressed in Endocrine Tumors by Magnetic Nanoparticles To Induce Cell Death", ACS NANO, vol. 8, no. 2, 25 February 2014 (2014-02-25), pages 1350-1363, XP055444829, US ISSN: 1936-0851, DOI: 10.1021/nn404954s cited in the application the whole document, in particular the figures and page 1356, col.2	1-7
X	MARIBELLA DOMENECH ET AL: "Lysosomal Membrane Permeabilization by Targeted Magnetic Nanoparticles in Alternating Magnetic Fields", ACS NANO, vol. 7, no. 6, 25 June 2013 (2013-06-25), pages 5091-5101, XP055444828, US ISSN: 1936-0851, DOI: 10.1021/nn4007048 cited in the application the whole document, in particular figure 7	1-7

-/--

1

C(Continuation). DOCUMENTS CONSIDERED TO BE RELEVANT

Category*	Citation of document, with indication, where appropriate, of the relevant passages	Relevant to claim No.
X	IOVINO NICOLE ET AL: "Magnetic nanoparticle targeting of lysosomes: a viable method of overcoming tumor resistance?", NANOMEDICINE, vol. 9, no. 7, May 2014 (2014-05), pages 937-939, XP009503106, the whole document, in particular page 939 -----	1-7

1